Cortical mechanisms for tinnitus in humans

Thesis submitted for the degree of Doctor of Philosophy

Institute of Neuroscience, Faculty of Medical Sciences, Newcastle University

William Sedley

Student number 099168816

Supervisors:

Tim Griffiths

Kai Alter

Andrew Blamire

Submitted August 2015, revised September 2015

Abstract

This work sought to characterise neurochemical and neurophysiological processes underlying tinnitus in humans. The first study involved invasive brain recordings from a neurosurgical patient, along with experimental manipulation of his tinnitus, to map the cortical system underlying his tinnitus. Widespread tinnitus-linked changes in low- and high-frequency oscillations were observed, along with inter-regional and cross-frequency patterns of communication. The second and third studies compared tinnitus patients to controls matched for age, sex and hearing loss, measuring auditory cortex spontaneous oscillations (with magnetoencephalography) and neurochemical concentrations (with magnetic resonance spectroscopy) respectively. Unlike in previous studies not controlled for hearing loss, there were no group differences in oscillatory activity attributable to tinnitus. However, there was a significant correlation between gamma oscillations (>30Hz) and hearing loss in the tinnitus group, and between delta oscillations (1-4Hz) and perceived tinnitus loudness. In the neurochemical study, tinnitus patients had significantly reduced GABA concentrations compared to matched controls, and within this group there was a positive correlation between choline concentration (potentially linked to acetylcholine and/or neuronal plasticity) and both hearing loss, and subjective tinnitus intensity and distress. In light of present and previous findings, tinnitus may be best explained by a predictive coding model of perception, which was tested in the final experiment. This directly controlled the three main quantities comprising predictive coding models, and found that delta/theta/alpha oscillations (1-12Hz) encoded the precision of predictions, beta oscillations (12-30Hz) encoded changes to predictions, and gamma oscillations represented surprise (unexpectedness of stimuli based on predictions). The work concludes with a predictive coding model of tinnitus that builds upon the present findings and settles unresolved paradoxes in the literature. In this, precursor processes (in varying combinations) synergise to increase the precision associated with spontaneous activity in the auditory pathway to the point where it overrides higher predictions of ‘silence’.

Dedication

This thesis is dedicated to those people whose time and suffering have been necessary for its creation: my volunteers, my wife Jordana, and my daughters Ava and Naia.

Acknowledgements

This work would not have been possible without a grant generously provided by the Medical Research Council. Much is also owed to the funding organisations supporting my key collaborators, principally the Wellcome Trust and the National Institutes of Health.

The expert and unwavering support of my principal supervisor Tim Griffiths, over the period of this thesis and preceding years, cannot be overstated in terms of its role in facilitating my development as a clinical academic. My co-supervisors, Kai Alter and Andrew Blamire, have also been essential in enabling this work to go ahead.

I also wish to acknowledge the following individuals for their valuable contributions as stated:

Doris-Eva Bamiou, Consultant Neuro-Otologist, University College London Hospitals NHS Trust: Assistance with patient recruitment

Gareth Barnes, Head of Magnetoencephalography, Wellcome Trust Centre for Neuroimaging, University College London: Methods guidance for magnetoencephalography

David Bradbury, Head of Imaging, Wellcome Trust Centre for Neuroimaging, University College London: Acquisition of magnetoencephalography data

Cora Burke, Radiographer, Wellcome Trust Centre for Neuroimaging, University College London: Acquisition of structural MRI data

Mitchell Chandler, Clinical Audiologist, University College London Hospitals NHS Trust: Assistance with control recruitment

Haiming Chen, EEG Technician, Human Brain Research Laboratory, University of Iowa: Assistance with intracranial electroencephalography data acquisition

Thomas Cope, Academic Clinical Fellow in Neurology: University of Cambridge: Helpful discussions about compensating for hearing loss and loudness recruitment

Richard Edden, Associate Professor of Radiology and Radiological Science, Johns Hopkins University: Guidance and methods for MR spectroscopy for GABA

Phillip Gander, Postdoctoral Researcher, Human Brain Research Laboratory, University of Iowa: Running of intracranial EEG experiments, assistance with some experimental design, helpful discussions about data interpretation and tinnitus models

Janice Glensman, Head Radiographer, Wellcome Trust Centre for Neuroimaging, University College London: MRI safety training, and acquisition of MRI and magnetoencephalography data

Andy Hanson, EEG Technician, Newcastle University: Assistance with EEG acquisition setup

Tim Hodgson, Radiographer, Newcastle Magnetic Resonance Centre: MR spectroscopy data acquisition

Matthew Howard, Neurosurgeon, Human Brain Research Laboratory, University of Iowa: Overseeing and facilitating intracranial EEG research, performing electrode implantation surgery

Hiroto Kawasaki, Neurosurgeon, Human Brain Research Laboratory, University of Iowa: Performing electrode implantation surgery

Christopher Kovach, Postdoctoral Researcher, Human Brain Research Laboratory, University of Iowa: Creating anatomical reconstructions for intracranial EEG datasets, helpful discussions about data analysis

Sukhbinder Kumar, Postdoctoral Researcher, Wellcome Trust Centre for Neuroimaging, University College London: Helpful discussions about data analysis methods and theory of predictive coding

Letty Manyande, Magnetoencephalography Technician, Wellcome Trust Centre for Neuroimaging, University College London: Acquisition of magnetoencephalography data

Kirill Nourski, Associate Professor, Human Brain Research Laboratory, University of Iowa: Overseeing intracranial EEG experiments

Hiroyuki Oya, Associate Professor, Human Brain Research Laboratory, University of Iowa: Creating anatomical reconstructions for intracranial EEG datasets

Rudrapathy Palaniappan, Consultant in Audiovestibular Medicine, University College London Hospitals NHS Trust: Assistance with tinnitus patient recruitment

Jehill Parikh, Postdoctoral Magnetic Resonance Physicist, Newcastle Magnetic Resonance Centre: Implementation and piloting of MR spectroscopy methods for GABA measurement, assistance with MR spectroscopy data analysis

Valerie Tait, Clinical Audiologist, Newcastle Upon Tyne Hospitals NHS Trust: Assistance with tinnitus patient recruitment

Sundeep Teki, Postdoctoral Researcher, Wellcome Trust Centre for Neuroimaging, University College London: Assistance with subject recruitment

Rich Tyler, Professor of Otolaryngology, University of Iowa Carver College of Medicine: Clinical audiological assessment of tinnitus patient for intracranial EEG study

Dorothy Wallace, Radiographer, Newcastle Magnetic Resonance Centre: MR spectroscopy data acquisition

Louise Ward, Radiographer, Newcastle Magnetic Resonance Centre: MR spectroscopy data acquisition

Contents

List of Tables and Figures

Section/item **Page(s)**

Chapter 7

Chapter 8

Chapter 9

Chapter 1. Introduction

1.1 Introduction to tinnitus

Tinnitus refers to the sensation of sound in one or both ears (or perceived inside the head) that does not correspond to an external sound source. Tinnitus can be categorised as objective, in which the sound is perceived from a source inside the body, in or close to the inner ear, or subjective, where no such physical sound source exists. This thesis is concerned only with subjective tinnitus.

1.1.1 Epidemiology of tinnitus

Subjective tinnitus is experienced transiently by almost everybody, for instance if triggered by loud sound exposure or a middle ear infection. If unselected adults are placed in a silent room for a few minutes, and asked to concentrate on what they can hear, then over half report a tinnitus-like percept (Levine et al., 2003; Tucker et al., 2005). Furthermore, over half of those not experiencing this type of 'tinnitus' in such a setting can reliably elicit a tinnitus-like percept by forceful contraction of certain orofacial muscles (orofacial movements; OFMs) or other muscles (Levine et al., 2003). Thus, subjective tinnitus, to a certain degree, can be considered a normal phenomenon, and thus must be explicable in a framework that does not require pathology of the auditory pathway or central nervous system. However, 14% of the adult population (in the United States) at some point experience chronic tinnitus prompting them to seek medical attention (Shargorodsky et al., 2010), and the prevalence of tinnitus increases with age and hearing loss. When surveyed, 2% of all adults report being constantly bothered by tinnitus (Axelsson and Ringdahl, 1989).

1.1.2 Tinnitus and hearing loss

Clinically detectable hearing loss is present in the majority of cases of bothersome tinnitus, and studies on patients with tinnitus and clinically normal hearing have found group-level evidence of subclinical hearing loss, as manifest by increased pure tone thresholds in supra-clinical frequencies above 8 kHz (Roberts et al., 2006), decreased performance in detecting stimuli in noise (Weisz et al., 2006) or decreased sound-evoked cochlear nerve evoked responses to sound (Schaette and McAlpine, 2011). It is thought that this 'hidden' hearing loss reflects relative sparing of low-threshold auditory nerve fibres, which

determine pure tone thresholds, with damage predominantly to high-threshold fibres. It has recently been shown in mice that selective acoustic trauma to these high threshold fibres, without permanently altering pure tone thresholds, is sufficient to induce tinnitus-related phenomena (Hickox and Liberman, 2014), including hyperacusis and a similar pattern of brainstem responses to that observed in tinnitus patients. However, behavioural evidence of tinnitus was inconsistent in these animals, as discussed in Section 1.3.1. The onset of tinnitus sometimes coincides with the development of hearing loss, but often the hearing loss is longstanding and tinnitus begins during a psychologically or physiologically stressful event (Eggermont, 2012). Studies examining the frequency spectrum of perceived tinnitus usually find that tinnitus is perceived in the frequency range corresponding to the hearing loss (Noreña et al., 2002), which is typically in the high frequency range, from around 4 kHz upwards.

1.1.3 Psychological and psychiatric influences on tinnitus

The idea of a two-part model of tinnitus has been popular for a long time (Jastreboff, 1990). In such models, the source of the tinnitus sound is at or below the level of auditory cortex (AC), and constitutes one part of the model. The second part involves conscious detection of the sound, along with cognitive, autonomic and affective reactions to it. Through this additional component, tinnitus may become habituated, or amplified depending on the individual's psychological reaction to it. Contemporary integrative models of tinnitus (De Ridder et al., 2013; Roberts et al., 2013) also feature this concept, and aim to explain the responsible neurobiological mechanisms. There is substantial evidence for psychological comorbidity in tinnitus, including that depression (and to an extent anxiety and neuroticism) are associated with increased tinnitus severity as determined by standardised questionnaires (Zöger et al., 2006), and that in general medical outpatients the presence of tinnitus is associated with depression, anxiety, autonomic arousal and somatoform disorders (Hiller et al., 1997). Subtyping tinnitus into help-seeking (patients attending a tinnitus clinic) and non-help-seeking (recruited from the general population) groups led to the finding that it was predominantly the help-seeking group that has high levels of somatoform disorders, whereas the non-help-seeking group was similar to controls (Scott and Lindberg, 2000). Likely possibilities are therefore that distress-causing tinnitus leads to psychiatric comorbidity, and that psychiatric and somatoform

disorders, while not necessarily causing tinnitus *per se*, cause increased distress associated with tinnitus.

1.1.4 Tinnitus and hyperacusis

Hyperacusis is a condition defined by perceiving as uncomfortably loud external sounds that are tolerable and comfortable to most normal-hearing people. This is distinct from phonophobia (fear of sound) and misophonia (hatred of specific sounds, accompanied by an extreme autonomic and/or behavioural reaction to these). Hyperacusis is related to, but distinct from, loudness recruitment, which can accompany cochlear damage. Loudness recruitment is caused by loss of the usual 'compression' of loudness by the ear, and effectively increases gain in the auditory periphery. A 'normal' degree of loudness recruitment, in response to a given pattern of cochlear hearing loss, can be estimated mathematically, based on compensatory processes mediated via cochlear outer hair cells (Moore and Glasberg, 2004). Both hyperacusis and loudness recruitment can be visualised using loudness growth functions, which are graphs of the presented volume of a sound (abscissa) and the perceived loudness (ordinate). Hearing loss results in a shallower slope, with its origin shifted, which becomes restored to near normal by loudness recruitment with increasing input level, whereas hyperacusis is characterised by a steeper than normal slope (see Figure 1).

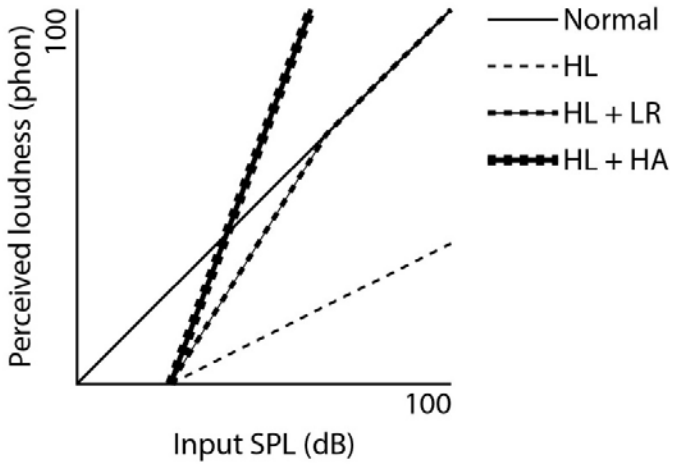

Figure 1: Loudness growth functions in normal and abnormal conditions
This figure shows a schematic of hypothetical loudness growth functions in normal hearing, hearing loss (HL), and with the addition of loudness recruitment (LR) and hyperacusis (HA). Steeper slopes indicate greater increases in perceived loudness for a given increase in input sound pressure level (SPL).

Hyperacusis can be quantified subjectively, through questionnaires, or by measuring subjective discomfort responses to sounds of varying volumes. Surprisingly, there is only a weak correlation between these two types of measure. There is overlap between hearing loss, tinnitus and hyperacusis, in that the presence of one is associated with an increased prevalence of the others (Hébert et al., 2004; Dauman and Frederic, 2005). Additionally, tinnitus patients in general appear to have steeper loudness growth functions than hearing-matched controls, even in the absence of reported hyperacusis, suggesting that mild subclinical hyperacusis may be the norm in tinnitus (Hébert et al., 2013).

1.1.5 Treatments for tinnitus

A very large number of treatments, including pharmacological, psychological, acoustic and electromagnetic, have been tried in tinnitus, and it is beyond the scope of this introduction to discuss these comprehensively, but the prevailing situation is that there does not exist a treatment for tinnitus that is both applicable to the majority of patients and proven to be successful in achieving a lasting reduction in perceived tinnitus loudness. Several meta-analyses of randomised controlled trials (RCTs) in tinnitus have been published in the Cochrane library, though in most cases the number of eligible trials was small and the strength of evidence obtained relatively weak. The strongest evidence exists for cognitive behavioural therapy (CBT), in significantly reducing the distress associated with tinnitus, but not its perceived loudness (Martinez-Devesa et al., 2007). Tinnitus-retraining therapy (TRT), a structured psychological intervention to promote habituation to tinnitus, also appears to be beneficial for tinnitus-related distress, though the evidence for this is weaker than for CBT (Phillips and McFerran, 2010). Repetitive transcranial magnetic stimulation (rTMS), a non-invasive technique to alter cortical excitability using sessions of periodic magnetic pulses, applied to auditory and other cortical regions has shown a small reduction in tinnitus loudness, in the short term, along with an equivocal benefit on tinnitus distress (Meng et al., 2011). Acoustic masking devices, which aim to suppress tinnitus using a competing sound, have not been found to be beneficial in RCTs (Hobson et al., 2012), but remain in clinical use. Hearing aids, for tinnitus in the presence of clinically significant hearing loss, are not supported by RCT evidence of a benefit in tinnitus loudness, but the evidence available is very limited (Hoare et al., 2014). Antidepressents, while sometimes helpful in managing associated mood disorders, are not associated with a benefit in tinnitus

loudness (Baldo et al., 2006). Anticonvulsants (Hoekstra et al., 2011) and the herbal remedy gingko biloba (Hilton et al., 2013) appear to be ineffective for treating tinnitus.

1.2 Studying tinnitus experimentally

A major barrier to effective treatments for tinnitus is an incomplete understanding of its pathophysiological mechanisms. However, a number of factors make tinnitus a difficult condition to study experimentally. Given the close association of tinnitus with hyperacusis and hearing loss, plus the myriad direct consequences of hearing loss throughout the auditory pathway (Gold and Bajo, 2014), it is difficult to isolate the key processes underlying tinnitus itself, and eliminate the confounds of hyperacusis and mechanistic consequences of hearing damage. Furthermore, as tinnitus is associated with (causal and/or consequential) alterations in cognitive, affective and attentional state, it is important that correlates of these changes are not mistaken for those of tinnitus itself. Animal and human studies present specific challenges, which are discussed in the following sections.

1.2.1 Animal models

Animal models of hearing damage allow auditory insults to be carefully controlled, and measurements of potentially any type to be made from any part of the auditory and central nervous system. As such, they represent an extremely powerful tool for understanding the normal functioning of the auditory pathway, and the effects of applying various sorts of insults or damage. Various animal models of tinnitus have been created, and broadly these fall into the category of either conditioned behaviour, or automatic reflex. Conditioned behaviour models (Jastreboff et al., 1988; Bauer and Brozoski, 2001; Heffner and Harrington, 2002; Ruttiger et al., 2003; Lobarinas et al., 2004) require animals to perform or stop performing a certain act during the presence or absence of a constant high-pitched sound resembling tinnitus. These models are most likely quite accurate at determining the presence of tinnitus (but not necessarily its loudness or character). The main downside is that they are extremely time-consuming and effort-intensive to implement, taking months of training. Conversely, the acoustic startle response is an involuntary reflex in response to unexpected loud sounds. This reflex can be attenuated by a preceding cue, and a cue in the form of a short silent 50 ms gap in an ongoing tinnitus-like tone has been found to be effective in attenuating the startle response, in a paradigm known as gap prepulse inhibition of the acoustic startle reflex (GPIAS) (Turner et al., 2006). This paradigm

theoretically serves as a marker of tinnitus, as a failure to suppress the startle reflex is taken as evidence of failure to perceive the gap, which putatively indicates filling in of the gap by tinnitus. Due to the low time commitment required for this method, it became rapidly adopted by multiple groups since its introduction. However, recent evidence has challenged the validity of this method, at least in its existing form. Firstly, it was found that rats classified as showing 'tinnitus' with the GPIAS model actually showed intact suppression of the startle response following the gap, provided the startle-inducing stimulus was presented in a frequency range of intact hearing (Lobarinas et al., 2013). This finding suggested that hearing loss reduced the magnitude of the startle response, and therefore there became less of a response to suppress. In humans, 50 ms gaps in a tinnitus-range stimulus (as in the GPIAS model) have been found to be no less detectible by tinnitus patients with hearing loss than hearing-matched controls (Campolo et al., 2013). Additionally, testing GPIAS paradigms in human tinnitus patients with normal hearing has found intact GPIAS, but increased startle reactivity in general in these patients (Fournier and Hébert, 2013), likely indicative of a degree of hyperacusis. Thus existing animal GPIAS studies, and any future ones until methods are made more robust, must be interpreted with the caveat that they represent an unknown combination of tinnitus, hyperacusis and hearing loss, as made clear in a recent review (Eggermont, 2013). Furthermore, the same review noted that, whichever method was used to induce tinnitus, no behavioural or neural measure following a tinnitus-inducing intervention has ever appeared bimodally distributed. This has two major implications; one is that either all of the exposed animals developed tinnitus, none of them developed tinnitus, or that the measure in question is not a measure of tinnitus *per se*. The other major implication is that it is not possible to clearly stratify animals that have all undergone the same intervention, and have the same degree of hearing loss, into a tinnitus group and a matched control group. Therefore at present, as discussed regarding GPIAS studies, all existing animal tinnitus studies must be considered inadequately controlled for hearing loss and hyperacusis. This is not an argument to disregard the animal tinnitus literature, but to simply acknowledge the limitations of its interpretation. However, these problems are not insurmountable, and future animal models may become robust by using tinnitus inducing insults that result in a bimodal distribution of tinnitus behaviour (perhaps by using lower intensities or durations of the insults applied), and then making key comparisons between equivalently exposed animal groups with contrasting tinnitus behaviour. High throughput

tinnitus screening methods, such as GPIAS, may also prove robust in future, but careful elimination of confounding factors, such as those discussed, must be achieved. Ideally, these methods should first be validated in animals trained on conditioned behaviour paradigms to ensure equivalent results. The methods used in animal studies to induce tinnitus have largely been overexposure to noise (excessive loudness and/or duration, so as to cause temporary or permanent hearing loss, or prolonged exposure to non-damaging sound levels), or administration of salicylate which causes peripheral hearing loss, direct effects on the central auditory system (Kenmochi and Eggermont, 1997) and altered firing in the auditory nerve (Stypulkowski, 1990; Cazals et al., 1998). The findings from these studies are discussed later, in the context of specific types of neural measurement.

1.2.2 Human studies

Because the diagnosis and quantification of tinnitus (both loudness and distress) relies on the subjective report of the patient, human studies have the substantial advantage of being able to confidently establish and quantify the presence of tinnitus and its various subjective dimensions. Not only this, but human subjects are able to report even subtle and short-term changes to tinnitus in response to interventions. The obvious downside to human studies is that no invasive measurements can be made (generally). This prevents any measurements of neuronal firing rates, and functional or chemical measurements in the subthalamic auditory pathway. Opportunities to record from the thalamus are very rare, as are chances to record activity directly from AC. Therefore, human studies are generally limited to indirect measures of neural activity; specific measures are discussed later. The inclusion of real-world patients is helpful, as it is reflective of clinical populations, but there is substantial heterogeneity in the aetiology, duration, laterality, perceptual character and loudness of tinnitus. Therefore studying unselected tinnitus populations might miss important differences relating to these factors, while studying stereotyped and highly selected groups might highlight changes not generalisable to tinnitus as a whole. A further limitation is that differences in psychological state and auditory-directed attention may confound studies of tinnitus. Finally, while the problem inherent in animal studies of not being able to disentangle tinnitus from hyperacusis and hearing loss can be overcome in human studies, it requires careful explicit matching of control groups, which has only been done in a minority of studies. Therefore the same caveats of interpretation apply to much of the human literature as to all of the animal literature. The three main approaches to

studying tinnitus in humans include making resting-state measurements, measuring responses to external sounds, and using experimental interventions to manipulate tinnitus loudness. Additionally, results can be compared between tinnitus and control groups, correlated with a subjective aspect of tinnitus such as perceived loudness, or within-subject comparisons between differing states can be made. Resting-state group comparisons (Llinás et al., 1999; Weisz et al., 2005a, 2007; Ashton et al., 2007; Moazami-Goudarzi et al., 2010; Adjamian et al., 2012) are potentially able to capture key correlates of tinnitus, but are particularly prone to confounding by poor matching for age and hearing loss. Furthermore, no attempts have been reported to ensure equivalence of attentional deployment between tinnitus patients, who know they are participating in a tinnitus study and are likely to attend to their auditory environment, and control subjects, who could be idly thinking about anything at all. Even if all of these factors were controlled, group comparison resting-state studies, in isolation, are fundamentally unable to separate core correlates of tinnitus (the minimum set of processes both necessary and sufficient for tinnitus to be perceived) completely from precursor processes and secondary consequences. Correlational analyses of resting-state measurements are also often performed, to highlight the neural correlates of specific aspects of tinnitus phenomenology such as distress (Weisz et al., 2005a; Vanneste et al., 2010a), loudness (van der Loo et al., 2009), chronicity (Vanneste et al., 2011c) and character (Vanneste et al., 2010b). Significant correlations often exist between various tinnitus-related and other factors, but provided these potential confounds are properly controlled for then these studies can be useful in identifying processes associated with specific aspects of the tinnitus experience. That said, it does not follow that any of these neural correlates is unique to tinnitus, or even significantly different in tinnitus compared to control groups, but just that there is an association. The presentation of sounds intended to match the perceptual character of tinnitus (for instance frequency-matched pure tones) has been used as a surrogate marker of tinnitus in searching for its central correlates (Smits et al., 2007; Lanting et al., 2008; Schlee et al., 2008; Melcher et al., 2009; De Ridder et al., 2011b). Such studies have the advantage of being able to easily create a contrast of relatively stimulated and non-stimulated states, and being able to do the same in control subjects. However, as well as susceptibility to hyperacusis as a confounding factor, such studies can only be interpreted to a limited extent without relying on the assumption that the external sounds are processed in the same way, using the same neuronal populations, as tinnitus. Presently there is a lack

of evidence to support this assumption. Short-term changes in tinnitus intensity can frequently be achieved using jaw movements or other OFMs (Lockwood et al., 1998), intravenous lidocaine (Reyes et al., 2002), direct electrical stimulation (De Ridder et al., 2011b), masking with a sufficiently loud sound (Adjamian et al., 2012), or remaining transiently suppressed after a masking sound finishes (residual inhibition; RI) (Kahlbrock and Weisz, 2008). Using within-subject contrasts, these interventions allow the core processes of tinnitus to be highlighted with greater selectivity than resting-state studies, provided direct consequences of the method of manipulation are controlled for. As well as group-level analyses, individual-level analyses are also possible. The latter type can highlight inter-individual differences, but risks potentially lacking a clear or straightforward 'take-home message'. It should also be kept in mind that these tinnitus manipulations may not cause observable changes in all of the core processes underlying tinnitus, but only necessarily a sufficient subset to cause the perception of tinnitus to change. Therefore interpretation must be made with the putative mechanism in mind by which the tinnitus manipulation operates.

1.3 Theoretical mechanisms of tinnitus

There are compelling arguments that, despite being strongly linked to hearing loss in the periphery, tinnitus is generated in the brain. These have been summarised in a previous review (Noreña and Farley, 2013) and, briefly, comprise three observations: 1) Tinnitus is often not cured by cutting the auditory nerve, and can be caused or exacerbated by this procedure; 2) Tinnitus is generally associated with reduced spontaneous and sound-driven firing in cochlea and auditory nerve; 3) Tinnitus is generally associated with excessive spontaneous activity (SA) in the central auditory pathway. However, a number of observations are not consistent with a purely central origin to tinnitus. Firstly, tinnitus (transient or permanent) resulting from a traumatically-loud sound tends to occur immediately, rather than after a sufficient delay to be consistent with the development of central compensatory processes. Additionally, increased SA in the central auditory pathway after noise trauma is strongly correlated to SA in the cochlea (Mulders and Robertson, 2009), particularly for the first 8 weeks, after which there is a shift towards independence of central activity (Robertson et al., 2013). Treatment with furosemide, which inhibits cochlear activity and has no central action, within this initial window results in abolition of tinnitus-related behaviour in animals (Mulders et al., 2014). Treatment of

human tinnitus patients with furosemide shows efficacy in some cases (Risey et al., 1995), suggesting at least a degree of peripheral dependence in a significant proportion of cases. Thus, while the perception of tinnitus is probably generated by SA in the central nervous system, the origin of this activity may, at least in part, lie in the periphery. The following sections discuss key evidence for the type(s) of spontaneous central activity that may underlie tinnitus, and how these may arise. These are grouped according to the type of neural process, rather than by species or recording methodology. Notably, there is significant overlap between these processes in several cases.

1.3.1 Central gain

Central gain refers to the amount that activity in the auditory pathway is amplified. Intuitively, it is akin to the volume dial on a radio, and neurophysiologically may be mediated by alterations in the balance of excitation and inhibition, re-weighting of neuronal connections and/or neuronal plasticity. In theory, central gain applied to external sounds could result in hyperacusis, and applied to intrinsic noise in the auditory pathway it could result in tinnitus (Schaette and McAlpine, 2011; Zeng, 2013). Peripheral gain also occurs via the activity of cochlear outer hair cells.

Psychophysical examination of human tinnitus patients has found steepened loudness growth curves, at tinnitus frequencies compared to those in hearing-matched controls (Hébert et al., 2013), suggesting increased gain mechanisms. However, it is difficult to know whether this relates specifically to tinnitus, or associated hyperacusis.

Auditory brainstem responses (ABRs) are the averaged electrical responses, across multiple stimulations, to acoustic stimuli, and comprise up to 7 waves, each representing a different stage in the auditory pathway (Moller, 2007). Wave I represents the compound action potential in the cochlear nerve; this has found to be reduced in amplitude in patients with tinnitus and clinically normal hearing compared to controls (Schaette and McAlpine, 2011; Gu et al., 2012). This has been taken as evidence of hidden hearing loss, which reduces the afferent drive to the auditory pathway. However, the same studies found recovery to normal or elevated response magnitudes at wave V, which indicates input to the inferior colliculus (IC), suggesting increased central gain between cochlear nerve and IC. A recent study in mice (Hickox and Liberman, 2014) found that noise overexposure at

a level sufficient to damage high-threshold auditory nerve fibres, but not permanently affect hearing thresholds, resulted in a similar pattern of brainstem responses to that observed in human tinnitus patients with normal hearing thresholds. The exposed animals also showed elevated acoustic startle responses in certain stimulus conditions, interpreted as behavioural evidence of hyperacusis. GPIAS deficits, however, were only found at short pre-stimulus gap latencies, raising some uncertainty about whether these animals experienced tinnitus.

Responses to acoustic stimulation, in tinnitus, have also been studied with functional magnetic resonance imaging (fMRI), which measures blood oxygenation as a surrogate marker of population neuronal activity. Initial reports of reduced sound reactivity in the contralateral IC (Melcher et al., 2000; Smits et al., 2007) and higher auditory centres (Smits et al., 2007) in tinnitus were initially taken to indicate increased SA, and hence reduced reactivity due to a 'ceiling' effect. However, subsequent work found that relatively quiet ongoing sound sources in the scanner environment led to 'baseline' activation of these structures, and that once these were removed there was actually a contralateral *increase* in sound reactivity in the IC onwards associated with tinnitus (Lanting et al., 2008; Melcher et al., 2009). While these findings support the presence of increased central gain in tinnitus patients, their methodology did not specifically aim to separate tinnitus from hyperacusis. More recent work that classified tinnitus patients according to the presence or absence of hyperacusis found that the hyperacusis group had increased sound reactivity in the IC, MGB and AC, whereas the non-hyperacusis group showed increased reactivity compared to controls only in AC (Gu et al., 2010). A more recent similar study (Boyen et al., 2014) has found a different pattern of results, with tinnitus patients showing elevated sound responses only in the cochlear nucleus and auditory thalamus (Medial Geniculate Body; MGB), compared to hearing and age matched controls. Notably, there was significantly greater hyperacusis in tinnitus patients, which could have at least partially explained the results. Similar work taking a different focus has found moderate increases in AC responses to sounds in tinnitus patients, and larger responses in the nucleus accumbens (Leaver et al., 2011). This has been interpreted as evidence of removal (via the nucleus accumbens) of subcortical gating of auditory responses, thus increasing gain at the level of the MGB. However, the subjects were unmatched for age and hearing, making the specific relevance of the results to tinnitus unknown. In considering the

relevance of AC studies of sound responses as a whole, it must be considered that attention affects the magnitude of cortical responses, and is therefore a potential source of differences between tinnitus and control groups. Attention might also influence subcortical parts of the auditory pathway via corticofugal pathways.

Auditory steady state responses (ASSRs) are evoked (time-locked) responses to amplitude modulated (AM) auditory stimuli, wherein the evoked response predominantly contains energy at the AM frequency (Galambos et al., 1981). This frequency determines the anatomical location primarily generating the measured response, with the most commonly used frequency of 40 Hz, for auditory studies, representing the level of initial processing in primary auditory cortex (A1) (Pantev et al., 1996). Early work found that the magnitude of ASSRs, using a carrier frequency corresponding to the tinnitus frequency, was proportional to subjective tinnitus distress, after correcting for the influence of hearing loss (Diesch et al., 2004). At group level, ASSRs to all frequencies measured showed increased amplitudes and displaced source locations compared to those in control patients (Wienbruch et al., 2006), however the controls were unmatched for age and hearing loss. More recent work has found no difference, at any carrier frequency, in ASSR magnitudes between tinnitus patients and matched controls (Paul et al., 2014), and also a selective decrease in ASSR magnitude at the tinnitus frequency (Roberts et al., 2015). Taken together, these observations do not make a compelling case for increased population-level frequency-specific amplification of auditory inputs in tinnitus patients, applicable to ASSR magnitudes. It is possible that the methods of correcting for hearing loss, which differed between these studies, were responsible for the conflicting results. This issue is discussed further in Chapter 7. Correlation with tinnitus distress (Diesch et al., 2004) might indicate that even if tinnitus patients do not show increased gain compared to controls, that the extent of gain might increase tinnitus distress. However an alternative and perhaps more parsimonious explanation, given that attention increases the strength of ASSRs (Gander et al., 2010), is that higher tinnitus distress leads to increased focused auditory attention, and hence increased ASSR magnitudes. The effect of attention on ASSRs has been explicitly studied in tinnitus (Paul et al., 2014), finding that attention increased all evoked response magnitudes (at sub-tinnitus and tinnitus frequencies, both N1 and ASSR responses) in controls, but in tinnitus patients the only attentional enhancement was for ASSRs at sub-tinnitus frequencies. The suggestion, therefore, is that modulation of auditory attention is

impaired in tinnitus, which is frequency-specific with respect to ASSRs and non-specific for N1 responses, and therefore there is no room for this to increase further with attention. Interestingly, healthy controls have been found to show ASSR increases with voluntary task-related deployment of attention to the auditory modality, but not further increases related to attending specific frequency ranges (Gander et al., 2010). This contrast, where voluntary attention increases ASSR magnitudes at all frequencies, except the tinnitus frequency in tinnitus patients, may therefore indicate that any resting-state increase in focused attention in tinnitus does not operate via a voluntary top-down mechanism, but instead might be driven in a bottom-up manner by the tinnitus signal. Short-term suppression of tinnitus, using RI, has been found to selectively increase the magnitude of ASSRs to tones with carrier frequencies in the tinnitus range (Roberts et al., 2015). Other work on ASSRs in tinnitus has found that the presence of multiple competing AM stimuli decreases the response magnitude in controls, but increases it in tinnitus (Diesch et al., 2010), raising the possibility of deficient lateral inhibitory mechanisms associated with tinnitus.

The first major negative evoked response to sound (and also the largest evoked response), N1 in electroencephalography (EEG) or N1m in magnetoencephalography (MEG), which localises to non-primary AC within the planum temporale. This represents a later stage of processing than the ASSR that is more dependent on wider brain states, including an equal or greater influence of attention. N1(m) responses have been extensively studied in the context of tinnitus, and have yielded mixed results without any consistent trends. In broad terms, N1 responses have been recorded to stimuli below and within the tinnitus frequency range. Below the tinnitus frequency, some studies have reported increased response magnitudes in tinnitus (Hoke, 1990; Hoke et al., 1998; Norena et al., 1999; Delb et al., 2008), while others have reported reduced magnitudes in tinnitus (Attias et al., 1993; Jacobson and McCaslin, 2003) and some have found no differences (Jacobson et al., 1991; Colding-Jørgensen et al., 1992). Theoretically, alterations in response amplitude below the tinnitus frequency range might indicate general auditory hyperexcitability, increased attention, or an effect of large-scale lateral inhibition or response reweighting as a result of high-frequency tinnitus. However, the overall evidence is not compelling for such an effect in tinnitus. Stimuli in the tinnitus frequency range have shown increased response magnitudes, in the form of steeper loudness growth functions, in tinnitus compared to

normal hearing controls (Kadner et al., 2002; Pineda et al., 2008), with partial normalisation after a course of sound-based therapy (Pineda et al., 2008), but in other studies has shown no difference in response magnitude (Weisz et al., 2005b), or reduced N1m amplitudes that were attributable to hearing loss but not tinnitus (Sereda et al., 2013). As with the conflicting findings for the sub-tinnitus frequency studies, overall there is no convincing evidence for altered N1m response magnitude to tinnitus-range tones that is specifically attributable to tinnitus.

Behaviourally, hamsters previously exposed to traumatic levels of noise have shown equal sound loudness thresholds, to unexposed controls, for triggering a startle response (Chen et al., 2013), but exaggerated startle responses, indicating increased central gain, have been observed in rats (Sun et al., 2012) and hamsters (Chen et al., 2013). These results are in keeping with the increased loudness growth functions, and increased hyperacusis, found in tinnitus patient groups. In terms of the anatomical level(s) of this increased amplification, sound-evoked local field potential (LFP) activity in rats, immediately following noise trauma, has been found to be decreased in the IC, but increased in AC (Sun et al., 2012). A chronic rat tinnitus model using noise trauma has also found increased sound-evoked responses in AC (Engineer et al., 2011). Non-traumatic prolonged acoustic exposure in cats, conversely, (an 'enriched acoustic environment') has been found to reduce sound-evoked responses in the frequency region of the prolonged exposure stimulus, and to increase responses at its edge frequencies (Noreña and Eggermont, 2006). In addition to noise-based models, salicylate has often been used as an animal model for tinnitus. Increased stimulus-driven responses in rat AC have been observed following salicylate exposure (Yang et al., 2007), which mirror the behavioural time course of tinnitus in rats (Sun et al., 2009) and cats (Zhang et al., 2011). Layer-resolved cortical recordings in rats have found granular and supragranular response amplitudes to be increased after salicylate administration, with responses in controls plateauing at 50 dB, but further increases beyond this in the salicylate group (Stolzberg et al., 2012).

1.3.2 Spontaneous firing rates

If increased central gain is responsible for tinnitus, then one might expect to see evidence of increased SA in the central auditory pathway associated with tinnitus. Spontaneous firing rate (SFR) of neuronal populations are a commonly-studied form of SA in animals,

but such recordings are not generally possible in humans In noise trauma models of tinnitus, SFR is increased in the dorsal cochlear nuclei (DCN) of chinchillas (Brozoski et al., 2002), hamsters (Kaltenbach et al., 2004; Zhang et al., 2006; Finlayson and Kaltenbach, 2009) and rats (Brozoski and Bauer, 2005), however subsequent ablation of the DCN has been found not to abolish behavioural evidence of tinnitus in rats (Brozoski and Bauer, 2005), suggesting that processes higher in the auditory pathway may be able to generate tinnitus in the absence of the DCN. Noise trauma models have also been associated with increased SFR in the IC in mice (Ma et al., 2006), chinchillas (Bauer et al., 2008) guinea pigs (Mulders and Robertson, 2009), the MGB in rats (Kalappa et al., 2014) and AC in cats (Noreña and Eggermont, 2006) and rats (Engineer et al., 2011). Paradoxically, attenuation of tinnitus behaviour following a targeted plasticity treatment was found to further increase SFR in rat AC, as opposed to restoring it to control levels (Engineer et al., 2011). While in isolation, barring the aforementioned paradoxical increase with successful treatment, these observations appear compelling for a basis of tinnitus in increased auditory SFR due to increased central gain, findings in salicylate models of tinnitus show very different results. Salicylate toxicity decreases SFR in the rat cochlear nerve (Stolzberg et al., 2011), as would be predicted by peripheral deafferentation, but has also been associated with decreased SFR in the rat DCN (Wei et al., 2010), mouse IC (Ma et al., 2006) and A1 in rats (Sun et al., 2009) and cats (Zhang et al., 2011). SFRs in cat A1 have also been found to be unchanged (Ochi and Eggermont, 1996), while increased SFRs due to salicylate toxicity have been observed in the extra-lemniscal part of the IC in rats (Chen and Jastreboff, 1995) and guinea pigs (Manabe et al., 1997), and in non-primary AC in cats (Ochi and Eggermont, 1996; Eggermont and Kenmochi, 1998). Given the broadly opposite findings in salicylate compared to noise trauma, unless salicylate and noise trauma induced tinnitus have different pathophysiological mechanisms, generalised increases in auditory pathway SFR seem to be an unlikely mechanism for tinnitus. The exception to this might be the extra-lemniscal pathway, projecting to non-primary AC, which as mentioned has shown increased SFR in salicylate models, though this has not been sufficiently studied across multiple models to make a strong claim that this is a basis for tinnitus.

1.3.3 Neural synchrony

Rather than simply examine the firing rates of single neurons or neuronal populations, other work has examined SA that is synchronous across neuronal populations. In human studies, this takes the form of extracranially-recorded electrical potentials or magnetic fields, and occasionally LFPs recorded intracranially. In animal studies, these types of measurement are all possible, but are rarely reported. Instead, the more typically-reported measurement is *neuronal synchrony*, defined as the strength of the cross-correlation between two or more spatially-separated neurons (usually over the order of a millimetre or so). In normal cat AC, this measure has been found to be a better predictor of acoustic stimulation than SFR (Eggermont, 2000).

Unlike SFR changes, which develop more slowly, noise trauma causes an immediate increase in neuronal synchrony in cat A1 (Noreña and Eggermont, 2003), mirroring the immediate onset of tinnitus in these circumstances. Furthermore, SFR actually decreases transiently before increasing, again demonstrating poor concordance of its time course with that of post—noise trauma tinnitus. This increase in synchrony is specific to the region of hearing loss (Seki and Eggermont, 2003). The chronic effects of noise trauma are similar, with persistent increases in SFR and neuronal synchrony (Noreña and Eggermont, 2006). Chronic exposure to non-traumatic levels of noise was found to increase neuronal synchrony in all parts of the tonotopic axis, especially within and above the frequency range of the noise (Noreña and Eggermont, 2006; Pienkowski and Eggermont, 2009). Notably, when followed up over a long period of time, the increased synchrony did not recover to normal (Pienkowski and Eggermont, 2009). Interestingly, while chronic non-traumatic acoustic stimulation can increase neural synchrony, the immediate and prolonged application of equivalent stimulation immediately after noise trauma prevents the usual changes in firing rate and neuronal synchrony (Noreña and Eggermont, 2006). Thus, it appears that chronic understimulation (from noise trauma) and overstimulation can induce persistent changes in neuronal synchrony, and a balance between the two prevents this from occurring.

SA of synchronised neuronal populations can be easily measured in humans, in the form of oscillations in extracranial or intracranial electrical potentials or magnetic fields. These can be divided into frequency bands, according to the frequency with which the signals oscillate, and analysis performed either at the level of the sensors, or at the level of

estimated brain sources. While altered oscillatory activity has been observed all over the brain, in association with various aspects of tinnitus phenomenology, this section concentrates on activity within the auditory pathway, specifically AC, as spontaneous subcortical activity generally cannot be recorded non-invasively.

Delta (1-4 Hz) and theta (4-8 Hz) oscillations appear to behave similarly in tinnitus, with some groups reporting delta and others theta. Given the lack of a clear theoretical difference, these are considered together here, and sometimes referred to just as 'low-frequency' oscillations. Early studies reported increased magnitude of spontaneous low-frequency oscillations in tinnitus patients compared to young, normal-hearing controls (Llinás et al., 1999; Weisz et al., 2005a, 2007; Moazami-Goudarzi et al., 2010). Given a similar frequency range to spontaneous bursting observed in extra-lemniscal parts of the human auditory thalamus (by direct recording in neurosurgical tinnitus patients) (Jeanmonod et al., 1996), it was hypothesised that the basis of the cortical delta/theta signal was in spontaneous thalamic bursting, in a model called *thalamocortical dysrhythmia* (TCD) (Llinás et al., 1999, 2005), which has been argued to underlie a number of neurological and neuropsychiatric conditions; more recently, a noise trauma animal model has shown similar bursting behaviour in MGB neurons (Kalappa et al., 2014). However, a more recent study including groups of tinnitus patients with and without hearing loss, and controls age and hearing matched to both (Adjamian et al., 2012), found no overall difference in low-frequency magnitude, but only a significant difference between tinnitus patients with hearing loss and normal-hearing controls. Thus, while it appears that spontaneous delta/theta magnitude may in some way relate to tinnitus, it does not appear to be a generic tinnitus signature. However, a number of other studies highlight the importance of delta/theta oscillations. Firstly, transient suppression of tinnitus through acoustic masking (Adjamian et al., 2012) and RI (Kahlbrock and Weisz, 2008; Sedley et al., 2012a) is associated with contemporaneous reductions in low-frequency amplitude at both group and individual level. Secondly, EEG neurofeedback techniques in which patients manage to suppress delta magnitude and increase alpha magnitude have been associated with significant reductions in tinnitus loudness (Dohrmann et al., 2007; Hartmann et al., 2014). Thirdly, tinnitus reduction by electrical stimulation was found to be accompanied by simultaneous reductions in delta/theta power (de Ridder et al., 2011b). Finally, improvement in tinnitus loudness following a tailored acoustic treatment was

associated with reductions in AC delta power at rest (Tass et al., 2012). As the phase of low-frequency oscillations is known to organise the timing of activity bursts in high frequency bands (Canolty et al., 2006), perturbations of low-frequency activity in tinnitus could have various consequences in other frequency bands.

Alpha oscillations (8-12 Hz) are the dominant rhythm in the awake resting EEG. While they are strongest in posterior parieto-occipital regions, there is a strong AC alpha rhythm also. This is strongest as rest, and decreases with attention or with auditory stimulation (Weisz et al., 2011). Like lower frequency oscillations, alpha oscillations also control higher frequency rhythms through phase-amplitude interactions (Jensen and Mazaheri, 2010). The initial report in tinnitus was of reduced alpha magnitude compared to unmatched controls (Weisz et al., 2005a), though subsequent work, again using unmatched controls, found alpha increases rather than decreases (Moazami-Goudarzi et al., 2010). In the only resting-state study with a well-matched control group (Adjamian et al., 2012), alpha oscillation magnitude was not found to be different between groups. However, as mentioned previously, neurofeedback successful in increasing alpha magnitude caused a significant reduction in tinnitus loudness (Dohrmann et al., 2007). Also, studies of illusory perception, in the form of Zwicker tones (perceived tones following the end of a notch-filtered noise stimulus) (Leske et al., 2014) and of illusory continuation of music during white noise (Müller et al., 2013) have found that the strength of AC alpha oscillations is inverse to that of illusory percepts.

Gamma oscillations occupy all frequencies above around 30 Hz. While initially favoured as a close correlate of conscious perception and solution to the binding problem of consciousness (Gray et al., 1989; Singer and Gray, 1995; Tallon-baudry and Bertrand, 1999), the initially-reported narrowband gamma oscillations, peaking at around 40-60 Hz, in the visual system have a number of features that point against them being a generic correlate of perception. Firstly, they occur only in response to high luminance contrasts, and not equally-salient colour contrasts (Adjamian et al., 2008). They also relate solely to contrasts within a fairly narrow range of spatial frequencies (number of contrasts per degree of visual angle) (Adjamian et al., 2004), which corresponds to the range generating visual illusions and unpleasant sensations in normal individuals, and triggering ictal discharges in patients with photosensitive epilepsy. They occur in response to large visual

patterns (Gieselmann and Thiele, 2008; Jia et al., 2013), of sizes that trigger surround suppression both perceptually (Tadin et al., 2003) and neurophysiologically, such that they are associated with reduced overall neuronal activity (Gieselmann and Thiele, 2008; Jia et al., 2013). Leaving aside narrowband gamma oscillations in the visual system, which do not appear to have an equivalent in other systems, there are higher-frequency more broadband gamma oscillations, with a distinct origin (Ray and Maunsell, 2011), observed in the visual (Lachaux et al., 2005) auditory (Edwards et al., 2005; Griffiths et al., 2010; Sedley et al., 2012b) and somatosensory (Bauer et al., 2006; Gross et al., 2007) systems. These broadband gamma oscillations appear to be a near-ubiquitous correlate of sensory stimulation, attention (Gruber et al., 1999; Fries et al., 2001; Tallon-Baudry et al., 2005; Bauer et al., 2006; Ray et al., 2008; Wyart and Tallon-Baudry, 2008; Chalk et al., 2010), task performance (Womelsdorf et al., 2006; Fujioka et al., 2009; Hoogenboom et al., 2010) and memory (Herrmann et al., 2004). While the origin of gamma oscillations has a basis in the rhythmic discharges of inhibitory neurons (Whittington et al., 1995), synchronous inhibition of neuronal populations can have a net excitatory effect, by aligning the firing of these neurons in time, and hence increasing temporal summation of excitatory post-synaptic potentials on their targets (Tiesinga et al., 2004). Long-range synchronisation of gamma oscillations, between functionally-distinct cortical areas, has been associated with increased conscious perception in the context of identical sensory stimulation (Melloni et al., 2007; Hipp et al., 2011). However, overall evidence does not support a singular role of gamma oscillations in promoting conscious perception, and instead finds that they can more parsimoniously be considered a generic signature of cortical activation (Merker, 2013). However, recent evidence (Arnal et al., 2011; Brodski et al., 2015) and theory (Arnal and Giraud, 2012; Bastos et al., 2012) suggests that gamma oscillations may constitute a *prediction error* signal, in that they signal incongruence between ascending sensory representations and prior predictions. These *predictive coding* models of perception are discussed in more detail later. In previous work (Griffiths et al., 2010) it was observed that the strong gamma responses to pitch stimuli only persist for the whole duration of the stimulus where there is ongoing irregularity in that stimulus, and do not in cases where the stimulus is completely deterministic (observation presently unpublished). Thus, basic auditory gamma responses might also be explicable in terms of prediction violations.

Early observations in tinnitus patients found gamma oscillations to be increased in scalp regions approximately overlying AC (Llinás et al., 1999; Ashton et al., 2007). It was claimed that these changes were absent in (young, normal-hearing) controls, but the control data were never presented, and not necessarily recorded in identical circumstances. At group level, tinnitus patients were found to have increased gamma power in AC compared to young, normal-hearing controls (Weisz et al., 2007), and a temporal correlation was observed between delta and gamma oscillation increases. A subsequent study by the same group, examining amateur rock musicians who regularly developed transient tinnitus and hearing loss following band practice, found that transient tinnitus plus hearing loss was associated with increased gamma power in the right AC (and no other changes), irrespective of tinnitus laterality, and that the gamma power was better explained by hearing loss than by tinnitus (Ortmann et al., 2011). The only inter-group comparison well-matched for hearing loss found no differences in gamma power related to tinnitus (Adjamian et al., 2012), supporting the interpretation that gamma power increases are not best explained as a direct correlate of tinnitus. Additionally, studies using tinnitus masking (Adjamian et al., 2012) and RI (Kahlbrock and Weisz, 2008) found no group-level changes in gamma power accompanying tinnitus suppression. However, correlational studies have reported that, within a tinnitus group, resting-state AC gamma power was positively correlated with self-rated tinnitus loudness (van der Loo et al., 2009). However, the influence of hearing loss and other factors on these self-ratings were not explored. Recent replications of this analysis, using much larger patient groups, have differed in their findings, with one such study, on whole-brain analysis finding no intensity-gamma correlation (Vanneste et al., 2015), and another finding a positive intensity-gamma correlation after correcting for hearing loss (De Ridder et al., 2015a). In the latter study, only subjectively-rated tinnitus, as opposed to loudness-matches to external sounds, correlated with brain activity, echoing the distinction made between these (relatively uncorrelated) ratings made in a recent study (Balkenhol et al., 2013). Also, successful treatment of a tinnitus group with acoustic therapy was associated with reductions in AC gamma power (Tass et al., 2012), and exacerbation of tinnitus by a failed sound therapy was associated with gamma increases (Vanneste et al., 2013b). Therefore, while there do not appear to be group-level gamma increases attributable to tinnitus, once hearing loss is controlled for, spontaneous gamma magnitude does appear to be linked to the perceived loudness of tinnitus. A further paradox comes from individual subject data examined in the

context of RI and its perceptual opposite, residual excitation (RE; a transient increase in tinnitus loudness following an acoustic stimulus) (Sedley et al., 2012a); the majority of patients experiencing RI showed significant coexistent reductions in gamma power (and delta/theta power as previously observed), however one patient's RI was accompanied by significant gamma increases. At the group level there were no gamma changes attributable to RI, suggesting the existence of further increases that were not individually significant, and potentially explaining the lack of group-level gamma changes seen during previous studies of masking and RI. The most striking finding was that in all four patients showing RE (tinnitus increase following a sound), this was accompanied by large isolated decreases in AC gamma power. These included one patient who also showed RI that was accompanied by gamma decreases. Thus the relationship between tinnitus intensity and gamma power can be in either direction, depending on the patient and the tinnitus manipulation used. This finding was interpreted as suggesting an inhibitory role of gamma oscillations, in that reducing the tinnitus drive (in RI) would reduce the amount to which inhibitory mechanisms were recruited, while interfering directly with the inhibitory signal (RE) would cause tinnitus to become louder. However, this claim was speculative. As an alternative explanation, a recently-proposed advance on the TCD model (De Ridder et al., 2015b) has suggested that these divergent gamma findings are a manifestation of gamma's role as a prediction error signal; i.e. that as tinnitus deviates from its 'baseline' state (as a reduction or increase relative to this), a prediction error is generated, manifest as increased gamma power. However, this claim would predict *increased* gamma power during RI or RE, whereas the opposite was observed. Overall, available evidence suggests that AC gamma oscillations are highly relevant to tinnitus, but do not have a straightforward relationship to the presence or perceived loudness of tinnitus.

While generally the measures of neuronal synchrony employed in human and animal studies are very different, one animal study has attempted to bridge the gap by measuring spontaneous LFP oscillations (Noreña et al., 2010) in the guinea pig. This study induced used two tinnitus induction methods: salicylate toxicity, followed by recovery and then noise trauma. Neither type of auditory insult was associated with alterations in delta/theta or gamma power in auditory cortex, but both types produced a decrease in oscillatory power in the 10-30 Hz range. The reasons for this discrepancy are unclear, but could include differences in the chronicity of 'tinnitus', attention and task requirements,

recording methods used, the spatial extent of synchrony measured with the different techniques, and whether the animals actually had tinnitus (this was not tested behaviourally). More recently, a novel rat assay for assessing tinnitus acutely has been developed (Stolzberg et al., 2013), which links evidence of current tinnitus with data recording epochs of several seconds duration. Initial recordings from a localised region of AC made during acute salicylate administration found evidence of tinnitus, accompanied by reductions in theta power, increases in low gamma power (around 50 Hz), and decreases in high gamma power. The acuteness of the tinnitus, and the method of induction, might have been contributed to the discrepancy between these results and the human literature. Regardless of the exact causes of the low correspondence between these studies and human ones, one must exercise a degree of caution in linking the human and animal literature in this respect.

1.3.4 Deficient inhibition

The previous discussion of increased gain and SA associated with tinnitus can potentially be explained, in whole or part, by alterations in excitation/inhibition balance. In addition to inhibitory mechanisms simply reducing the gain on neuronal activity, inhibition takes other forms. These include forward inhibition/masking, as in RI (Roberts et al., 2008, 2015), and also lateral/surround inhibition, in which activation of excitatory ascending projections in one frequency inhibits activity in adjacent frequency regions through diagonal or lateral connections. Lateral inhibitory mechanisms are necessary to refine and sharpen perceptual representations, and may be responsible for the exquisitely narrow frequency selectivity observed in auditory cortex neurons (Bitterman et al., 2008). The principal inhibitory neurotransmitter is gamma-aminobutyric acid (GABA), which has received the most attention in tinnitus. The glycinergic inhibitory system has been less studied in tinnitus, but has shown evidence of altered function in the DCN as a result of ageing in chinchillas (Brozoski et al., 2002) and rats (Caspary et al., 2005) and hearing loss-related tinnitus in rats (Wang et al., 2009).

A rapid consequence of noise trauma in cats is reduced SFR in exposed frequency regions of AC, which then resolves, accompanied by increased SFR in the frequency ranges immediately above and below the region of trauma (Noreña and Eggermont, 2003). This finding has been interpreted as a reduction in lateral inhibition arising from the traumatised

frequency range, and is a likely precursor of tonotopic map changes (which are discussed later). It is not only traumatic noise exposure that induces such changes, but chronic exposure to non-traumatic noise has been found to have the same effect (Noreña and Eggermont, 2006). The longer-term effects of noise trauma, as well as increased SFR and neuronal synchrony as discussed previously, include re-tuning of neurons in the range of hearing damage to the edge frequency (i.e. the highest unaffected frequency) (Norena, 2005; Noreña and Eggermont, 2006). Reduced lateral inhibition, from first principles, is likely to result in larger neuronal populations responding to a given stimulus, which might underlie increased neural synchrony observed in tinnitus.

A body of work has sought to treat tinnitus by restoring the balance of lateral inhibition. In this, patients listen to music containing a frequency 'notch' corresponding to their perceived tinnitus frequency (Okamoto et al., 2010; Stein et al., 2015a), thereby exerting asymmetrical lateral inhibitory effects that are the opposite of those putatively associated with tinnitus. This was found to reduce the perceived loudness of tinnitus and the magnitude of cortical evoked responses. Further work on the subject has found that amplifying narrow frequency regions at the notch edges, increasing lateral inhibition effects further, led to a stronger subsequent reduction in evoked response magnitude, but no difference in effects on tinnitus perception (Stein et al., 2013, 2015b). A further study also found that tinnitus-linked cortical activity was only attenuated by actively, not passively, listening to notched music stimuli (Pape et al., 2014).

Both ageing and various peripheral auditory insults induce widespread alterations to GABA systems in the central auditory pathway, and have been extensively reviewed previously (Gold and Bajo, 2014). In the rat IC, ageing was associated with reduced free GABA (Banay-Schwartz et al., 1989), GABA-ergic neuronal density (Caspary et al., 1990), labelling of glutamic acid decarboxylase (GAD; an enzyme responsible for GABA synthesis) (Burianova et al., 2009) and stimulus-evoked GABA release (Caspary et al., 1990), and hearing loss was associated with reduced levels of GAD in rats (Argence et al., 2006) and GABA(A) receptor transcription in guinea pigs (Dong et al., 2010). Similarly, ageing rat AC was found to have reduced GAD levels (Ling et al., 2005) and free GABA (Banay-Schwartz et al., 1989). While the above evidence is exclusively from animal studies, there has been a recent human study which found that presbyacusis (age-related hearing loss) was associated with reduced GABA in AC (Gao et al., 2015).

Mice exposed to noise trauma, with behavioural evidence of tinnitus, were found to show excessive magnitude and lateral spread of neural responses to focal stimulation of the DCN (Middleton et al., 2011). Applying GABA antagonists produced the same response pattern in control animals, but did not change the responses in tinnitus animals. Therefore, the findings were interpreted as evidence of GABA-ergic deficiency. GABA concentration has been measured in noise trauma rats with behavioural evidence of tinnitus, and was found to be reduced in the contralateral MGB, but not significantly altered at other levels, including AC (Brozoski et al., 2012). However, despite a lack of evidence of reduced GABA concentration, there is evidence of AC GABA-ergic deficiency in rodent models of noise trauma-induced tinnitus, in the form of reduced GAD expression in rats (Yang et al., 2011), and increased magnitude and spread of cortical responses in mice, to thalamic afferent stimulation, similar to those in the DCN (Llano et al., 2012). In summary, there is substantial evidence of reduced GABA-ergic activity in both ageing and hearing loss, and also in animals with behavioural evidence of tinnitus from either or both of these causes. However, given that reduced inhibition is likely to be a homeostatic response to deafferentation, it is difficult to assess which findings, if any, relate specifically to a maladaptive deficiency of inhibition that might underlie tinnitus. Human studies including tight matching for age and hearing loss might help to answer this question, but presently have not been conducted. The nearest study in humans did not use matched controls, and reported reduced benzodiazepine binding sites in the mesial temporal lobes of patients with severe chronic tinnitus (Shulman et al., 2000).

1.3.5 Plasticity in tinnitus

Neural plasticity broadly refers to the capacity of the nervous system to change its behaviour in response to physical changes and/or past experiences. This encompasses the previously discussed changes in firing rates, inhibitory connections, neural synchrony, gain controls and other correlates associated with tinnitus and its inducers. This section focuses on a few key aspects of plasticity, related to tinnitus, that have not already been covered.

The *tonotopic map* refers to the distribution of neurons or neuronal populations, at all levels of the auditory pathway, according to the stimulus frequencies to which they most strongly respond. Further to the previously discussed observation that noise trauma exposed animals exhibit consequent changes in lateral inhibition and SFRs, the subsequent

re-tuning of neurons in the noise trauma region to the lower edge frequency constitutes tonotopic map plasticity (Noreña and Eggermont, 2006). The finding in this study of cat AC that immediate immersion in an enriched acoustic environment prevented most of these changes from taking place indicates that the observed changes are not inevitable consequences of the noise trauma, but most likely gradual plastic processes resulting from consequent alterations in excitation and inhibition. However, when the same approach of enriched acoustic environments was used to treat human patients with chronic tinnitus (Vanneste et al., 2013b), there was no benefit, and in many cases a worsening of tinnitus loudness. Therefore it seems like there may be a window of opportunity, beyond which acoustic stimulation may further activate and enhance the maladaptive plasticity rather than preventing it. Human evidence of tonotopic map plasticity in tinnitus was originally reported from MEG studies of N1m responses and ASSRs, which found that the tinnitus frequency source locations were displaced in space compared to controls (Mühlnickel et al., 1998; Wienbruch et al., 2006). However, these studies (and inherently, all animal studies on the subject) were not controlled for hearing loss. More recent work using fMRI to examine tonotopic maps in AC in tinnitus patients, against age and hearing matched controls, found no differences in tonotopic maps (Langers et al., 2012). This evidence builds upon the previous observations that noise trauma-exposed cats with less than 25 dB hearing loss did not demonstrate tonotopic map plasticity, but still showed increased SFR and neural synchrony (Seki and Eggermont, 2002, 2003). Therefore tonotopic map plasticity does not seem necessary for tinnitus, though an optional role cannot be discounted. Furthermore, if tonotopic map plasticity were primarily responsible for the tinnitus sensation, one might expect the overrepresented edge frequency to relate to the perceived tinnitus pitch, whereas evidence on the subject based on psychophysical matching has found that tinnitus is experienced across the whole range of hearing loss frequencies (Noreña et al., 2002; Roberts et al., 2006).

The notched music approach already described can be considered a way of using lateral inhibition to reverse plasticity associated with tinnitus. Another method exploits the action of the basal forebrain (BF) cholinergic system which, via its rich cholinergic projections to AC, has a major role in shaping sensory responses and promoting plasticity (Sarter et al., 2001; Hasselmo and Sarter, 2011). This treatment involves using vagus nerve stimulation (VNS), which activates the BF in order to cause brief windows of acetylcholine release in

which high levels of plasticity can occur. VNS is paired with tone stimulation in the tinnitus frequency range that is precisely timed to induce plastic reductions in neuronal responses and connections (Engineer et al., 2011). This approach has been successful at eliminating behavioural evidence of tinnitus in animals, and early trials in humans are encouraging (De Ridder et al., 2014). Another approach has exploited spike timing dependent plasticity (STDP) which, depending on the timing with which neuronal populations are stimulated, can induce long-term potentiation (LTP) or long-term depression (LTD), which refer to strengthening and weakening (respectively) of synaptic connections between co-stimulated neurons. This approach, known as coordinated reset (CR) neuromodulation (Tass et al., 2012) is applicable only to tinnitus with a pure tone character, and involves presenting tones in neighbouring frequencies in a sequence and timing that theoretically induces LTD. This has been found to reduce perceived loudness of tinnitus, and to reverse the neuronal oscillatory signatures that have previously been associated with tinnitus plus hearing loss (Weisz et al., 2007). In summary, plasticity relating to asymmetrical lateral inhibition, the BF cholinergic system and STDP all appear to be related to the perception of tinnitus.

1.3.6 Cross-modal interactions

Further to numerous observations of tinnitus coinciding with musculoskeletal disorders of the neck and jaw, suggesting a subtype of tinnitus that is sometimes referred to as 'somatic tinnitus', it has been found that 80% of all people with tinnitus can reliably modulate their tinnitus percept through forceful contractions of the head, neck and/or jaw (OFMs), and 60% of people with no tinnitus can elicit a tinnitus-like sensation with such manoeuvres (Levine et al., 2003). Thus, somatomotor-auditory interactions appear not only fundamental to tinnitus, but to auditory perception in general. Regarding the mechanism(s) for this interaction, it has long been known that such interactions occur in the cat MGB (Wepsic, 1966), and it has also been found that fibres from the trigeminal nerve nucleus project to the DCN in guinea pigs (Zhou and Shore, 2004). Functionally, the guinea pig DCN shows significant responses to trigeminal nucleus stimulation (Shore, 2005), and the magnitude of these responses is increased in the presence of hearing loss (Shore et al., 2009). Therefore these cross-modal inputs are a potential source of SA in the ascending auditory pathway. However, it must be remembered that there are cross-modal interactions

at all levels of the auditory pathway, and so interactions at other levels less well explored may also be relevant.

1.3.7 Deficient noise cancelling

A model of tinnitus has been proposed, in which the fundamental underlying pathology is deficiency of normal noise cancelling mechanisms (Rauschecker et al., 2010). This model is based on observations of grey matter (GM) loss in the subcallosal region of cingulate cortex (Mühlau et al., 2006; Leaver et al., 2011), which is argued to act as a key centre for suppressing certain subcortical auditory inputs. The nucleus accumbens was found to be overactive in response to tinnitus-matched tones, in tinnitus patients, and the degree of overactivity was related to the extent of subcallosal GM loss (Leaver et al., 2011) and the perceived loudness of tinnitus. The proposed noise cancelling mechanism is that the thalamic reticular nucleus (TRN) sends rich inhibitory connections to other thalamic regions, including auditory regions relevant to hearing loss and tinnitus. The nucleus accumbens acts on the TRN to reduce this inhibition, and hence increases the magnitude of subcortical activity. The subcallosal region is argued to inhibit the nucleus accumbens, and therefore restore subcortical inhibition. It is deficiency of this region, and its consequent subcortical inhibitory action, that is proposed to allow subcortical activity to escape from inhibition and thus go on to be consciously perceived. While this model has face validity, it is supported by limited evidence, and the evidence described above used young, normal-hearing controls and did not apply any correction for hearing loss. Therefore it is unclear whether such a mechanism, if existent, is acting adaptively (to compensate for hearing loss) or maladaptively (so as to cause tinnitus).

-

1.3.8 Attention and acetylcholine

As discussed already, attention is an important factor to consider when studying tinnitus, as it is known to enhance sound-evoked responses (Hall et al., 2000; Petkov et al., 2004; Gander et al., 2010), and to have neural correlates in sensory cortex that are similar to those described for tinnitus (e.g. increased gamma and reduced alpha oscillations). From first principles directed attention, as a means of selectively enhancing representations of certain stimuli at the expense of others, may also increase the perceptual intensity of tinnitus. The importance of the BF cholinergic system in tinnitus has already been

discussed in the context of plasticity. This system is also known to be recruited by attention, and to facilitate attention by increasing the synaptic gain associated with cortical representations of attended stimuli (Hasselmo and Sarter, 2011). Evidence suggests that cholinergic action of the BF acts to strengthen thalamocortical connections and weaken cortico-cortical ones (Sarter et al., 2005), thereby sensitising cortex to ascending sensory inputs (Metherate and Ashe, 1993). Unexpected stimuli evoke a characteristic response, called mismatch negativity (MMN), which quantitatively relates to the unexpectedness of stimuli (Garrido et al., 2013), and automatically orients attention via a circuit involving primary and non-primary sensory cortex and ventrolateral prefrontal cortex (vlPFC) (Schönwiesner et al., 2007). vlPFC has a key role in directing attention (Petrides et al., 2002), and one of several prefrontal cortical regions exhibiting rich bidirectional connectivity with the BF (Sarter et al., 2005). A recent EEG study using dynamic causal modelling (DCM), which models observed neural activity based on underlying layer-resolved neuronal populations and their relative connection strengths (Friston et al., 2003; David et al., 2006), found that application of a cholinesterase inhibitor (which acts to potentiate cholinergic projections) had the effect of increasing the gain of the superficial pyramidal cells in the cortex, which receive afferent sensory inputs (Moran et al., 2014). This effect explained the differences observed in MMN evoked responses. Directed attention is also known to alter the spectrotemporal receptive fields of auditory cortical neurons, based on work in ferrets (Fritz et al., 2003), which may also be a precursor to long-term plasticity. Further evidence has found that the BF system is linked to task-related plasticity in rats, but not 'passive' plasticity such as reorganisation following deafferentation (Ramanathan et al., 2009). In humans, attention not only enhances responses to sounds, but increases the activation of sensory cortex in the absence of stimulation (Voisin et al., 2006; Sadaghiani et al., 2009), and alters its ongoing pattern of oscillations (Ray et al., 2008). The potential confounding effect of attention makes tinnitus difficult to study, as both the presence and intensity of tinnitus, plus psychological reactions to it, are likely to result in alterations of attention, which have their own effects on spontaneous and driven neural activity. For instance, the increased cortical sound-driven activity seen in tinnitus (Gu et al., 2010), after matching for hearing loss, could represent intrinsic hyperactivity specific to tinnitus, or simply increased auditory-focused attention as a result of tinnitus. An alternative, or complementary, explanation is that attention is actually *causal* to tinnitus, rather than consequential (Roberts et al., 2013). In

this model, a central representation of tinnitus is created through aberrant plasticity following deafferentation. Ascending sensory input, as it is compromised by deafferentation, is incongruent with this central representation, and the mismatch automatically orients attention towards the modality and frequency region at which it occurs. The increased attention can be thought of as a way to resolve this discrepancy, by strengthening central auditory representations, and could be mediated by the BF cholinergic system. While it does not use the term specifically, this model describes a similar framework to *predictive coding*, which is discussed in more detail later.

1.3.9 Global brain networks

As well as changes occurring within the auditory system, the involvement of wider cortical and subcortical networks in tinnitus has received considerable attention in human studies.

Early studies of altered SA in tinnitus reported changes across large parts of the cerebral cortex (Weisz et al., 2005a; Moazami-Goudarzi et al., 2010), and not just auditory regions. A study of functional connectivity, using MEG source reconstructions, found abnormal connectivity between certain cortical areas, particularly mesial temporal lobe and midline cortical regions (Schlee et al., 2009). However, these studies were not controlled for age or hearing loss, so there is some uncertainty about what the observed changes represent. A series of correlational EEG studies, from a major tinnitus clinic, has reported the within-group correlates of various aspects of tinnitus phenomenology, including distress (Vanneste et al., 2010a), duration (Vanneste et al., 2011c), perceptual character (Vanneste et al., 2010b) and laterality (Vanneste et al., 2011b). These findings together implicate an extensive array of areas which combined cover most of the brain. A synthesis of these and other findings proposes that the multifaceted experience of tinnitus arises due to distinct sub-networks each representing a different aspect of tinnitus (for instance, the above characteristics, plus loudness), and that these communicate with each other through inter-regional coherence and cross-frequency interactions (De Ridder et al., 2013). A brain region of particular focus is the parahippocampal cortex (PHC), which exhibits increased gamma band activity contralateral to the tinnitus percept (Vanneste et al., 2011a), and is argued to be part of a ‘core’ tinnitus network, defined as the areas necessary and sufficient for conscious tinnitus perception, as well as a specific role in auditory memory relating to tinnitus (De Ridder et al., 2013). Other prominent areas are the ventromedial prefrontal

cortex (vmPFC) and the adjacent subcallosal cingulate region, which have already been discussed in the context of deficient noise cancellation models. Ongoing oscillatory delta, theta and beta activity in vmPFC (and adjacent anterior cingulate regions) correlates with the proportion of the time in which tinnitus is perceived (Song et al., 2015), which has been interpreted as evidence in support of a noise cancellation role. These areas also correlate with tinnitus-related distress. Other areas highlighted by these studies include anterior and posterior cingulate cortex, precuneus, vlPFC, dorsolateral prefrontal cortex (dlPFC) and inferior parietal cortex (IPC). However, a caveat to the interpretation of these studies in isolation is that these global brain networks are likely generic (for instance, the same distress network is activated regardless of the cause of distress), and thus it is difficult to separate generic correlates of cognitive and affective processes from processes specific to tinnitus.

Certain functional imaging (fMRI and PET) studies have used short-term tinnitus manipulations to create a contrast between 'high' and 'low' tinnitus states in order to isolate tinnitus correlates within the brain. One study, of transient tinnitus suppression, found tinnitus-linked activity in right non-primary AC, plus prefrontal and mesial temporal lobe sites (Mirz et al., 2000). However, other studies used OFMs or lidocaine to enhance or suppress tinnitus, and (once the direct correlates of the interventions were contrasted out of the analyses) found activity changes in AC but not wider cortical regions (Lockwood et al., 1998; Reyes et al., 2002). In a resting-state study, tinnitus duration and distress were associated with increased activation in frontal and limbic regions respectively (Schecklmann et al., 2013a), mirroring the EEG findings discussed in the previous section. Most recent fMRI studies of SA in tinnitus have not measured the mean level of activity in particular brain regions, but have focused instead on resting-state connectivity, which infers communication between brain regions based on correlation of slowly-fluctuating signal magnitudes between them. There are two broad approaches to this: seed-based connectivity techniques specify a particular brain region and quantify correlations between that area and the rest of the brain; independent component analysis (ICA) based methods identify anatomical patterns in the brain in which spontaneous signal magnitudes correlate over time, and do not require specification of a prior 'seed' or other location of interest. In healthy controls, ICA based methods reveal the presence of multiple distinct resting-state networks (RSNs), which are reproducible across individuals (Biswal et al., 1995; Greicius

et al., 2002). These RSNs have been named according to their likely functions in light of their anatomical constituents and activation patterns (Beckmann et al., 2005). A pair of studies (Burton et al., 2012; Wineland et al., 2012) used a seed-based approach to compare resting-state connectivity in groups with bothersome and non-bothersome tinnitus against age (but not hearing) matched controls. They found a negative correlation between auditory and visual cortex in the bothersome group only. The first reported study using ICA based methods found reduced connectivity between left and right AC in the tinnitus group (Kim et al., 2012), but a subsequent study using near-identical methods but matching the controls for hearing loss found no differences of any kind between tinnitus and control groups (Davies et al., 2014). However, a more recent study used a different metric to quantify interhemispheric connectivity, and found the degree of interhemispheric correlation in AC to correlate positively with the presence of tinnitus, and its distress and duration, even after correction for hearing loss and other subject variables (Chen et al., 2015). One study used both ICA and seed based methods to compare tinnitus patients to hearing loss matched and normal hearing controls (Schmidt et al., 2013). The ICA analyses found abnormal connectivity within the default mode network (DMN) (Raichle et al., 2001), in the medial prefrontal cortex in both tinnitus and hearing loss groups, and in IPC in the tinnitus group only. The seed-based analysis showed a different pattern of results, with tinnitus patients showing connectivity increases between auditory and PHC compared to normal hearing controls, between PHC and the dorsal attentional network compared to hearing loss controls, and decreases between the precuneus and the DMN compared to both control groups. Another pair of studies, by the same group, used differing methodologies to compare equivalent patient populations (i.e. tinnitus patients and normal hearing controls). An ICA-based analysis (Maudoux et al., 2012) found numerous differences, including increased connectivity in the brainstem, basal ganglia, cerebellum, parahippocampal, parietal and sensorimotor cortex in the tinnitus group, and various decreases). The analysis using a variant of ICA-based network selection, based on graph theory, compared tinnitus patients to healthy controls, and found increased connectivity between AC and PHC. Therefore increased connectivity between AC and PHC has been observed in three separate studies with different methodologies, one with correction for hearing loss, but not in some other studies. The significance of this finding is not fully clear, but is consistent with other studies, both resting-state EEG and tinnitus manipulation-based PET, highlighting involvement of this area.

1.3.10 Structural brain changes

In addition to the possibility of abnormal ongoing activity in the auditory pathway being responsible for tinnitus, there has been a number of studies examining whether structural changes in auditory or non-auditory areas might be associated with tinnitus. The predominant methodology used has been voxel based morphometry (VBM) (Ashburner and Friston, 2000), which warps individual subjects' T1 weighted structural magnetic resonance imaging (MRI) images to conform to a common template, segments the images into GM, white matter (WM) and cerebrospinal fluid (CSF), then tests for group differences in tissue composition. However, some studies, alternatively or additionally, have measured cortical thickness as a metric of structural changes. An initial study compared tinnitus patients with clinically normal hearing to controls matched for age and sex, but not hearing (Mühlau et al., 2006), and found tinnitus patients had GM increases in MGB, and decreases in the subcallosal cingulate region. A later study by the same group, this time using tinnitus with marked hearing loss and normal hearing controls, replicated this finding (Leaver et al., 2011). Yet another study by the same group (Leaver et al., 2012) compared tinnitus patients to hearing impaired age-matched controls, though the controls had better hearing thresholds by an average of 8 dB. This study again replicated the GM losses in the same approximate region, though this time in the adjacent vmPFC region, rather than the subcallosal cingulate. Cortical thickness in the subcallosal cingulate region itself was correlated with anxiety and depression scores. The study also found that tinnitus-related distress correlated with cortical thickness in the anterior insula. However, a study using tightly-matched controls for hearing loss (Melcher et al., 2013) found no differences attributable to tinnitus specifically, including in a subcallosal/vmPFC region of interest (ROI). What the study did find was that GM loss in the subcallosal region was correlated with hearing loss at frequencies above 8 kHz, which had not previously been measured in structural studies. Supra-clinical hearing loss also correlated with structural changes in posterior cingulate and dorsomedial prefrontal cortex. Six further studies, with and without the use of control groups (some of which were matched for hearing loss), have not found any structural changes in the subcallosal region attributable to tinnitus, and their positive findings were as follows. Reduced volume of A1 (corresponding to all frequencies in tonotopic axis) was associated with both tinnitus and hearing loss (Schneider et al., 2009). Tinnitus patients were found to have reduced GM in right IC and left hippocampus

compared to hearing matched controls (Landgrebe et al., 2009). GM decreases in anterior cingulate, medial frontal gyrus and superior temporal gyrus (STG) were found to be associated with hearing loss but reversed by the presence of tinnitus, in that they were found in a non-tinnitus hearing loss group compared to both normal hearing and tinnitus groups (Husain et al., 2011). Another study comparing these three group types found that both hearing loss groups, irrespective of tinnitus, had GM increases in middle and superior temporal gyri, and only a ROI analysis showing increased GM in A1 attributable specifically to tinnitus (Boyen et al., 2013). Two large correlational studies each including over 200 patients, but examining only tinnitus patients, found the following: tinnitus distress correlated with GM loss in Heschl's gyrus (HG) and auditory insular regions, even after partialling out the effects of age and hearing loss (Schecklmann et al., 2013b); no significant correlations were present with any tinnitus variables, except a correlation in the cerebellum with tinnitus duration and distress (Vanneste et al., 2015). This latter study also correlated brain structure with spontaneous source space EEG oscillations, and found no significant correlations between the two measures.

In summary, the various studies of brain structure in tinnitus have focused on auditory regions and subcallosal regions. Changes in auditory regions have been variably observed (often only in ROI analyses), occurred in both directions, and appear to relate more to hearing loss than tinnitus. Subcallosal changes have been observed only by one group, though repeatedly, and never in a study well-controlled for hearing loss. The one study by another group finding changes in this area found these to relate to supra-clinical frequency hearing loss and not tinnitus. The overall synthesis of these findings is that there is no convincing evidence of any brain structural abnormality that is consistently associated with tinnitus, and also that brain structure does not appear to have any impact on ongoing brain oscillations relevant to tinnitus.

1.3.11 Predictive coding

While this thesis examines brain bases for abnormal auditory perception in tinnitus, there are aspects of normal auditory perception relevant to tinnitus that remain controversial. One such model of perception which is gaining substantial popularity, due to multiple converging lines of evidence, is *predictive coding*, which is introduced here before proceeding to a discussion of how it might help to explain tinnitus. It has been apparent for some time that perception is not simply the unidirectional processing of information from

out sensory organs, but is shaped heavily by prior experience and expectation, at both conscious and unconscious levels. Well-recognised phenomena in stimulus-evoked brain responses such as repetition suppression, priming and MMN require such a framework in order to be explained. Furthermore, omission of expected stimuli elicits brain responses that are in many ways similar to presentation of those stimuli (Fujioka et al., 2009). Generative accounts of perception propose that the brain creates, maintains and tests internal models of the environment. Furthermore, they state that observed brain responses relate to the testing and updating of these models, rather than the content of perception *per se*. In predictive coding (Rao and Ballard, 1999; Friston et al., 2006; Friston and Kiebel, 2009), perceptual systems are organised hierarchically, with each level communicating with the levels immediately above (forward or bottom-up connections) and below (backward or top-down connections) it. Backward connections convey predictions, or changes to existing predictions, and forward connections convey prediction errors, which are discrepancies between predictions and bottom-up sensory representations. Prediction errors may be reconciled by modifying internal models of the environment, or by acting in such a way as to change the way the environment is sampled (Friston et al., 2006). Sensory perception is more concerned with reducing prediction errors by changing internal models. At each level of the hierarchy, the two factors being compared are the (top-down) *prior* (prediction), and the (bottom-up) *likelihood*, the latter representing ascending sensory information. Each of these, mathematically, constitutes a probability distribution (over some dimension of perceptual space) characterised by its mean and *precision* (inverse variance). The discrepancy between the two distributions is the prediction error, one formulation of which is *surprise*, which is defined as the negative log probability of the likelihood distribution (its mean value) based on the prior. Surprise takes into account the precision of the prior, whereas a more generic formulation of prediction error need not necessarily do so. Overall inference at each hierarchical level (the *posterior*, which balances prior predictions and new sensory information) is based on comparison of the prior and the likelihood, each weighted by its precision. Precision may be determined both by stimulus properties (*actual* precision) and by internal beliefs about the reliability of the information (*estimated* precision). Weighting is also influenced, by the significance of a given event or object, for instance the reward or danger associated with it. The system aims to minimise surprise in the long term (Friston et al., 2006), which in the context of perception is generally achieved by optimising internal models of the environment by

making them maximally correspond to sensory input. Thus, prediction errors often result in changes to predictions, particularly when the sensory environment is unstable. In a stable situation, an equilibrium is reached where predictions are optimised and prediction errors are minimised. In the face of noisy, sub-optimal or missing sensory input, the precision of the likelihood is low, and therefore the posterior inference is dominated by the prior prediction, which has relatively higher precision. Conversely, attention is explained in these frameworks as an increase in the precision of bottom-up sensory representations, mediated by cholinergic activity increasing the gain of superficial pyramidal cells (Moran et al., 2014), thereby biasing perception towards the ascending sensory input. Theoretical models of predictive coding based on the functional unit of neocortex, the canonical microcircuit (Haeusler and Maass, 2007), have identified suitable neuronal architecture for performing and conveying the operations necessary for predictive coding (Bastos et al., 2012). This theory predicts that superficial pyramidal cells (in the supragranular layers) encode prediction errors, manifest as gamma band oscillations, while predictions are encoded by deep neuronal population (in the infragranular layers), and manifest as beta band oscillations. Prediction errors are conveyed to higher levels, while predictions are conveyed to lower levels. Evidence for these theories is largely indirect, and includes the following: layer resolved recordings showing the segregation of gamma and sub-gamma frequency responses to supra- and infra- granular layers respectively, with antagonism between the two (Spaak et al., 2012); feed-forward connections occurring in the gamma band, and feed-back in lower frequency bands (Fontolan et al., 2014; van Kerkoerle et al., 2014); gamma responses correlating with the unexpectedness or incongruence of sensory stimuli (Arnal et al., 2011; Brodski et al., 2015); beta rebound responses to omission of expected auditory stimuli (Fujioka et al., 2009). For review, see (Arnal and Giraud, 2012).

There are several reasons why it is an attractive prospect to try and explain tinnitus in a predictive coding or equivalent framework, as has been proposed (De Ridder et al., 2012, 2015b). Firstly, these frameworks seem to offer the best account for the range of brain responses seen in normal perceptual systems, therefore if normal perception operates in this manner then phantom perception (e.g. tinnitus) probably does too. Also, given the prominent involvement of PHC in tinnitus networks, it has been proposed that tinnitus and phantom limb pain may arise due to ‘filling in’ of missing sensory information from memory (De Ridder et al., 2011a). This idea fits neatly into predictive coding frameworks,

by stating that precision of sensory input is lowered in deafferentation, and that relevant memory circuits therefore generate predictions based on past experience, which dominate perception due to their relatively higher precision than the sensory input. Additionally, because in these frameworks observed neural oscillations represent only changes to the perceptual system, not the percept itself, any given correlate (e.g. gamma oscillation magnitude) can potentially correlate with the percept in paradoxical or opposite ways, depending on the context (De Ridder et al., 2015b), making such a model easier to reconcile with the highly inconsistent literature on neural tinnitus correlates. Other points include that a predictive coding-based perceptual system could theoretically generate tinnitus without showing any measureable differences versus a system without tinnitus, provided both systems were in steady state, and also that predictions and their estimated precision can be influenced by a variety of psychological factors, thereby offering a potential explanation of how these factors impact upon tinnitus perception. Presently-proposed predictive coding or equivalent models of tinnitus (De Ridder et al., 2012, 2015b; Roberts et al., 2013) thus offer the potential to explain certain paradoxes in the experimental tinnitus literature, but presently are under-specified in their level of detail, and fail to account for certain observations with respect to tinnitus. This issue is discussed further in Section 1.5.

1.4 Unresolved paradoxes in tinnitus research

While there has been extensive research into tinnitus mechanisms, in both humans and animals, at all levels of the auditory pathway and beyond, including structural, metabolic, neurochemical and neurophysiological markers, there are several major paradoxes remaining that have not been explained, including:

1.4.1 No neural correlate separates tinnitus patients from matched controls

The situation remains that not even one candidate process or mechanism has been identified that consistently differs between tinnitus patients and controls matched for age and hearing loss. Furthermore, whatever the processes underlying tinnitus are, and wherever they occur, they should have a signature that is present in SA within the auditory system. Given the significant peripheral dependence of the central activity underlying tinnitus, it is likely that the spontaneous precursors of tinnitus should be present throughout the whole auditory pathway as well. As auditory perception is widely assumed to involve

AC, even if it also has to involve wider cortical areas, it seems reasonable to assume that even if tinnitus originates subcortically, it should still have a detectable signature in AC.

1.4.2 Variable relationship with closest correlates

The cortical correlates of tinnitus that have previously been proposed (delta/theta and gamma oscillations) do not have a consistent relationship with tinnitus across subjects, in the context of short-term tinnitus manipulations. Furthermore, gamma oscillations appear to have a paradoxical relationship with tinnitus intensity, being positively or negatively correlated depending on the manipulation used (Sedley et al., 2012a).

1.4.3 Variable dissociation of hearing loss and tinnitus

In humans, only certain cases of hearing loss ever result in tinnitus, and the onset of tinnitus, perceptually, is often significantly separated in time from the underlying hearing damage, meaning that additional processes must sometimes need to operate for tinnitus to be caused. Precipitating processes are often psychological, or related to general physiological state, yet once these factors are removed, tinnitus generally persists. Conversely, in animals, tinnitus behaviour begins immediately after the auditory insult, and appears to generally be present in every animal exposed. Given the controversies in the validity of certain animal models, one must consider that the behavioural tests for 'tinnitus' may actually be measuring precursor processes rather than perceived tinnitus.

1.4.4 Most people have a degree of chronic tinnitus

Tinnitus, to a minor extent, is experienced by the majority of healthy, normal hearing adults, if they are in a sufficiently quiet environment, and if they perform orofacial movements. Therefore tinnitus models must not absolutely require cochlear or any other pathology, but can only include this as an exacerbating factor. The other alternative is that if, strictly speaking, the majority of adults have a degree of hearing damage, and tinnitus only requires this 'normal' level of hearing loss.

1.4.5 Peripheral and central origins

Initially, tinnitus seems to be dependent on SA in the auditory periphery, and later to be dependent predominantly or solely on activity in the central auditory system. Therefore, models relying on the thalamus or cortex as the primary generator of the signal that drives

tinnitus can only ever be a partial explanation, and require an additional peripheral model that produces the same phenomenology.

1.5 Shortcomings of current models

While all tinnitus models discussed so far and to be discussed, show considerable merit, and may well correctly explain certain aspects of tinnitus mechanisms, a comprehensive model must be able to account for all the above paradoxes, and presently such a model has not been proposed. A host of models has been proposed to explain how SA in the ascending auditory pathway is amplified by gain mechanisms (Schaette and Kempter, 2006; Noreña, 2011; Schaette and McAlpine, 2011), which can easily be extended to encompass enhanced neural synchrony and other forms of plasticity. However, these models ultimately require that this enhanced SA needs to be propagated to AC (and beyond), in which case there should be some measurable abnormality that separates tinnitus patients/animals from tightly-matched controls. As explained in the previous sections, evidence of such a correlate is presently lacking, despite numerous attempts to define one. Furthermore, the closest candidate correlate for the tinnitus percept, AC gamma oscillations, behaves paradoxically with respect to short-term modifications in tinnitus intensity, in a way that is inexplicable by existing models. As discussed previously, the possibility of a predictive coding based model of tinnitus, building on the TCD model, has been suggested (De Ridder et al., 2012, 2015b), in which deafferentation causes the 'missing' central auditory representations to be filled in by neighbouring cortical representations or from auditory memory; while attractive in many ways, these initial attempts are unable to resolve several of the above paradoxes for the following reasons. They require a total independence of central tinnitus-related activity from peripheral activity, and homeostatic gain increases in the ascending auditory pathway (which are strongly suggested by extensive evidence) would actually reduce the cortical deafferentation that prompted the filling in process. They predict increased delta/theta oscillations in tinnitus, driven by the hyperpolarised thalamic state, and rely on these to trigger the cortical activity underlying tinnitus perception; however increased delta/theta oscillations are not observed in tinnitus patients as a whole once hearing loss is controlled for. Because they explain gamma oscillations as a prediction error signal (mismatch between prediction and sensory input or SA), they allow opposite relationships between gamma oscillations and tinnitus intensity (i.e. if tinnitus increases or decreases from its

prediction, which corresponds to baseline intensity, then gamma-mediated prediction errors will increase), however they predict such changes in the opposite direction to what has actually been observed (in that gamma generally decreases when tinnitus deviates from its baseline state). A similar prediction-based explanation of tinnitus, but in this case driven by persistent bottom-up attention, has also been proposed (Roberts et al., 2013). This model is based on a central origin to the tinnitus percept, arising in non-primary AC and/or auditory memory centres (perhaps due to previous auditory experiences). This central representation corresponds poorly to ascending inputs, which are diminished due to cochlear pathology, and persistent auditory attention is recruited to resolve the discrepancy, which only amplifies the central representation further. This model is also very attractive, and the multifaceted influences on attention can potentially explain diverse aspects of tinnitus phenomenology via a single converging mechanism. However, like the predictive coding based model, this account requires a total independence of the central tinnitus-related activity from the ascending auditory pathway and periphery. Furthermore, both models require a significant void of peripheral auditory input, and therefore struggle to explain tinnitus in the presence of minimal hearing loss, and the 'normal' tinnitus experienced by the majority of normal-hearing individuals in quiet enough environments. Another aspect that is hard to reconcile with the phenomenology of tinnitus is that these models propose that directed attention strengthens the centrally-generated tinnitus representation at the expense of the (compromised) peripheral input. However, in normal sensory systems, attention biases perception towards the peripheral representation by increasing the gain on thalamocortical connections. The concept of 'misdirected' attention has been proposed in the context of functional neurological symptoms (also called 'hysterical' or 'psychosomatic' disorders), whereby attention is applied to the consequences of the symptom, not to the sensation itself, and therefore reinforces maladaptive internal predictions (Edwards et al., 2012). However, this describes a psychological/psychiatric pathology that is applicable to only a small minority of individuals, and has particular correlates in terms of personality traits. Given the high prevalence of tinnitus, and the identification of particular psychological and personality traits only in highly-distressed tinnitus patients (as discussed earlier), tinnitus must be explicable within a normal psychological framework, though misdirected attention could theoretically apply to explain a minority of severe cases. Finally, these models stop short of explaining how the process of phantom perception actually arises within the specified

framework, and instead begin with the assumption that a fully-formed tinnitus-like percept exists already in the brain, and simply needs to 'fill in' a gap left in AC due to deafferentation, but do not explain the origin of this representation. More generally, certain models can potentially explain diverse aspects of tinnitus phenomenology, including the sound itself, attention, emotional, cognitive and autonomic reactions, but are far from complete, on account of not being linked to specific neurobiological processes (Jastreboff, 1990; Searchfield et al., 2012), or by including ever-increasing numbers of brain processes, regions and networks to incorporate these functions, without specifying the details of how tinnitus is actually generated and manipulated within such a framework (De Ridder et al., 2013).

Chapter 2. Aims

The broad aim of this body of enquiry was to work towards a model of tinnitus capable of accounting for all the paradoxical aspects described in the previous sections. Specifically, the experimental approaches taken aimed to satisfy as many of the following criteria as possible:

- Studies in humans, where all subject variables not directly relating to perceived tinnitus could be controlled (e.g. age, hearing loss, hyperacusis)
- The inclusion of hearing loss as a variable, and controlling this between groups
- The separation of current from baseline tinnitus loudness, in order to disentangle fixed predictors of loudness from factors affecting current state (i.e. a 'state-trait' distinction)
- The use of direct brain recordings from human tinnitus patients where possible, in order to maximise signal to noise ratio (SNR) and spatial localisation accuracy
- Measurements of neurochemical concentrations, particularly GABA, from human AC
- Explicit linking of neuronal oscillations to the processes involved in predictive coding

A number of hypotheses were tested in the execution of these experiments, including that:

- Tinnitus patients would show neurochemical evidence of relatively decreased inhibition compared to controls, manifest as either absolute reductions in cortical GABA concentration, and/or a negative concentration between GABA concentration and tinnitus loudness
- Gamma oscillations may reflect a signature of local inhibition, in which case they should either be reduced in tinnitus, or have a negative relationship with state or trait tinnitus loudness
- Gamma oscillations may reflect prediction errors, or a related process, rather than an inhibitory process
- Tinnitus might be associated with altered cortical acetylcholine (ACh) concentration, reflective of abnormalities of attention and/or perceptual weighting of sensory information

Chapter 3. Generic methods

Certain methods used herein are applicable to multiple individual experiments, and thus are discussed in detail here, and briefly referred back to in the respective experiments.

3.1 Spectral and time-frequency analysis of local field potentials and MEG/EEG data

LFPs reflect the synchronised ensemble activity of large numbers of neurons, recorded from a sufficiently large distance from any individual neuron that it does not dominate the recording. Contributing neurons must be oriented the same way, such that their activity is summed rather than cancelling itself out, and must fire with a common periodicity on order that the ensemble activity varies meaningfully over time. LFPs are influenced by axonal and synaptic activity, both of which are transmitted from source to recording site through volume conduction. EEG measures ensemble electrical activity from outside the scalp, which is thus volume conducted over a large distance, and is attenuated and spatially smeared as it passes through the skull. MEG measures magnetic fluctuations resulting from locally synchronised neuronal activity at sensors outside the head. The magnetic field fluctuations pass unimpeded through the skull, unlike EEG. Also, magnetic fields generated by electrical activity project perpendicularly to electrical potentials, making MEG only sensitive to sources not oriented radially to the brain's outer surface. Both EEG and MEG can only detect sources that operate as equivalent current dipoles. Action potentials do not behave as dipolar sources, and instead these modalities record excitatory and inhibitory post-synaptic potentials.

Despite their differences, intracranial EEG (iEEG) measuring LFPs, EEG and MEG all measure the synchronous ensemble activity of large numbers of neurons. Brain activity of this sort comprises ongoing oscillations within a number of frequency bands. The bands most commonly studied include delta (1-4 Hz), theta (4-8 Hz), alpha (8-12 Hz), beta (12-30 Hz) and gamma (>30 Hz). Note that precise definitions vary, and these bands are often subdivided, particularly the beta and gamma bands. Any experimental effects of interest are generally very small in comparison to the much larger ongoing brain activity in these frequency bands, and thus specific techniques exist to extract these effects.

Early techniques involved quantifying effects by conducting a number of 'trials', and averaging the brain activity within each trial. This has the effect of averaging out all

ongoing brain activity not related to the experiment, and highlighting activity that has a time-locked relationship to the experimental stimulus or event. Such recordings are known as event-related potentials (ERPs) or evoked potentials. While ERPs have many advantages, such as a high SNR, it is understood that many responses to experimental events are not rigidly time-locked to the stimulus, but instead represent an interaction of the event with ongoing brain rhythms. These effects, known as 'induced' responses, are not detected in ERPs. Additionally, where no experimental event exists (e.g. in the study of spontaneous brain activity), ERPs cannot be calculated at all. The study of spontaneous or induced brain activity requires the quantification of brain activity within specific frequency bands, and is termed 'spectral' analysis. Induced responses also require brain activity to be quantified within specific time windows with respect to the event, in a process termed 'spectrotemporal' or 'time-frequency' analysis. Both approaches involve transforming the recorded time series into the frequency domain, with the difference being that this is done for the whole time series in spectral analysis, and for multiple subdivisions of the time series in spectrotemporal analysis. Various methods exist for transforming data into the frequency domain, including the Fourier and wavelet transforms, but ultimately they produce similar results, with the main difference being the exact pattern of signal leakage between frequencies. Of greater impact than the method used is the trade-off chosen between time resolution (samples per s) and frequency resolution (samples per Hz); in that the product of these cannot exceed 1. Thus, a researcher must decide how to optimally balance these for the specific data being analysed and research question being addressed. In Fourier-based analyses, time and frequency resolutions are determined by the length of time window used for analysis, with a Fourier transform being performed for each time window. Data are generally tapered before Fourier transformation, for example by applying a Hanning window, to smooth the edges and hence reduce leakage between frequencies. In wavelet based methods, a family of wavelets is created, with a wavelet being a complex sinusoid of a specified frequency, multiplied by a Gaussian function. One wavelet is created per desired frequency, and the time/frequency resolution is determined by the width of the Gaussian function applied. The wavelets are then sequentially time shifted and convolved with the time series to yield spectrotemporal data. In both kinds of methods, one can have overlap in time or frequency points sampled (e.g. by having time windows or wavelet frequencies overlap), and thereby obtain output data with as high a time and frequency resolution as desired. However, this amounts to oversampling, which

does not add any actual information, but just affects the results aesthetically. Output results from any spectral or spectrotemporal analysis are complex, in that they contain both a real and imaginary component. A complex data value can be represented as a point in two-dimensional Cartesian space with the origin at (0,0), and each dimension taking either a positive or negative value. A more intuitive and useful representation is in polar coordinates, where each point is represented by its phase (angle with respect to the origin) and amplitude (distance from the origin). In a polar representation, a time series can be represented in a cylindrical space, and in the case of a sinusoidal time series the amplitude remains constant while the phase rotates around the origin over time. Thus, in cylindrical space a sinusoid takes a helical path, as opposed to the more familiar sinusoidal shape in two dimensional space that only considers time and the real component. Analysis of the strength of activity in a particular frequency band (which can be influenced by either the magnitude of underlying neural activity, and/or the degree of synchronisation between neurons) is performed by just taking the amplitude values and discarding phase information. These values are sometimes squared to represent power, and are sometimes subsequently log transformed to normalise the values. If averaging across trials (or regression against an experimental parameter) is performed before converting to amplitude, then the evoked response is obtained, as only activity with consistent phase across trials will remain (plus a small amount of residual noise). Conversely, if conversion to amplitude or power is performed before averaging over trials then total amplitude/power is obtained. The term 'induced' is often used to refer to the remaining amplitude/power after the evoked response has been subtracted. As well as contributing to the evoked response, phase information can be used to infer communication between anatomically separate brain regions. One such measure used herein is the phase locking value (PLV). PLV values range from 0 to 1, and indicate the consistency of the phase relationship between two different time series (here the data from two different brain sites) sampled at the same time-frequency point(s). A value of 1 (perfect consistency) is still possible even if there is a phase difference between the two signals, as long as that phase difference is consistent over time or across trials. Both Fourier and wavelet based, plus amplitude and phase based, analyses are used in the experiments described herein, with the particular analysis determined by the dataset under analysis.

3.2 Source space projection of MEG data

MEG samples brain activity at a number of sensors outside of the head: 275 in the setup used in these experiments. While it is straightforward to process the sensor data directly, interpretation of results is problematic for a number of reasons. Firstly, the majority of signal at the sensors does not originate within the brain. Non-brain sources include intrinsic noise in the sensors, environmental electromagnetic activity, ocular, muscular and cardiac activity. While the physical design of modern MEG setups reduces environmental activity significantly, other sources, particularly muscle artefacts, are less straightforward to remove from the data. Secondly, the position of each subject's head relative to the sensors is different, therefore there is no direct correspondence of activity recorded at any particular sensor between subjects. Thirdly, the magnitude of activity is influenced by head size (larger heads have brain tissue closer to the sensors which therefore gives a stronger signal) and position. Finally, any results obtained cannot be attributed to specific brain areas, limiting the usefulness of the results. Issues of muscle artefact are very important in resting-state studies of brain activity comparing patient populations, as even small differences in arousal, mood, attention, apprehension, or chronic symptoms could manifest as small differences in resting muscle tone, which would have large effects on sensor data. A complete or partial solution to all of these problems is to project brain activity into source space, i.e. to use the sensor data to make inferences about activity within specific brain locations.

As mentioned previously, sources of brain activity can be modelled as equivalent current dipoles, with a particular strength (or 'moment') and orientation. For a given brain location and dipole orientation, the pattern of projection to the MEG sensors can be calculated quite precisely and easily. Information required is the size and shape of the subject's brain (which can be obtained from their MRI scan, or estimated using a template), the volume conduction properties of brain tissue, the position of their head relative to the sensors, the location of interest within the brain, and the strength of activity at that location. This pattern is known as the lead field, and calculating it is known as solving the 'forward problem'. Less trivial is the 'inverse problem', which is how to use the pattern of activity recorded at the sensors to infer the location and pattern (e.g. time-frequency profile) of brain activity that caused it. Theoretically, the inverse problem has no unique solution, and infinite possible solutions for each instance of the problem. However, there are widely-used approaches to solving the problem, which each allow a unique solution to be reached through the use of certain assumptions. Broadly speaking, approaches are sparse or

distributed (sometimes termed ‘volumetric’). In sparse solutions, the brain activity of interest (either all the activity, or a contrast between brain states) is modelled using a limited number of dipoles, with the number, locations, orientations and moments of these dipoles as free parameters which must be optimised using an appropriate algorithm such as to best fit the sensor data. Distributed methods divide the brain into a large number of sources (typically with 2 or 3 dipole orientations at each), and assume that each source makes a contribution to the signal measured at the sensors. One such approach, known as ‘beamforming’ (Van Veen et al., 1997; Gross et al., 2001), uses the assumption that sources of brain activity are not correlated with each other over long distances (though in reality the method is robust to most correlations within the physiological range). For each brain location, the covariance matrix of the sensor data (or its frequency domain counterpart, the cross-spectral density matrix) is used in conjunction with the inverse of the lead field in order to create a spatial filter that converts sensor data to activity at a particular source, by taking a weighted contribution from each sensor. By incorporating the covariance matrix, the filter is optimised to the subject’s own data, and prioritises the contributions from sensors that better match the lead field from a particular location, and greatly reduces the influence from non-brain sources of activity. Disadvantages of beamforming include insensitivity to highly correlated sources, occasional difficulty resolving extremely strong sources (spatial resolution is related to signal strength, and very strong sources can appear so small as to be missed with the spatial sampling used), and decrease in performance in the face of inaccurate lead field estimation (for instance with errors in co-registration between MEG and MRI data, or due to excessive head movement within the MEG recording).

3.3 Non-parametric analysis of large, multivariate datasets

MEG, EEG and iEEG datasets are often particularly rich in information. For instance, even just the analysis of spontaneous brain activity can involve thousands of source locations, each with activity measured at multiple frequency bands. When a time dimension is also included, in event-related experiments, the number of observations is increased several-fold. Where communication between different brain regions is measured (within different frequency bands, and often at different time points), the number of potential comparisons can become very large indeed (for instance, 1000 brain locations by 1000 brain locations by 8 frequencies by 8 time points, giving 64,000,000 points in data analysis space). On top

of computational demands, two main issues arise from this situation: how to appropriately correct for this large number of comparisons, statistically, and how to maintain statistical sensitivity to experimental effects. More conservative measures of multiple comparison correction, such as the Bonferroni method, assume independence between the multiple tests used. Clearly this is not the case in multivariate brain data sets, where neighbouring spatial, time and frequency points often show similar trends, and where there is dependence between observations, conservative measures incur an inappropriately heavy penalty. A commonly employed solution is to use a permutation approach (Maris and Oostenveld, 2007). In this method, the data analysis is repeated for each of a large number of permutations (typically 1000 or more), with the difference that in each case a shuffling process is performed. This is often across trials (e.g. by randomising the trial category labels), but can theoretically be any kind of shuffling that abolishes the relationship with the experimental parameter under study while preserving other important data relationships. A particular method of quantification is performed in each permutation, which is at the experimenter's discretion, so as to give a single or maximum statistic for each permutation. The permutations are then sorted according to the value of this statistic, and a threshold for significance set according to the appropriate point on this distribution (e.g. for $p < 0.05$ corrected, with 1000 permutations, the threshold would be the 50^{th}-largest statistic). The method of quantification used for each permutation, and for the actual data, can potentially be anything, provided it is consistently applied, but common approaches include the following: 1) taking the largest single value in each permutation, then all points in the actual data exceeding that value are considered significant – this method is relatively conservative, with the advantage of strong confidence in positive results obtained, but the disadvantage of relative insensitivity to large, flat areas of experimental effects; 2) identifying contiguous clusters of activation within the data space, based on neighbouring points exceeding an arbitrary threshold – this method can potentially be over-inclusive, in that some peripheral parts of significant clusters might not 'truly' be significant in and of themselves, but it has the advantage of having sensitivity to large flat areas of activation, and rewards consistency across regions of brain/time/frequency space, which may reflect the character of brain activity. Both methods are appropriate, and are inherently corrected appropriately for multiple comparisons, and the choice of a particular method should be determined by the characteristics of the dataset and the particular research question. In the experiments described herein, both methods are used.

Chapter 4. Direct neurophysiological recordings of core tinnitus processes

This work exploited a rare opportunity to directly study electrophysiological brain activity associated with tinnitus, in a patient undergoing invasive electrode monitoring for incidental focal epilepsy. The experimental facility was set up and maintained by the Human Brain Research Laboratory team at the University of Iowa. The neurosurgical team within this group recruited the patient and performed the surgery. Clinical audiological testing was performed by Dr Rich Tyler and Dr Phillip Gander. Experiments were designed and coded by me, and run by Dr Gander. Data analysis methods were planned and implemented by me. This work has now been published in Current Biology (Sedley et al., 2015).

4.1 Aims

Working with this patient provided a unique opportunity to obtain brain recordings of tinnitus that combined: high temporal resolution, high spatial resolution, precise anatomical localisation, high SNR, contemporaneous subject report of tinnitus phenomenology. The principal aim was to test existing models of tinnitus against empirical evidence of significantly greater sensitivity and detail than had been previously possible. In particular, the model of TCD (Llinas et al., 1999; Llinas et al., 2005; de Ridder et al., 2015) predicts delta/theta oscillations to occur in regions of hearing loss, and gamma oscillations to occur at the cortical 'edge' regions between abnormal delta-manifesting areas and normally functioning areas. The high spatial resolution would allow this hypothesis to be explicitly tested. A related assertion that could be tested was that tinnitus correlates are limited to tonotopic cortical areas corresponding to the tinnitus frequency (i.e. that frequency-matched tones might be a viable surrogate marker for tinnitus), as again the high spatial resolution would allow this to be examined. Finally, the previous findings of gamma oscillations correlating positively or negatively with tinnitus intensity, depending on the manipulation used (Sedley et al., 2012a), are at odds with current models of tinnitus proposing gamma oscillations as an intensity code of tinnitus. As these results were derived using a beamformer source reconstruction, which theoretically can be blind to

heavily correlated but anatomically separated sources, corroboration of these findings with direct recordings would lend support to the validity of the results.

4.2 Methods

As this was a study of a single case, the most crucial aspect of any experiment conducted was to be able to create a within-subject contrast of tinnitus loudness or intensity. There are a limited number of ways to achieve this, which include the following: exploit spontaneous variations in tinnitus intensity (these were sought, but did not occur); manipulate tinnitus pharmacologically, such as with intravenous lidocaine (this could not safely be done in an epileptic patient); use orofacial sensorimotor stimulation to modulate tinnitus (this creates very large electrophysiological artefacts); use cortical electrical stimulation (this was attempted in limited time available, but did not succeed); use acoustic stimulation, i.e. RI or RE. Pre-implantation psychophysics was performed, using acoustic masker stimuli, and RI was found to be modestly successful, thus this was used as the basis of actual experimentation.

4.2.1 Subject and clinical case study

The subject was 50 years old, male and left-handed, with left hemisphere language dominance confirmed by Wada test. He had moderate-severe high-frequency hearing loss bilaterally, as the result of noise trauma from handgun firing recreationally. His tinnitus had been present for 15 years, was described as tonal in character, and was bilateral and symmetrical. It had begun gradually, and remained constant perceptually over most of the 15 year period since its onset. Frequency matching revealed a 5 kHz frequency to his tinnitus, and loudness matching a 24 dB HL loudness, based on a 500 Hz tone. Minimum masking level, using speech-spectrum noise was 54 and 60 dB in left and right ears respectively. These audiometric data are shown in Figure 2.

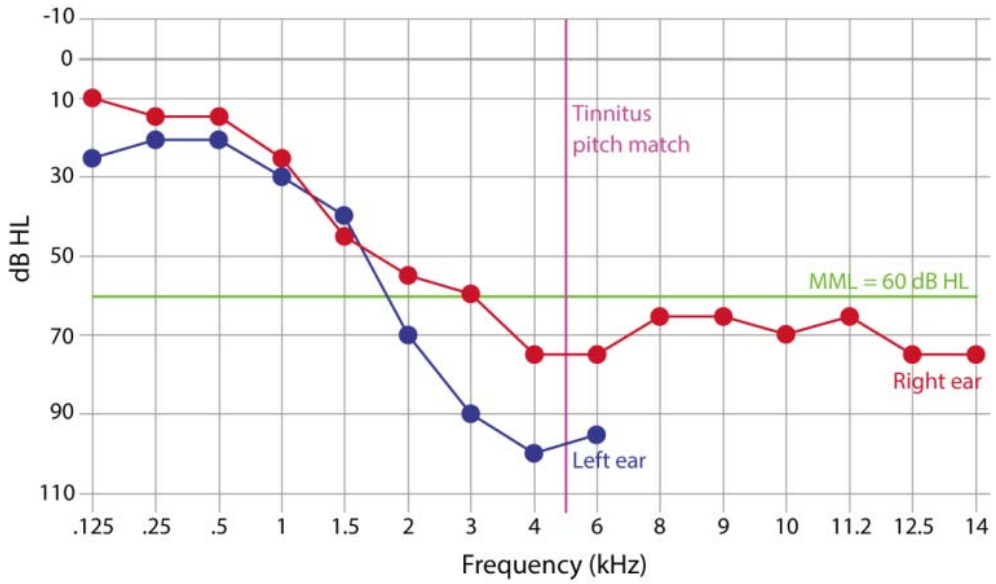

Figure 2: Audiometric profile of the subject
Red and blue plots indicate pure tone thresholds for right and left ears respectively. MML = minimum masking level, in the right ear, using noise with a speech-shaped spectrum.

His Tinnitus Handicap Inventory (THI) (Newman et al., 1996) score was 20, corresponding to 'mild' tinnitus severity.

The subject's epilepsy had begun when he was 10 days old, and took the form of complex partial seizures, which did not feature an auditory aura. Due to sub-optimal seizure control on various anticonvulsants, most recently levetiracetam monotherapy, he underwent two weeks of invasive electrode monitoring, prior to resection of the presumed location of seizure onset. He did not have any seizures during the first week of monitoring, so his levetiracetam was discontinued for the second week in order to try and provoke a seizure. The experiments described herein were performed during this second week, during which he took no medications. No seizures occurred during the second week either, so subsequently a subtle congenital malformation in the left posterior inferior temporal lobe was resected.

4.2.2 Recording setup

iEEG data were recorded from 164 intracranial electrode contacts (Ad-Tech Medical Instruments, Racine, WI). 18 of these contacts on depth electrodes, placed along left HG (which included A1), into left anterior and posterior temporal lobes, the cortical malformation, and right anterior temporal lobe. 146 electrodes were on subdural grids and

strips, covering most of the temporal lobe convexity, inferior temporal lobe, temporal pole, parts of parietal, occipital and sensorimotor cortex on the left, and the temporal pole and PHC on the right. Electrode numbering, from 1 to 250, was based on connection position to the amplifier (Tucker Davis Technologies, Alachua, FL), and some connections were left empty. Signals were recorded at 2034 Hz, with a bandpass of 0.7-800 Hz, and downsampled to 1 kHz offline. Electrical noise was removed by notch filtering.
Experiments were run from a computer in a dedicated research room, using functions from the Cogent 2000 (Wellcome Laboratory of Neurobiology, London, UK) toolbox for Matlab (MathWorks, Natick, MA). Auditory stimuli were generated at a 44.1 kHz sampling rate, and presented via insert headphones (ER4B; Etymotic Research, Elk Grove Village, IL).

4.2.3 Auditory response characterisation

In order to establish responses to normal auditory stimuli, and those matched to tinnitus, the following stimuli were presented passively, in separate experiments:
1) 125 repetitions of a 1 s duration tone of 5 kHz carrier frequency (his tinnitus frequency match). This was loudness matched to a 55 dB tone at a relatively normal hearing frequency (1 kHz). A 40 Hz sinusoidal amplitude modulation was applied to the tones, in order to be able to characterise both onset and steady-state responses at the tinnitus frequency.
2) 50 repetitions of each of two types of click train: one with 100 Hz click rate and the other with 25 Hz. These were 200 ms in duration each.
3) 50 repetitions of a consonant-vowel /da/ stimulus of 180 ms duration.

4.2.4 Residual inhibition paradigm

The main results were obtained from an experiment using broadband Gaussian noise maskers, presented for 30 s duration diotically at the loudest comfortable volume, to achieve reductions in tinnitus loudness lasting beyond the end of the masker stimuli (RI). A total of 60 identical maskers were presented, across two days. After each masker the subject was immediately verbally prompted to provide a verbal rating of his current tinnitus loudness, on an integer scale from -2 (very quiet) through 0 (normal loudness) to +2 (very loud). After this rating was given, a 10 s time period was designated during which there was no task to perform, no stimulus and no speech or action by subject or experimenter. This was followed by three further ratings of his tinnitus loudness, each

separated by a 10 s gap (total 4 ratings, 3 gaps after each masker). Data during these 10 s inter-rating periods were used for further analysis, except where otherwise specified.

4.2.5 iEEG data processing

Spectral analysis was performed to decompose the data into nine pre-defined frequency bands which aimed to achieve a tradeoff between adherence to pre-defined functional bands, and logarithmic spacing: delta (1-4 Hz), theta (4-8 Hz), alpha (8-12 Hz), beta1 (12-20 Hz), beta2 (20-28 Hz), gamma1 (28-44 Hz), gamma2 (44-60 Hz), gamma3 (60-92 Hz) and gamma4 (92-148 Hz). The delta band was analysed as two separate bands (1-2 Hz and 2-4 Hz), and then the results averaged, as certain measures of signal quality can be compromised if bandwidth exceeds lowest frequency.

To analyse oscillatory power, averaged across the whole 10 s time period, each 10 s epoch was subdivided into ten one-second sub-epochs. Each sub-epoch was mean-centred and multiplied with a Hanning window in the time domain, before calculation of the FFT. To compensate for the 1/f amplitude distribution over frequency, each spectral amplitude value was multiplied by its frequency. Amplitude values were then squared (to yield power) and log transformed, before being averaged across sub-epochs and across frequency. This yielded one power value per epoch per frequency band per electrode. A *tinnitus regressor* was calculated, containing one value per epoch, which consisted of the average of the tinnitus loudness ratings immediately before and after that epoch. The regressor was partialised with respect to the recency of the end of the most recent masker stimulus, and the time with respect to the start of the experiment. Although the experimental design largely eliminated any direct stimulus-related effects, this partialisation corrects for any small residual influences (for instance if response times differed according to the level of tinnitus suppression, or tinnitus suppression systematically changed over the course of the experiment). Notably, the results did not change qualitatively after application of the partialisation process. Finally the regressor was inverted, so that positive values reflected tinnitus *suppression*, and mean centred. For each electrode/epoch/frequency band combination, a Pearson product moment correlation coefficient ('r') value was calculated, across the 179 epochs used for analysis, between oscillatory power values and the tinnitus regressor.

To analyse power changes over time, before, during and after maskers, the procedure described in the paragraph above was followed, but with the following differences. Instead of using the 10 s epochs between ratings for analysis, epochs (one per masker presentation) covered a time period of 5 s before the start of the masker to 30 s after masker offset (total 65 s). The sub-epoch length was 2.5s instead of 1 s, and power values were not averaged over time, so as to retain the time dimension in the data. Power values were averaged across electrodes within a pre-defined ROI covering HG and all of STG (electrode numbers 23, 24, 61, 66, 82, 87, 161, 162, 163 and 164), representing all AC sites sampled. For display purposes, the mean 'baseline' power in the 5 s preceding masker onset was log subtracted for each frequency, such that power values were expressed relative to this baseline value. Epochs were then categorised based on whether the first tinnitus loudness rating after the masker offset was zero (non-RI trials) or negative (RI trials). Note that some RI did occur on non-RI trials, but was simply so short-lived as to have ceased by the time the first tinnitus loudness rating was given. For statistical analysis, each time-frequency point was subject to a two-sample T test (comparing RI to non-RI trials).

To analyse local cross-frequency coupling, for each electrode/epoch combination, the time domain signal was Hanning windowed across the whole 10 s window, band-pass filtered in the frequency domain into the nine frequency bands, and Hilbert transformed to yield a complex time series. The Hilbert envelope (absolute value) was taken, squared (to yield power), log transformed, mean-centred, shifted to mean zero and normalised to unit standard deviation. Normalised envelopes were then Fourier transformed to yield the complex spectrum of the power envelope for each frequency. These time series could be directly compared across frequencies. To do this, the cross-spectral density (CSD) was calculated for each possible pair of frequencies (except identical or adjacent frequencies) by averaging over frequency the product of the lower frequency spectrum with the complex conjugate of the higher frequency spectrum, then averaging across frequency. The resulting complex valued metric thus indicates the strength of the correlation between the amplitudes of the two frequency bands, by its magnitude, and the phase lag inherent in the coupling, by its phase. The measure is similar to covariance, but offers the advantage that lagged relationships can also be detected. For each electrode/frequency pair combination a (complex) pair of r values was calculated against the tinnitus regressor. These were converted to polar coordinates to reflect magnitude and phase lag of coupling.

To analyse long-range coupling PLV was calculated, within each frequency band, between each possible pair of electrodes. This involved taking the complex time series of the Hilbert transformed raw data, dividing it by its magnitude (to retain only phase information). The resulting time series were then used to calculate instantaneous phase differences, for each electrode pair, at each point during the epoch. Phase differences were complex-valued, and the vector sum of these was taken, over time. The magnitude of the resultant vector is the PLV (range 0 to 1, with 1 indicating a perfectly consistent phase relationship between the two signals), and the angle of the vector is the phase lag inherent in the coupling. Complex PLVs were regressed against the tinnitus regressor, to yield a complex pair of r values. At the request of a reviewer, the analysis was performed using bipolar electrode montages, in order to eliminate the influence of widespread synchronous coherence on measured results. i.e. Individual (common reference) time series were converted into bipolar pairs, by subtracting one time series from that of its immediate neighbour, and PLV was calculated between the time series of one bipolar pair and that of another pair. This approach is highly conservative; although it reduces the chance of signal leakage influencing results, it also discards any genuine widespread zero lag synchrony. Specifically, instead of using individual electrode time series, adjacent electrode pairs were used as bipolar montages, and PLV was calculated between each electrode pair and each other electrode pair. Because there is no straightforward interpretation of 'positive' and 'negative' phase coherence in bipolar pairs (because some signals become inadvertently inverted), the results were expressed as the absolute magnitude of PLV change with tinnitus suppression, ignoring direction. It was putatively assumed (based on inspection of PLV changes between pairs of individual electrodes rather than bipolar pairs) that all changes occurring during tinnitus suppression would be reductions in PLV.

Induced oscillatory responses to external sounds were analysed in two ways. To identify electrodes showing significant stimulus responses, an equivalent analysis was performed to that described for oscillatory power during tinnitus suppression, except that only a 0-300 ms post-stimulus time window was used, coinciding with the maximum stimulus response. This was compared to an equal length pre-stimulus baseline. For display purposes, time-frequency decomposition with Morlet wavelets was performed, and the results expressed on a decibel scale relative to prestimulus baseline power at a given frequency (i.e. event-

related spectral perturbations; ERSPs). Evoked responses were calculated by averaging the time domain waveforms for each stimulus across trials, middle latency responses by doing the same after high-pass filtering from 10 Hz, and frequency following responses to 100 Hz click trains by band-pass filtering around 100 Hz.

4.2.6 Statistical analysis

In light of the large size of the data spaces involved, the basis of all statistical analysis was permutation testing, as discussed in Section 3.3. Permutations involved randomly shuffling regressor values, trial labels, or time points, depending on the experiment being analysed. For spectral power changes accompanying tinnitus suppression, the statistic of interest was simply the largest absolute r value obtained for any electrode/frequency combination. For the actual data, all r values exceeding this threshold were deemed significant.

For peri-masker time-frequency analysis, T scores were assessed for significance using a cluster-based non-parametric permutation approach, with clustering determined by adjacency in time-frequency space. A point threshold of $p < 0.25$ was used, and a cluster significance threshold of $p < 0.05$ (corrected) was set.

For cross-frequency coupling analysis, two metrics were subject to statistical analysis: 1) the magnitude of cross-frequency CSD change; 2) the cross-frequency CSD angle (phase) change, multiplied by the mean magnitude. For each permutation, the largest absolute change occurring for any electrode/frequency pair combination was used to generate the null distribution.

For long-range within-frequency coupling, the largest magnitude of PLV change occurring for any frequency/electrode pair combination was used to generate the null distribution.

4.3 Results

4.3.1 Responses to external sounds

Responses to external sounds were limited to HG only, and the 5 kHz (tinnitus-matched) tone significantly activated only the most medial two electrodes, corresponding to A1. These results are shown in Figure 3. From physiological classification criteria based on the presence of a 100 Hz frequency following response (FFR) (Brugge et al., 2008), it was determined that electrodes 161 and (to a lesser extent) 162 sampled A1.

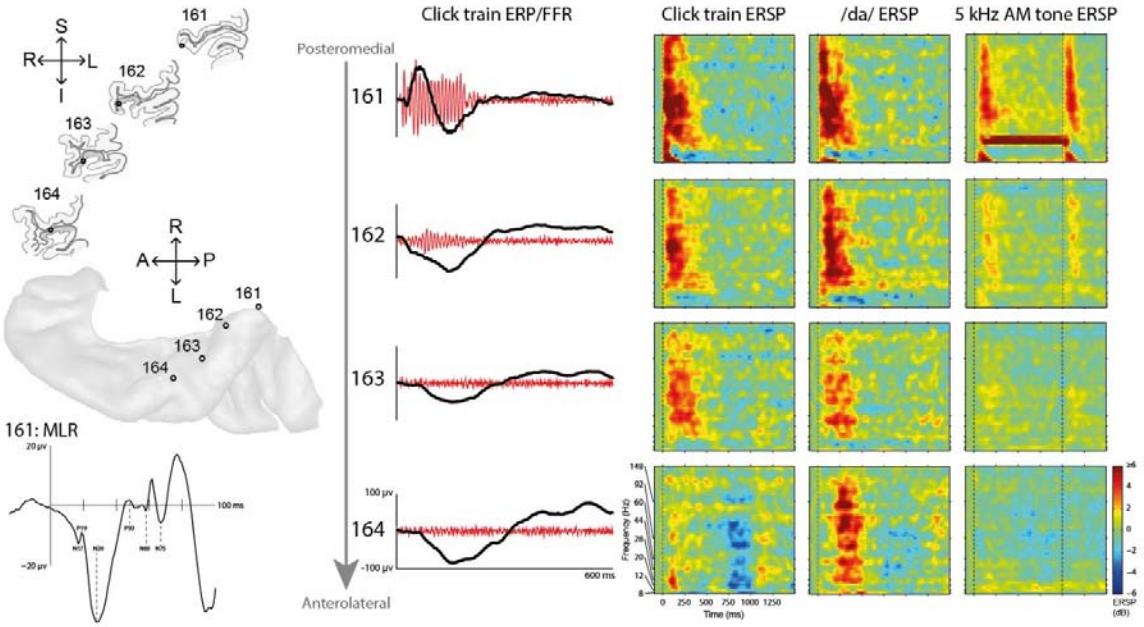

Figure 3: Responses to external broadband and tinnitus-matched sounds
Left column: anatomical location of the four electrodes in Heschl's gyrus (HG; 161:164) in the context of coronal sections (top), and superior view of superior temporal plane (middle), and also middle latency response to 100 Hz click train in electrode 161 (bottom). Middle column: ERP (black) and frequency following response (FFR; red) to 100 Hz click train from medial (top) to lateral (bottom). The transition from primary to non-primary auditory cortex is defined physiologically by the disappearance of the FFR, and occurs around electrode 162. Right columns: time-frequency responses to click trains, speech syllable and 5 kHz tone with 40 Hz AM (left to right) in the four HG electrodes. Colour scale indicates event-related spectral perturbations (ERSP; 10 x base-10 logarithm of power ratio versus baseline). Note the 40 Hz sustained response to the AM tones, corresponding to the 40 Hz modulation frequency.

4.3.2 Psychophysical RI responses to masker stimuli

On each day, half of the masker presentations resulted in RI that lasted until after the first tinnitus rating was given (RI trials). A higher proportion of trials yielded RI in the first half of the experiment than the second half, in both cases. Response times were slightly longer for RI trials than non-RI trials. These results are illustrated in full in Figure 4.

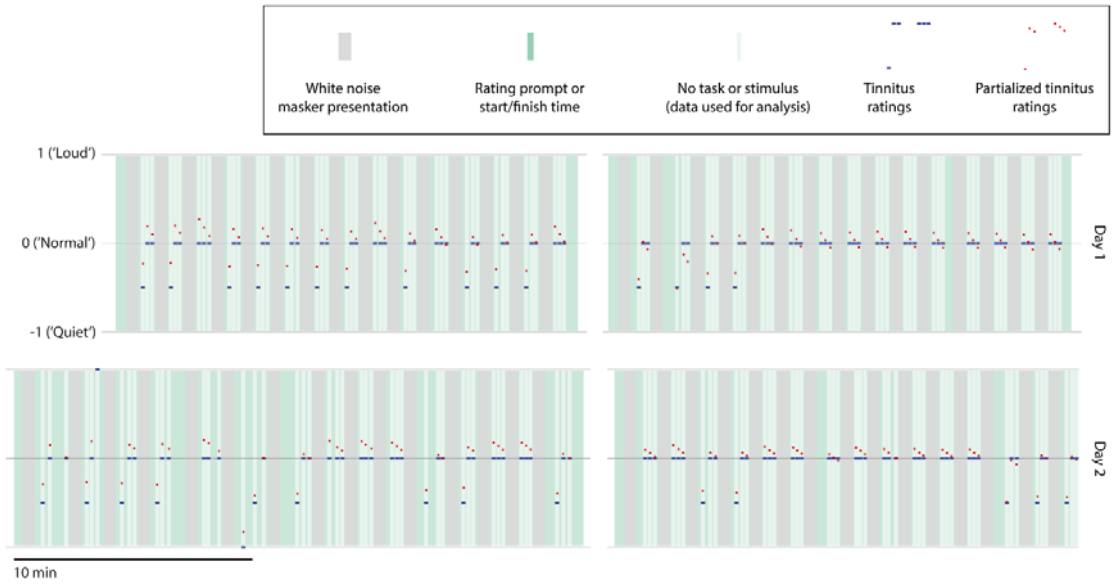

Figure 4: Psychophysical results of residual inhibition (RI) experiment
The horizontal axis represents time, and the two rows the two days on which the same experiment was performed. Masker stimuli (grey blocks) were 30 s each, and were each followed by four prompts (green) to provide a current rating of tinnitus loudness, separated by 10 s blocks in which no stimuli, task or responses occurred. Note the variable duration of the (green) response blocks, depending on response time, which resulted in a longer overall experiment duration on Day 2. Also note the halfway break in each day. The vertical axis on each row indicates tinnitus loudness in the range -1 to 1, which were the minimum/maximum ratings given during the experiment. Each value displayed is the mean of the ratings that immediately preceded and followed the 10 s epoch to which the rating applies. In all but one instance, the first two post-masker ratings were -1 and 0, or 0 and 0, respectively. Averaging these thus yielded mean ratings of -0.5 or 0, which are displayed in the figure as blue rectangles. Later responses were generally all zero, except in one instance on Day 2 where a mean rating of 1 occurred. This trial was removed from analysis due to incongruence with the rest of the experiment. Red circles indicate the tinnitus rating after partialisation, for masker recency and position in the experiment, and mean centring. Note the waning efficacy of the maskers in producing RI over the duration of each experiment.

4.3.3 Reproducibility across days

As illustrated in Figure 5, the results of the experiment were highly reproducible across the two days. Therefore, the results were pooled for further analysis. A striking pattern of widespread low frequency (delta, theta and alpha) power decreases and high frequency (beta2 and gamma) power increases accompanied tinnitus suppression. These changes are discussed in more detail in Section 4.3.4.

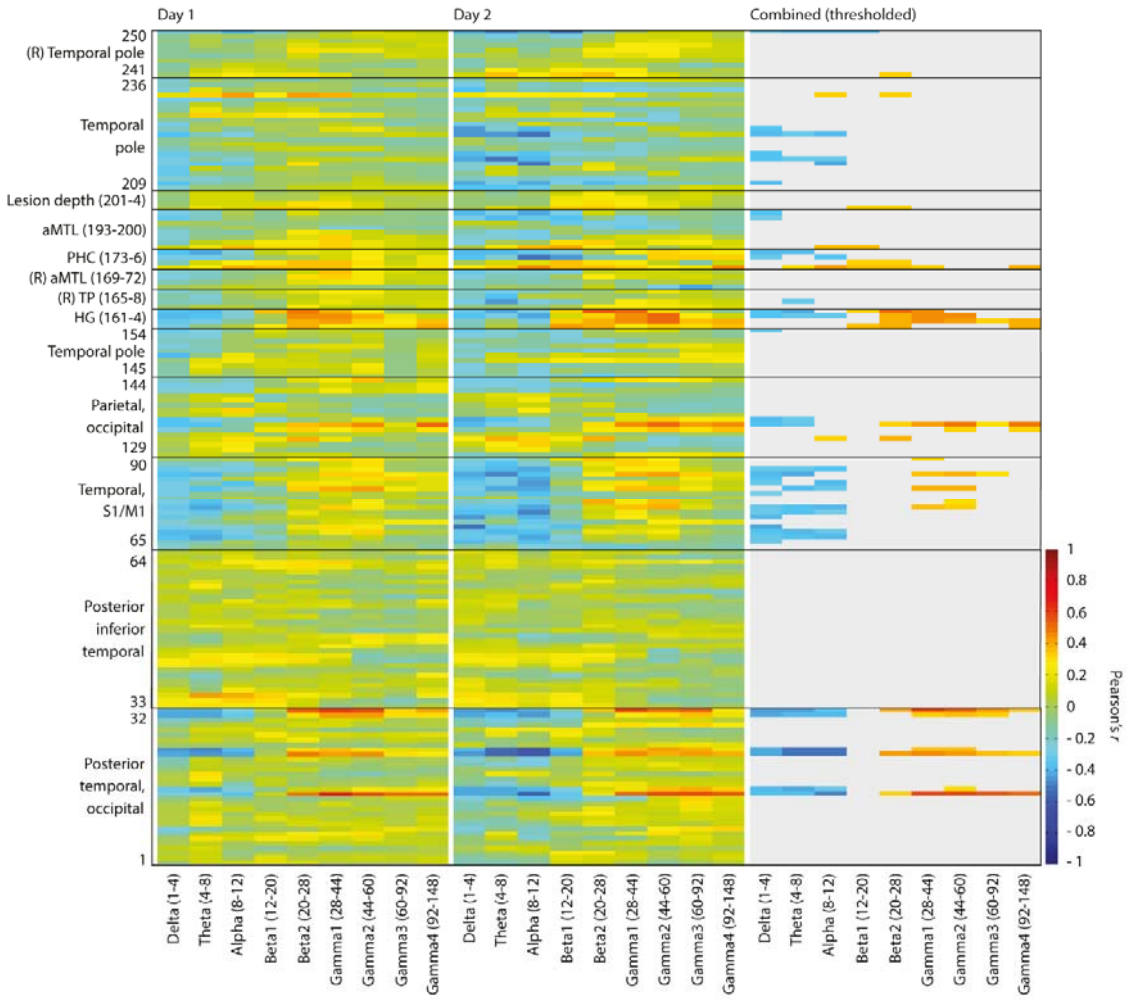

Figure 5: Full oscillatory power change matrix across the two experimental days
Left and middle plots indicate Pearson's r values from the two experimental days. In each plot, the columns indicate the nine frequency bands (bracketed numbers denote Hz), and rows indicate individual electrodes. The right plot is organised equivalently, and shows only significant power correlations based on the described permutation approach. All electrodes are in left hemisphere except where (R) indicates right hemisphere. aMTL = anterior mesial temporal lobe, including possible contributions from lateral nucleus of amygdala and anterior hippocampus. HG = Heschl's gyrus. PHC = parahippocampal cortex. TP = temporal pole. S1 = primary somatosensory cortex. M1 = primary motor cortex.

4.3.4 Oscillatory power changes

The oscillatory power correlates of tinnitus suppression are shown in full in Figure 5, and mapped onto brain anatomy in Figure 6. The most widespread changes were reductions in delta, theta and alpha (1-12 Hz) power, which encompassed lateral HG (a non-primary region of AC), STG, posterior middle temporal gyrus (MTG), IPC, primary sensorimotor cortex (S1/M1) and inferior temporal pole (iTP). The next-most widespread changes were

increases in high frequency beta and gamma (20-148 Hz) power with tinnitus suppression, which occurred in primary and non-primary AC, MTG, IPC, S1/M1 and PHC. The distribution of beta/gamma power changes covered almost all AC areas sampled, well beyond areas tonotopically representing or responding to the tinnitus frequency. A limited number of electrodes showed theta and alpha (4-12 Hz) power *increases* during tinnitus suppression. These were confined to PHC, aMTL and IPC.

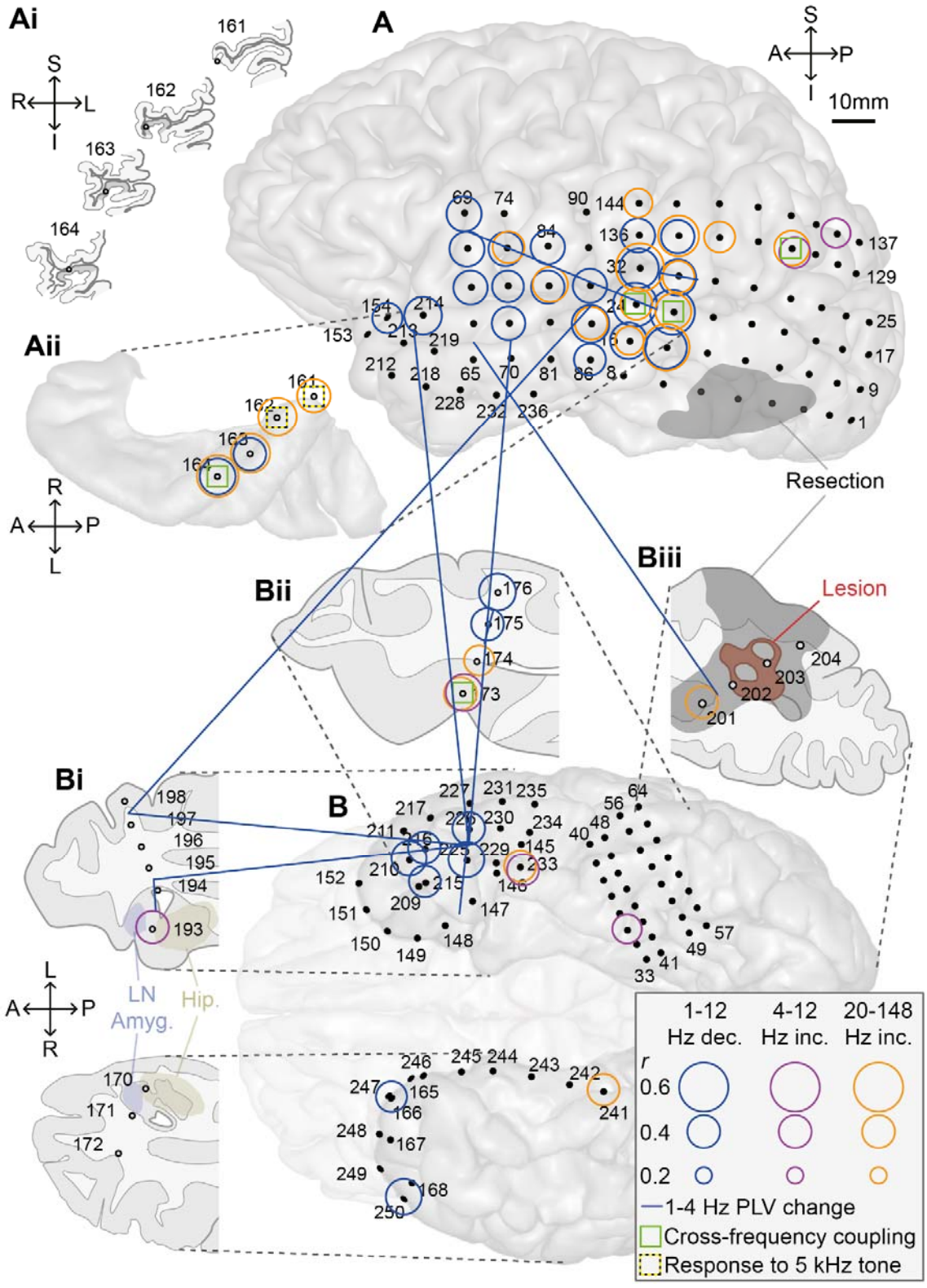

Figure 6: Changes in oscillatory power and phase locking value (PLV) with tinnitus suppression

Each black circle denotes one electrode from which data were analysed, with hollow circles indicating depth electrodes and solid circles subdural electrodes. Hollow coloured

circles indicate significant oscillatory power changes accompanying tinnitus suppression, with circle radius proportional to strength of correlation. The three circle colours indicate the three main response types observed, with blue, magenta and orange circles indicating delta-alpha suppression, theta-alpha enhancement and beta2-gamma enhancement respectively. Circle radius specifically indicates the largest r value for any of the frequencies within the indicated range. Blue lines indicate PLV changes (all within the delta band of 1-4 Hz) accompanying tinnitus suppression, and link two bipolar electrode pairs (with each line end midway between the two electrodes comprising the bipolar pair). Green squares indicate the five electrodes showing significantly altered cross-frequency coupling with tinnitus suppression. Black and yellow dashed squares indicate electrodes showing significant responses to the passive presentation of a tinnitus-matched (5 kHz) tone. A: Lateral view of the left hemisphere surface. Ai: Coronal sections illustrating the positions of the Heschl's gyrus (HG) electrodes (no activations shown on these). Aii: Superior view of the superior temporal plane surface. B: Inferior view of the inferior brain surface, with parts other than the temporal lobes faded. Bi: Sections through the anterior temporal lobes. Bii: Section through the left mid-posterior temporal lobe, with mesial grey matter corresponding to parahippocampal cortex (PHC). Biii: Section through posterior temporal and occipital lobe, including the lesion responsible for the focal epilepsy (red) and the area that went on to be resected (dark grey). In this section, the deepest electrode is in posterior PHC. LN Amyg. = lateral nucleus of amygdala. Hip. = hippocampus proper. S = superior. I = inferior. A = anterior. P = posterior. L = left. R = right.

4.3.5 Peri-masker time-frequency power changes

Figure 7 shows the mean peri-masker time-frequency power changes, across all AC electrodes. Both RI and non-RI trials were associated with transient broadband power increases at masker onset, followed by weak sustained gamma responses for the masker duration. Masker offset was associated with a similar, but weaker, response to the onset response. After this, both RI and non-RI trials showed strong low-frequency power decreases and high-frequency power increases. In non-RI trials, these finished by around 6 s post-masker, while in RI trials they persisted, gradually waning over tens of seconds. These power changes from around 6 s were significantly different between RI and non-RI trials, but no earlier, intra-masker or pre-masker changes showed a significant difference.

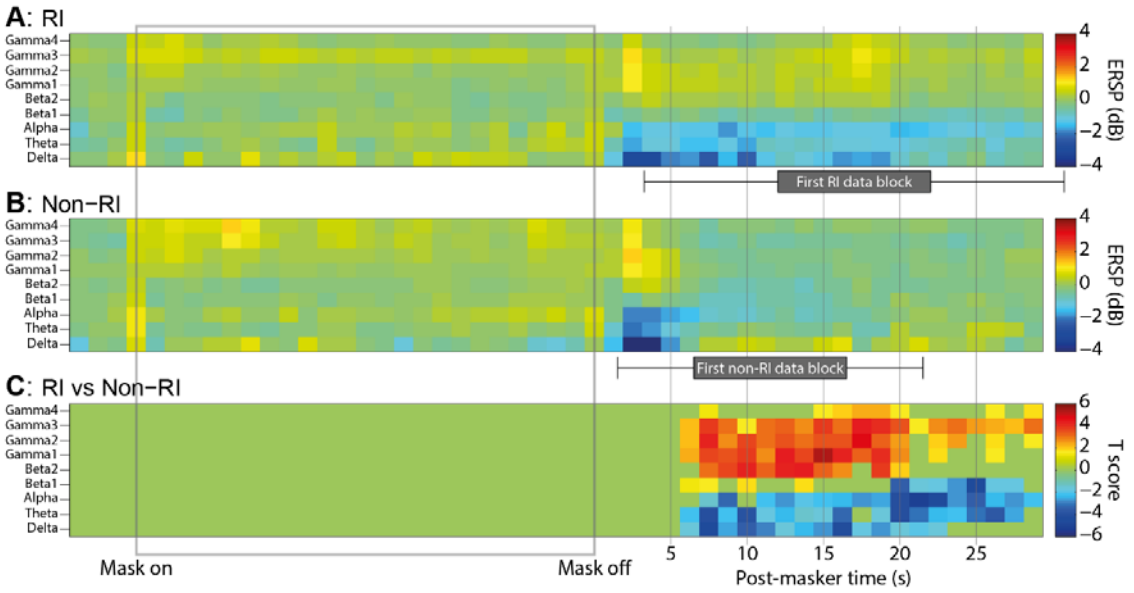

Figure 7: Peri-masker time-frequency power changes across auditory cortex
Each plot shows the power at each point in time (horizontal) and frequency (vertical) space, averaged across auditory cortex and expressed relative to the last 5 s before masker onset. Masker timing is indicated by the grey outline box. Hot colours indicate power increases and cool colours decreases. A: in RI trials, where tinnitus suppression persisted into the first inter-rating epoch (mean position and standard deviation indicated by horizontal box plot), were characterised by post-masker low frequency power decreases and high frequency increases which persisted for tens of seconds. B: In non-RI trials, where tinnitus returned to normal before the first epoch, similar power changes were observed, but these returned to baseline by around 5 s post masker. C: RI trials, compared to non-RI trials, were characterised by significantly greater high frequency, and lesser low frequency, power from around 6 s post masker onwards. Only clusters of significant difference are shown in this plot. ERSP = event-related spectral perturbations (10 times the base-10 logarithm of the power ratio versus baseline).

4.3.6 Cross-frequency coupling changes

Unlike the widely-distributed power changes, significant cross-frequency coupling changes occurred only in five discrete electrodes. These were in lateral HG, posterior STG, IPC and PHC. The overall pattern of coupling changes was complicated (Figure 8). A summary of the main observations accompanying tinnitus suppression is that in auditory regions (lateral HG and posterior STG) delta-alpha inverse coupling changed to weak positive coupling, and the coupling of low (delta, theta and alpha) frequency to high frequency (beta2) oscillations either shifted from positive to inverse, or from inverse to more strongly inverse. In PHC and IPC, a strengthening of positive coupling was observed between low (theta and alpha) and high (beta2 and gamma1) frequencies. Cross-frequency coupling

changes in other electrodes, even immediately adjacent ones did not come near to the threshold for statistical significance.

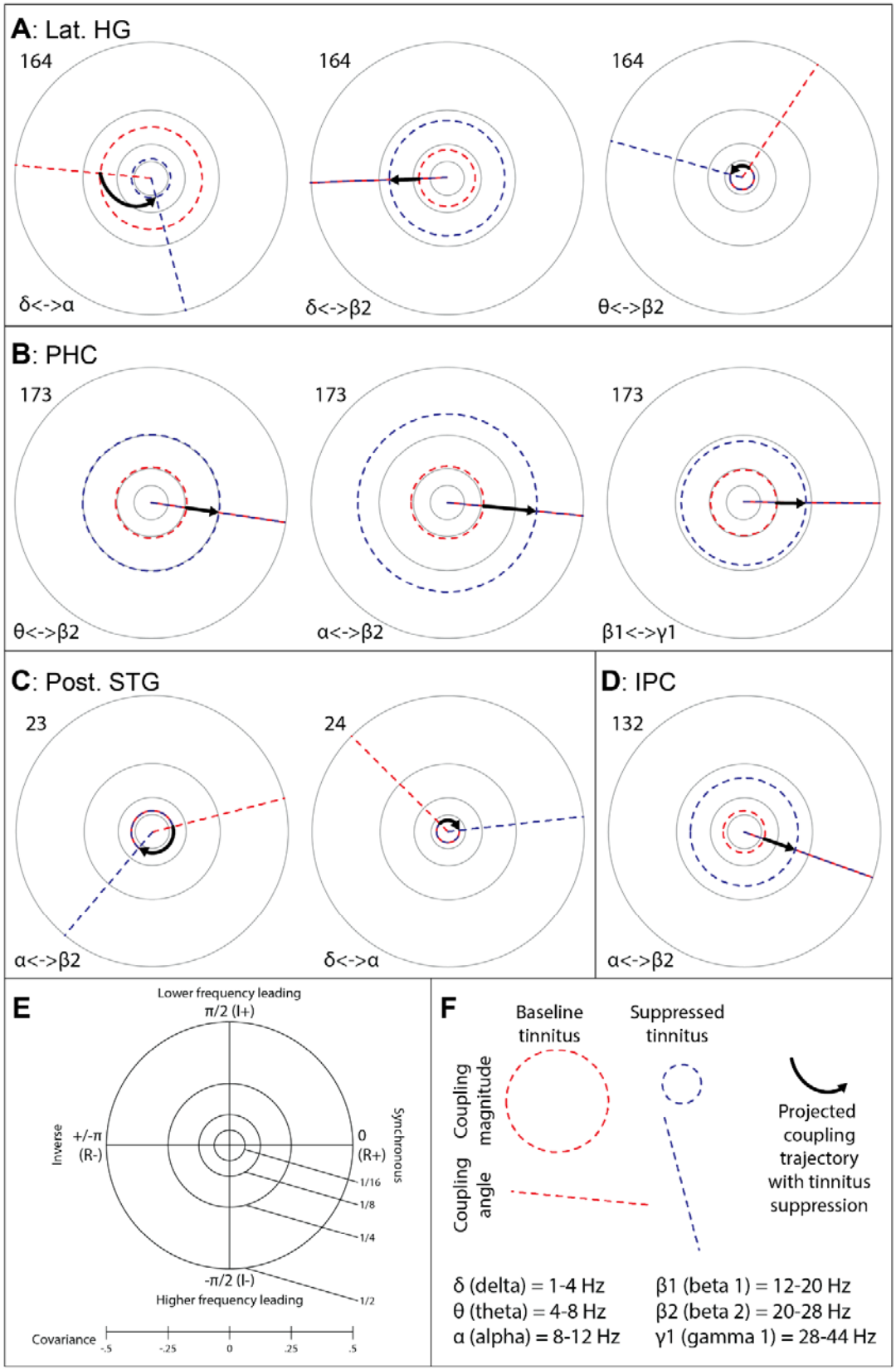

Figure 8: Cross-frequency coupling changes accompanying tinnitus suppression

Each polar plot indicates one electrode where cross-frequency coupling (its magnitude, angle, or both) changed significantly during tinnitus suppression. The origin and terminus of each black arrow indicate the coupling state during non-suppressed and maximally-suppressed tinnitus intensity respectively, and the path of the arrow indicates the projected trajectory between these. Each point in polar space is characterised by its magnitude (distance from the origin, with greater distance indicating stronger coupling: indicated by dashed circles) and its phase lag (angle: indicated by dashed line). Greek letters below each plot indicate the frequency pair in which coupling is denoted. Within polar plots, the horizontal distance from the origin (real component) indicates the covariance of the coupling. Vertical distance from the origin indicates the imaginary component of coupling, with points above the origin indicating the lower frequency is leading (on account of its phase being further ahead), and points below indicating the higher frequency leading. Numbers above each plot indicate the electrode number in which the changes were observed, and these are grouped into boxes according to anatomical region. HG = Heschl's gyrus. PHC = parahippocampal cortex. STG = superior temporal gyrus. IPC = inferior parietal cortex.

4.3.7 Long-range PLV changes

PLV changes were found only in the delta band, and are displayed in Figure 6. These occurred between STG and iTP, PHC, S1/M1, and between aMTL and iTP.

4.4 Discussion

In a study where subjective tinnitus loudness was manipulated through RI, while keeping stimulus factors (and others such as task) constant, widespread significant changes in the power and both local and widespread coupling of LFP oscillations were observed. Given the tight control over factors not directly related to tinnitus, the observed changes can be considered directly related to the processing of tinnitus itself. That said, it must still be kept in mind the putative route by which tinnitus was manipulated. RI can be considered a temporary reversal of deafferentation, by forward masking, and therefore is likely to suppress any subcortical drive underlying tinnitus (if one exists), and exert its effect on cortical correlates of tinnitus via that route. However, other possibilities cannot be discounted. The most striking, and immediately-apparent, finding was that tinnitus-linked oscillations were not confined to the tonotopic part of AC relating to the tinnitus, or hearing loss, frequency, or even to all of AC, but instead spanned a large and generally contiguous area of cortex including extra-auditory temporal regions, plus sensorimotor, parietal and PHC. A more detailed discussion of the observed changes follows.

4.4.1 Low frequency (delta/theta) oscillations

It was predicted that tinnitus suppression would coincide with suppression of delta/theta oscillations in AC, based on previous observations of suppression in these frequencies accompanying short-term (Kahlbrock and Weisz, 2008; Adjamian et al., 2012; Sedley et al., 2012a) and long-term (Tass et al., 2012) suppression of tinnitus. These oscillations are likely to relate to thalamocortical connections, based on observations of spontaneous burst firing of auditory thalamic neurons, in this frequency range, in both human tinnitus patients (Jeanmonod et al., 1996) and noise-exposed animals with behavioural evidence of tinnitus (Kalappa et al., 2014). Changes in this oscillatory band were the most widespread of all observed tinnitus-linked oscillations, and the delta band was the only frequency in which long-range phase coherence (PLV) changes were linked to tinnitus suppression. Based on these observations, it seems reasonable to speculate that this pattern of low-frequency changes, particularly in the delta (1-4 Hz) frequency band, represents a 'tinnitus drive' network, which links the thalamic input, and the multiple cortical regions involved in the processing of tinnitus. The lack of low-frequency changes in A1 is notable. This could indicate that non-primary regions play a more crucial role in brain tinnitus systems, or alternatively that there is tinnitus-linked low-frequency activity in A1 that does not suppress with the degree of RI achieved in this experiment.

4.4.2 Alpha oscillations

Early reports of spontaneous brain oscillatory abnormalities in tinnitus found alpha oscillations to be reduced in magnitude (Weisz et al., 2005a, 2007), though at least one similar study found the opposite (Moazami-Goudarzi et al., 2010). Also, neurofeedback-aided increases in alpha power (albeit coinciding with reductions in delta power) have been found to cause reduction in subjective tinnitus loudness (Dohrmann et al., 2007), and successful acoustic-based treatment of tinnitus was associated with increases in alpha power, along with decreases in all other bands (Tass et al., 2012). Additionally, during studies of illusory percepts (Zwicker tones and imagined music during noise) in healthy individuals, alpha power reductions were associated with increased presence and strength of illusory percepts (Müller et al., 2013; Leske et al., 2014). In light of these findings, the observed reduction in alpha power with tinnitus suppression is surprising, but not unprecedented. Recent tinnitus theory proposes a much less strict distinction between theta and alpha oscillations than has previously been applied, highlighting instances where theta behaves like 'low alpha' and alpha behaves as 'high theta' (De Ridder et al., 2015b). In the

present results, alpha oscillations behave almost identically to theta, which would be consistent with this assertion.

In addition to the widespread areas of alpha power decrease with tinnitus suppression, a few areas (circumscribed parts of PHC and IPC) showed theta and alpha increases. Based on recent tinnitus theory, these regions are associated with auditory memory (De Ridder et al., 2013), and may have a role in generating tinnitus through 'filling in' of missing central auditory representations from memory (De Ridder et al., 2011a, 2012, 2013, 2015b; Roberts et al., 2013). Though the following assertion is speculative, it could be that the increased activation in these regions during RI signalled an increased reliance on memory during suppression of the afferent tinnitus drive.

4.4.3 High frequency (beta/gamma) oscillations

The theory of TCD proposes that the underlying drive to tinnitus is the delta/theta oscillations in deafferented tonotopic regions, and that the cortical interfaces between deafferented, delta/theta oscillating, and normal, alpha oscillating, cortical regions generate gamma oscillations in a phenomenon called the 'edge effect' (Llinás et al., 1999, 2005; De Ridder et al., 2015b). This theory therefore makes the explicit prediction that gamma oscillations are present only in circumscribed parts of AC corresponding to these normal-pathological cortical interfaces. The present finding of tinnitus-linked gamma oscillations throughout all of AC, and a wider array of cortical regions, strongly contradicts this hypothesis, suggesting either that it is not correct, or that a secondary mechanism must operate via which gamma oscillations are widely propagated across AC and beyond. While gamma oscillations have previously been argued to represent the conscious perception of tinnitus, or its perceptual intensity (Llinás et al., 1999; Weisz et al., 2007; van der Loo et al., 2009), more recent evidence has either not detected gamma changes at all (Adjamian et al., 2012), or found variable relationships between tinnitus intensity and gamma power, which could be either positive or negative depending on individual and context (Sedley et al., 2012a). Given these findings, the prior hypothesis was that tinnitus suppression would be associated with changes in gamma power, but that these could be positive or negative. Given that contemporary accounts of the role of gamma oscillations either propose that they are a generic signature of local cortical activation (Merker, 2013), or a signal of incongruence between prediction and ascending sensory information (Arnal and Giraud, 2012; Bastos et al., 2012), it seems reasonable that a change in a chronic stable percept

should be associated with increased gamma power, regardless of whether it were a change towards a stronger or weaker percept. While the present finding of increased gamma power with tinnitus suppression can be explained in such a manner, previous findings of reduced gamma power during tinnitus increases (Sedley et al., 2012a) are harder to explain, and are beyond the scope of this individual study; further discussion on this issue occurs in Chapter 9.

4.4.4 Local cross-frequency interactions

The first striking characteristic of the cross-frequency coupling changes observed is that, in contrast to the widespread power changes, they occurred only in a few highly localised cortical regions. Therefore, even if very large cortical areas are involved in tinnitus, the orchestration of these large-scale systems may be conducted only in circumscribed areas. In interpreting the patterns of cross-frequency coupling within these areas, it is helpful to consider 'normal' patterns of coupling based on invasive layer-resolved recording from monkey visual cortex (Spaak et al., 2012). These found a strong anti-correlation (negative covariance) between alpha power, generated in deep cortical layers, and higher frequency power, generated in superficial layers. In the present results, auditory cortical regions showed either weakly negative, or positive, alpha-beta2 coupling in the baseline tinnitus state, with a shift to negative, or more strongly negative, coupling during tinnitus suppression. This could be considered a shift from abnormal to normal coupling. Other coupling changes in auditory cortical regions are harder to interpret, given the lack of established reference ranges. In putative auditory memory regions, PHC and IPC, all coupling (between theta, alpha, beta and gamma oscillations) was positive, and became more positive during tinnitus suppression. Again, these findings are difficult to interpret, but follow a distinctly different pattern to those in auditory regions. The anatomical distribution of these cross-frequency coupling 'hubs' (AC, PHC and IPC) closely matches the hypothesised layout of a 'core tinnitus network' (De Ridder et al., 2013), comprising the minimum set of areas necessary for tinnitus perception to occur, and which interacts with other wider networks responsible for non-essential parts of the tinnitus experience.

4.4.5 A cortical 'tinnitus system'

The observations discussed in the preceding sections are summarised in Figure 9. Distinctions of activity patterns based on frequency band and direction of power changes,

anatomical regions, long-range connectivity and cross-frequency coupling suggest the existence of three distinct but overlapping sub-networks, which together can be considered a cortical tinnitus system. As discussed previously, the low frequency (especially delta) oscillatory decreases appear to delineate a network of areas subject to a common afferent tinnitus drive (blue in Figure 9). These exhibit delta-band coherence linked to tinnitus, which appears to be the predominant or sole frequency band of coherent communication. Also as discussed previously, the areas showing theta and alpha increases appear to relate to auditory memory, and may comprise a sub-network relating to mnemonic contributions to tinnitus representations (magenta in Figure 9). As beta and gamma oscillations, at a minimum, relate to local cortical activation and processing (Merker, 2013), and may well constitute changing predictions and prediction errors respectively (Arnal and Giraud, 2012; Bastos et al., 2012), the areas showing tinnitus-linked gamma oscillations can be considered to be showing altered processing of local representations coincident with changes to the tinnitus percept. Thus, these are putatively considered to comprise a 'tinnitus perception' network (orange in Figure 9). Importantly, this includes not only auditory cortical areas, necessary for auditory perception, but multimodal global perceptual areas (MTG and IPC) which, based on previous research, appear to relate to high-level perceptual responses such as whether or not equivalent stimuli are consciously perceived (Brancucci et al., 2011; Turken and Dronkers, 2011; Hoffman et al., 2012).

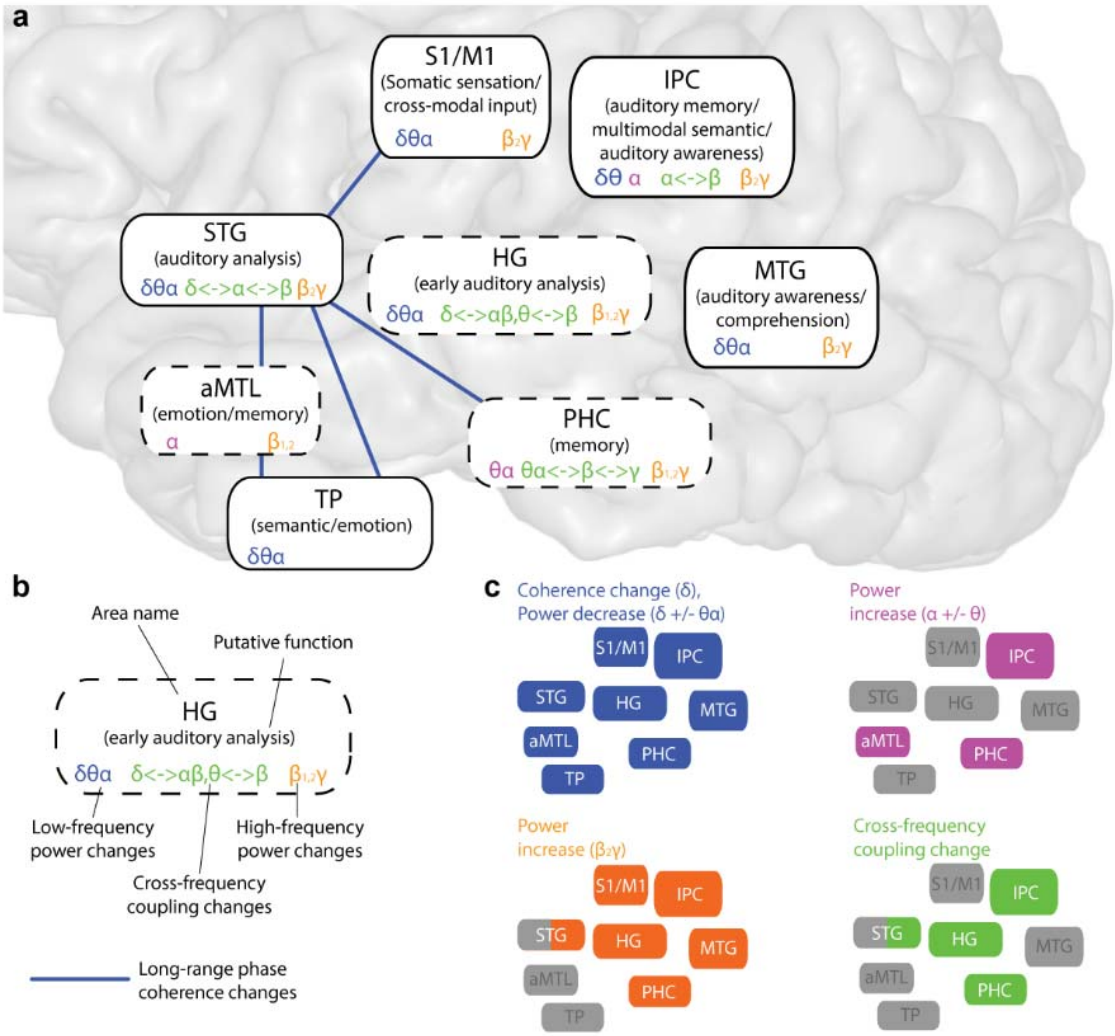

Figure 9: Summary of findings from the study, expressed in terms of a three-part tinnitus system

Text boxes represent distinct anatomical regions in which tinnitus-linked activity changes were observed. Note that for reasons of clarity these are not necessarily placed in their correct locations. Dashed outlines indicate deep areas, and solid outlines superficial areas. Boxes contain the area name (top), its putative function with respect to tinnitus (middle), and the local neural activity changes accompanying tinnitus suppression (bottom). Long-range delta phase coherence (PLV) changes are shown as blue lines. Part c shows a separation of these activity changes into four patterns (three frequency ranges, plus the distribution of cross-frequency interactions), based on the type, frequency, direction and distribution of activity changes. S1/M1 = sensorimotor cortex. IPC = inferior parietal cortex. STG = superior temporal gyrus (in some cases subdivided into anterior and posterior parts). HG = Heschl's gyrus (including A1). MTG = middle temporal gyrus. aMTL = anterior mesial temporal lobe (including amygdala and hippocampus). PHC = parahippocampal cortex. TP = temporal pole. δ = delta (1.4 Hz). θ = theta (4-8 Hz). α = alpha (8-12 Hz). β = beta (12-30 Hz). γ = gamma (>30 Hz).

4.4.6 Limitations of study

The most obvious limitation of this study is that it is just based on a single case. While a group study of this type is unfeasible, a small number of further cases would help to determine how homogeneous or heterogeneous these observed changes are. While the subject's laterality, character, loudness and distress of tinnitus were all typical, the degree of hearing loss was perhaps greater than average. Furthermore, it is not yet clear whether there are neurobiological subtypes of tinnitus, even within groups of patients with similar phenomenology. Attention is a very important factor in all tinnitus research measuring cortical activity. While the present study was based on a contrast of states between which attention should not have differed, the absence of small attentional changes cannot be confidently assumed. However, this study was in this respect far more tightly controlled than all resting-state studies performed so far, which almost certainly features large differences in attention between groups. Furthermore, it is unlikely that attention could have been the sole explanation for the observed findings, as previous iEEG examination of auditory attention affects found only weak and highly localised changes in AC in association with a switch from somatosensory to auditory task-related attention (Ray et al., 2008). As well as attention as a potential confound, attention could also alter the magnitude or anatomical extent of tinnitus-linked activity changes, and as such would be an interesting variable to explore. Future research might use varying tasks, during the epochs from which iEEG data are processed, to manipulate the focus and degree of attention.

Chapter 5. Group-level MEG correlates of tinnitus

This study was conducted at the Wellcome Trust Centre for Neuroimaging, University College London. I received limited assistance with patient recruitment from Dr Rudrapathy Palaniappan, Consultant Neuro-Otologist at University College London Hospitals, who provided two patients. MEG and MRI scans were performed with the assistance of radiographers and technicians at the centre, in accordance with local policy. Experimental conception, design, piloting, creation of experimental scripts, running of experiments, data analysis and interpretation was performed entirely by me.

5.1 Aims

The principal motivation for this experiment was to better understand the relationship between resting-state AC gamma oscillations and the perception of tinnitus, in light of two unresolved discrepancies in the literature. Firstly that resting-state AC gamma power increases in tinnitus subjects compared to controls, which form a crucial part of prominent tinnitus models, have only been found in certain studies which were poorly controlled for hearing loss (Llinas et al., 1999; Weisz et al. 2007; Ashton et al., 2007), and not others including particularly a recent study well-controlled for hearing loss (Adjamian et al., 2012). Furthermore, when resting-state gamma changes in tinnitus have been found, they have always been positively correlated to either the presence or perceived loudness of tinnitus (Weisz et al., 2007; Ashton et al. 2007; van der Loo et al., 2009; Balkenhol et al., 2013; de Ridder et al., 2015a). However at group level, gamma correlates of short-term changes in tinnitus loudness have always been absent (Kahlbrock and Weisz, 2008; Adjamian et al., 2012) and individual-level changes can take the form of positive or negative correlations depending on the tinnitus manipulation used (Sedley et al., 2012a). Positive correlations reported between subjective tinnitus loudness and gamma power have either lacked detail about the loudness quantification used (van der Loo et al., 2009), or only used sensor-level EEG as the measure of gamma power (Balkenhol et al., 2013), which is dominated principally by muscle activity at that frequency range and hence likely confounded. The aims of this study were therefore to examine group-level differences in gamma power, where the control group was well-controlled for age, sex and hearing loss, and also to make a detailed and explicit assessment of subjective tinnitus loudness with which to correlate gamma power, taking account of confounds such as tinnitus distress and

hearing loss. Other frequency bands would also be examined, with the delta/theta bands of particular interest. These have shown the most consistent group and individual level correlations with tinnitus presence and loudness (Llinas et al., 1999; Weisz et al., 2005a, Weisz et al., 2007, Kahlbrock and Weisz, 2008; Sedley et al., 2012a; Tass et al., 2012), but a recent well-controlled study found that delta power only differed between the 'tinnitus with hearing loss' and 'no tinnitus with normal hearing' groups, as opposed to being increased in tinnitus groups in general (Adjamian et al., 2012). Importantly, the quantification of oscillatory power must be in source space, where confounds of muscle and other artefacts are greatly reduced, and localised in AC.

5.2 Methods

5.2.1 Subjects

Sixteen subjects with chronic tinnitus were recruited, through a local neuro-otology clinic, and via advertisement on a local mailing list for potential research participants and in the magazine of the British Tinnitus Association, 'Quiet'. Inclusion criteria included chronic subjective tinnitus of over 6 months duration, age 18 years or over, the absence of a wider neurological condition, and the absence of medications causing sedation or acting on GABA-ergic systems. Importantly, subjects were required to have tinnitus that was entirely or predominantly lateralised to one ear (half left, half right). The reason for this was to be able to assess whether any observed tinnitus correlates had either a contralateral or right/left hemisphere bias. Half of the subjects had clinically normal hearing, defined as mean hearing threshold between 0.25 and 8 kHz less than 20 dB, no individual frequency exceeding 30 dB threshold, and a maximum of one frequency per ear exceeding 20 dB threshold. Once each tinnitus patient participated in the study, a search began for a control subject individually matched for age, sex and hearing thresholds. For the normal hearing tinnitus subjects, matched controls were sought through advertisement on the same research participant mailing list. For the hearing loss subjects, limited computerised records, consisting of just age, sex, latest audiogram results, name and contact details, were screened within the database of the Royal National Throat Nose and Ear Hospital. Individuals identified who provided a close match for age, sex and hearing profile were then contacted to explain the study and offer an invitation to be screened for participation. The screening procedure and contacting of patients was performed by me, who held an

honorary clinical contract with the hospital trust, and participated in occasional clinics within Neuro-Otology. Importantly, the procedure was approved by the trust's R&D department, and the research ethics committee that assessed the study as a whole. 15 out of 16 required matched control subjects were successfully recruited. As age, sex and hearing were matched at group level with these numbers, it was decided that these numbers would suffice.

5.2.2 Psychophysical assessments

Pure tone audiograms were performed for each subject as follows. For each frequency from 0.5 to 8 kHz, in octave steps. A series of tones started at -10 dB, and was gradually increased until the subject could perceive it. The procedure was done three times per frequency per ear, starting with 5 dB steps, followed by 1 dB steps. The median of three repetitions was taken as the final result. For tinnitus subjects, tinnitus 'spectra' were determined based predominantly on a previously published method (Norena et al., 1999). Briefly, a number of frequencies were tested in random order. For each frequency, the subject first tuned the loudness of a pure tone at that frequency to match the loudness of their tinnitus in each ear in turn. Next they were presented the tone in both ears at the specified loudness, and gave a rating of 0 to 10 for how much it resembled their tinnitus in pitch. Each frequency was tested twice, and the mean rating used. Spectra were then scaled such that the lowest rating given was 0, and the highest was 1. Group averaging took place after this scaling process. Frequencies from 1 to 8 kHz, in 1 kHz steps, comprised the spectra.

Questionnaires completed by subjects were as follows. All subjects completed the Modified Hyperacusis Questionnaire used by the Tinnitus Practitioners Association (http://csd.wp.uncg.edu/wp-content/uploads/sites/6/2014/01/Hyperacusis-Qx1.pdf), which is similar in content to the Khalfa Hyperacusis Questionnaire (HQ) (Khalfa et al., 2002), the Hospital Anxiety and Depression Scale (HADS), and the Physical Health Questionnaire 15 (PHQ-15). The inclusion of general chronic symptom scales was so that if abnormalities outside AC were observed then it could be assessed whether they were tinnitus-specific or related to chronic unpleasant symptoms in general. Tinnitus subjects also completed the THI (Newman et al., 1996), and gave subjective ratings of tinnitus phenomenology on bespoke visual analogue scales (VAS). VAS scores were given for tinnitus loudness and tinnitus distress. For each of these, an 'overall' rating was given, to

reflect the score on a typical day, with 0 being silence or no distress, and 10 being the loudest or most distressing thing in existence. Additionally, a 'current' rating was given, where 0 and 10 represented the quietest/least distressing and loudest/most distressing their tinnitus had been within the last 6 months, with 5 being a typical or average day. The purpose of making this distinction was to distinguish between theoretically distinct 'static' and 'dynamic' processes. Static processes could include correlates of cortical plasticity or the underlying tinnitus drive, while dynamic processes could include compensatory processes, attention and/or interaction with global perceptual networks (GPNs). To aid the distinction of these factors, subjects were preferentially recruited if they indicated that their tinnitus showed significant day to day or week to week variation, though this was not a strict inclusion criterion.

5.2.3 Magnetoencephalography (MEG) data acquisition

Subjects were requested to refrain from alcohol for 24 hours prior to the MEG recording, and from caffeine on the day of the recording. The recording setup used was a Canadian Thin Films (CTF MEG International Services Ltd., Coquitlam, BC, Canada) magnetometer incorporating 275 axial third order gradiometers. Recordings were performed in a magnetically-shielded and vibration-damped room, which was moderately-lit, and quiet. Before the recording, subjects had three fiducial points marked on their heads, namely the nasion, plus left and right preauricular points. Radiofrequency coils were attached to these locations for the MEG recording, and used for constant head localisation. Sessions lasted 600 seconds, during which a black screen with a white cross was in front of the subjects. Subjects were instructed to remain relaxed and still, to keep their eyes open and to fixate on the point on the screen. A video feed, and the MEG data, was monitored throughout to ensure the subjects remained awake and kept their eyes open. Data was recorded with a sampling rate of 600 Hz.

5.2.4 MRI data acquisition

After MEG, subjects underwent acquisition of a structural T1-weighted MRI scan of their whole head. The same fiducial locations used for the MEG recording were marked with vitamin E capsules, which appear as high signal on T1-weighted images due to their high lipid content.

5.2.5 MEG Data analysis

Data analysis was performed in Matlab, using the SPM12 toolbox (Wellcome Trust Centre for Neuroimaging, London, UK) and custom analysis routines. Preprocessing of MEG data was performed in the FieldTrip (Oostenveld et al., 2011) toolbox for Matlab.

MRI scans were segmented into GM, WM and CSF tissue types, which were used to generate a cortical mesh by warping a template brain mesh to fit the individual's scan. A single shell head model was created from the mesh, and co-registered manually by alignment of the fiducial markers used in the MEG and MRI scans. A regular 3D grid was created, with 10 mm spacing, throughout the brain substance, and at each grid point the lead fields were calculated for each of three orthogonal dipole orientations. To ensure equivalence of grid points across subjects, SPM12 implements an approach in which the grid is created in a template brain common to all subjects, and for each individual it is warped to fit their individual anatomy. Thus, any given grid point can be considered to represent the same brain area in all subjects.

MEG data was divided into 60 epochs of 10 s duration each. Epochs were visually inspected, and those with significant muscle or other artefacts were rejected. Eye movements and blinks were not removed. ICA was performed on the data after artefact rejection. Components that included line noise, eye movements, blinks or cardiac activity were removed from the data.

Source space analysis was preferred to sensor space, as sensor level data is relatively insensitive to brain activity in the gamma range, with most observed activity representing muscle artefact. As changes in orofacial muscle tone could plausibly accompany tinnitus presence and/or distress, this type of analysis could not be relied upon to be valid. Data were initially divided into the following frequency bands, and the sensor covariance matrix calculated within each band: delta (0-4 Hz), theta (4-8 Hz), alpha (8-12 Hz), beta1 (12-20 Hz), beta2 (20-30 Hz), gamma1 (30-45 Hz), gamma2 (45-70 Hz), gamma3 (70-150 Hz). +/- 1 Hz from line noise harmonics (i.e. 50, 100 and 150 Hz) were excluded from analysis. A dynamic imaging of coherent sources (DICS) beamformer (Gross et al., 2001) was used to create a set of spatial filters for the transformation of sensor space into source space data. One filter was created per frequency per brain location. Oscillatory activity in source

space was expressed as power. Due to the theoretical limitations of beamformers in resolving widely coherent sources, an initial comparison was performed between the beamformer source power estimates, and those obtained using eLORETA (Pascual-Marqui et al., 2011). This is a similar method in many ways to beamforming, but assumes maximum smoothness of activity across brain sources rather than independence of sources. As the intracranial study of tinnitus (Chapter 4) found highly correlated activity across large areas of cortex, it seemed important to ensure that such widely coherent activity was not missed due to the technical limitations of methods used. The comparison found similar results in the two modalities, with higher spatial resolution with the beamformer. Thus the beamformer method was used for final analysis.

The principal area of interest was AC. Given that the intracranial study of tinnitus (Chapter 4) found AC activity to be extensive, and confluent with inferior parietal lobe activity, a cuboidal ROI was defined, in each hemisphere, that encompassed the whole superior temporal plane, and extended posteriorly and superiorly enough to encompass IPC. Analyses were then performed in the regions of interest, and in the whole brain. A permutation approach was used, treating each subject as a single observation for each brain/frequency point, with shuffling of subjects for each permutation. Analyses were performed separately for each frequency band, but with the two beta bands forming one analysis, and the three gamma bands forming one analysis. A cluster, rather than single point, thresholding approach was used, as large, flat areas of activation were identified in the intracranial study of tinnitus (Chapter 4), which would be better captured with a cluster approach. Correlations were calculated for each point in source space. The point threshold applied before sorting into clusters was $p < 0.05$ uncorrected. Comparisons of interest included tinnitus vs. control groups, and regression against subjective tinnitus loudness (overall and current), THI score, and mean hearing thresholds. Group comparisons used T tests, and regression used Pearson's product moment correlation coefficient ('r'). When used with permutation approaches, parametric statistics are appropriate, even if data are not normally distributed, as any violations of normality will apply equally to generation of the null distribution used to determine the significance threshold.

5.3 Results

5.3.1 Subject characteristics

16 tinnitus subjects and 15 matched controls were studied. The tinnitus group comprised 8 left ear and 8 right ear predominant tinnitus. Within each set of 8, half had hearing loss and half clinically normal hearing. Overall, control subjects had higher pure tone thresholds (i.e. worse hearing), but the difference was not significant at any frequency at $p < 0.05$ uncorrected. Figure 10 shows the group hearing thresholds, and Table 1 summarises subject characteristics.

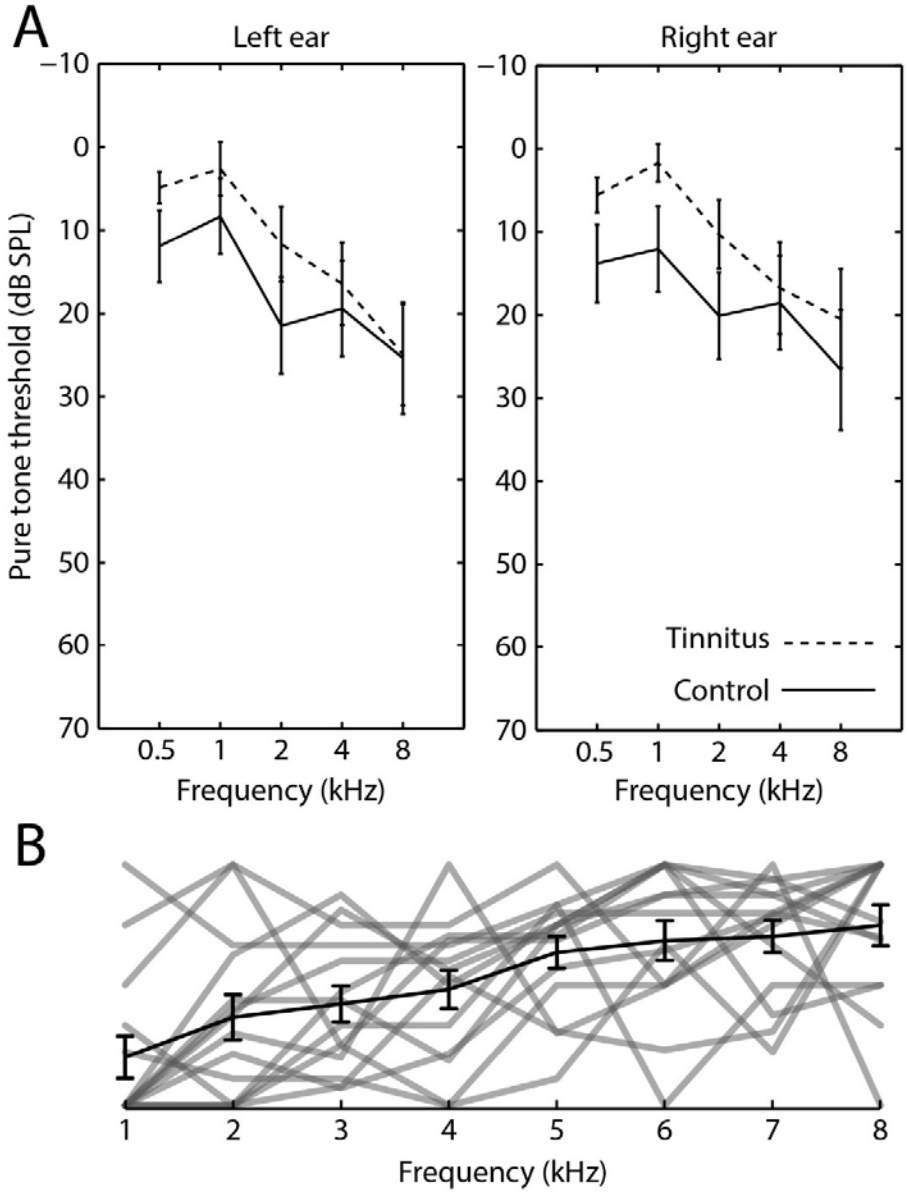

Figure 10: Audiometric assessments

A: Pure tone thresholds for tinnitus and control groups. Error bar plots indicate the group mean and standard errors for the tinnitus (dashed) and control (solid) groups. No difference, at any frequency, was significant at $p < 0.05$ uncorrected. B: Tinnitus spectra for tinnitus group. Grey lines indicate individual spectra, and black line represents mean spectrum, with error bars indicating standard error of the mean. The ordinate axis ranges from 0 to 1 (lowest and highest rating, respectively, given by each subject).

	Tinnitus (n = 16) Mean (SD)	Control (n = 15) Mean (SD)	p =
Age	46.1 (14.8)	43.3 (14.5)	0.59
Female:male	5:11	5:11	
Mean HL (dB) left	12.1 (14.4)	17.3 (19.0)	0.40
Mean HL (dB) right	10.9 (13.6)	18.2 (19.9)	0.24
mHQ score	17.8 (8.6)	6.5 (6.9)	**0.0004**
HADS anxiety	4.1 (2.7)	2.7 (2.1)	0.14
HADS depression	4.3 (4.3)	2.6 (2.9)	0.20
PHQ15	5.9 (4.1)	2.5 (2.7)	**0.01**
T duration (years)	7.5 (7.5)		
T laterality (left/right)	8:8		
THI score	30.4 (18.8)		
VAS loud overall	4.2 (1.9)		
VAS loud current	6.2 (2.1)		
VAS distress overall	4.6 (2.7)		
VAS distress current	5.3 (2.0)		

Table 1: Subject characteristics
Where applicable, open and bracketed numbers indicate group mean and standard deviation (SD) respectively. p values, based on two-tailed Student's T tests are shown where a comparison between tinnitus and control groups can be made. Significant ($p < 0.05$ uncorrected) group differences are indicated by bold p values. HL = hearing loss. mHQ = modified Hyperacusis Questionnaire. HADS = Hospital Anxiety and Depression Scale. PHQ15 = 15-point Physical Health Questionnaire. T = tinnitus. THI = Tinnitus Handicap Inventory. VAS = visual analogue scale (0-10).

While there were no significant group differences in age, sex or hearing thresholds, tinnitus subjects had significantly higher mHQ scores ($p = 0.0004$) and the PHQ15 ($p = 0.01$), which measures somatic symptoms. Two control subjects had unforeseen contraindications to MRI, and thus had template MRI scans used to generate their head models and lead fields.

5.3.2 MEG source space power

There were no significant group level differences in source space power between tinnitus and control groups, either in the whole brain or ROI analyses, in any frequency band.
In the ROI analyses, overall subjective tinnitus loudness, rated by VAS score, correlated positively with delta power in left auditory cortical regions (Figure 11A). Current tinnitus loudness correlated positively with alpha power in the left ROI (Figure 11B), but inspection of the distribution of the changes suggested that the main site of power change was in IPC, with little involvement of AC itself. In the tinnitus group, mean hearing threshold (hearing loss) correlated positively with activity in all three gamma bands in the right AC ROI (Figure 11C), whereas in the control group the correlation was much weaker and did not reach significance.

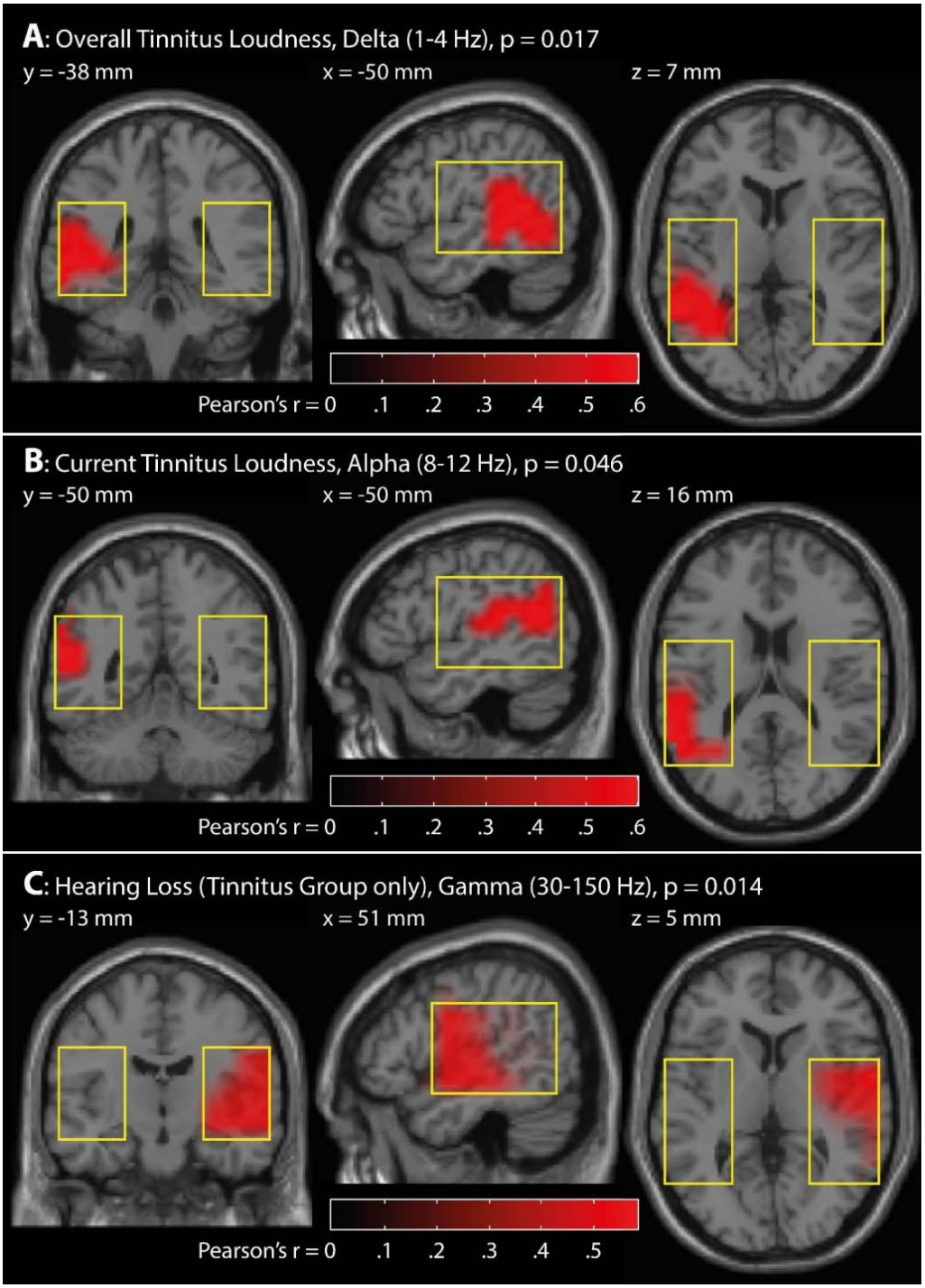

Figure 11: Significant correlates of tinnitus and hearing characteristics within the tinnitus subject group, in left and right auditory cortex regions of interest (ROIs)
Images are shown in neurological convention (i.e. left on the left), and ROI boundaries are indicated in yellow. Coordinates refer to MNI space. Significant clusters of correlation, between source power in the particular frequency and the parameter of interest, are highlighted in red. All significant correlations were positive. A: Correlation between delta power and overall subjective tinnitus loudness. B: Correlation between alpha power and current subjective tinnitus loudness. C: Correlation between gamma power and mean hearing loss.

None of these correlations were present contralaterally (i.e. in right AC for tinnitus loudness measures, or in left AC for hearing loss), even after relaxing statistical thresholds. Also, none of the observed effects were influenced by tinnitus laterality (i.e. the effects were not observed if the analyses were performed in ipsilateral and contralateral ROIs, as opposed to left and right). No significant correlations were found in the whole brain analysis.

5.4 Discussion

No group-level source power differences were found between tinnitus patients and matched controls, either in whole brain analysis or a ROI AC analysis, despite the use of optimally sensitive MEG processing and statistical analysis techniques. However, frequency band-limited correlations were found with tinnitus and hearing phenomenology, and these are discussed below according to the frequency band concerned.

5.4.1 Gamma oscillations

A principal hypothesis under investigation, driven by previous findings, was that AC gamma oscillations would correlate with the presence and/or subjective intensity of tinnitus. The present results suggest against any hypothesis of this sort, and favour the null hypothesis. While previous studies have reported increased resting state gamma power in tinnitus patients (Llinás et al., 1999; Ashton et al., 2007; Weisz et al., 2007), these studies were not controlled for hearing loss. The present finding of a strong correlation between hearing loss, in tinnitus patients, and gamma power raises the question of whether previous results can be explained by matching for hearing loss in control groups. Notably, a recent resting-state MEG study of tinnitus patients against hearing-matched controls, using sensor and beamformer source power comaprisons, found no difference in AC gamma power between groups (Adjamian et al., 2012). This is consistent with an explanation that hearing loss is a bigger determinant of gamma power than tinnitus, but does not provide any directly supportive evidence. A separate MEG beamformer study recorded from amateur rock musicians before and after band practice (Ortmann et al., 2011). During the post-practice recordings the subjects had transient hearing loss and experienced transient tinnitus; in these recordings, they exhibited localised gamma power increases in right AC (irrespective of perceived tinnitus laterality), and no other changes in oscillatory source

power. The present findings are entirely consistent with these (provided acute and chronic hearing loss share certain neural correlates), including in the laterality of power changes, and support the authors' conclusion that the gamma power probably relates more to hearing loss than to tinnitus. The present results go further, in suggesting that the gamma power is not simply a correlate of hearing loss, but also represents an interaction between hearing loss and tinnitus. In considering how these gamma power changes relate to tinnitus and hearing loss, it is helpful to bear in mind that, based on the study just described, they seem to appear very quickly after the underlying auditory insult; thus they are unlikely to represent long-term plastic changes, although changes in receptive fields and lateral inhibition can occur rapidly after auditory insults. One possibility for why gamma oscillations should increase in hearing loss is that they are a manifestation of increased spontaneous firing or neural synchrony in the auditory pathway, as is observed subcortically in animal models (Eggermont, 2013). However, this does not explain why the relationship is stronger in tinnitus patients than controls, nor why short term changes in tinnitus perception seem to usually be accompanied by significant changes in gamma power (Sedley et al., 2012a). Alterations in attention in tinnitus patients could explain the stronger relationship in tinnitus patients, in that attention to the auditory modality would be expected to increase the gain of the superficial pyramidal cells that generate gamma oscillations. An explicit attention-driven model of tinnitus has recently been proposed (Roberts et al., 2013), in which there is a mismatch between higher predictions and ascending auditory input, which drives persistent auditory attention and thereby generates or amplifies the perception of tinnitus. The present findings are consistent with increased attention in tinnitus patients (i.e. in this account, hearing loss would cause the gamma oscillations, and increased attention due to tinnitus would enhance them). This hypothesis could be explicitly tested by experimentally manipulating auditory-directed attention in future studies. Furthermore, while not explicitly expressed in these terms, the description of this model bears significant similarity to predictive coding accounts of brain function (Rao and Ballard, 1999; Friston, 2005). Given that gamma oscillations have been proposed as a generic prediction error signal (Arnal and Giraud, 2012; Bastos et al., 2012), one would therefore expect that gamma oscillations in tinnitus reflect ongoing prediction errors, rather than the tinnitus percept *per se*. This assertion has very recently been made explicitly (De Ridder et al., 2015b). Increased prediction errors in hearing loss could come about for either of two reasons. Firstly, if perception is dominated by top-down predictions

which are not accompanied by compatible sensory information then a prediction errors would arise due to the missing sensory information. Secondly, and perhaps more relevantly, the prediction errors might occur in the absence of any particular perception, simply because there is spontaneous sensory activity which does not match higher predictions or the overall percept (including not matching a prediction of silence). In the latter case, higher parts of the sensory hierarchy would act to 'tune out' this prediction error signal, which would amount to noise. Regardless of the type of prediction error, if increased attention were present in tinnitus patients, this would be expected to increase the gain on prediction error signals and hence lead to stronger gamma signals. The role of prediction errors in brain tinnitus systems is discussed in more detail in Chapter 9. An alternative, or complementary, explanation for stronger gamma correlations with hearing loss in tinnitus patients is that the stronger gamma signal arises from greater gamma synchrony between different parts of AC, which would give the appearance of a single more powerful source. Increased synchrony could arise through attention, differences in certain neurotransmitter systems such as GABA or ACh, changes in lateral inhibition or connectivity, synchronisation through lower frequency oscillations, or other tinnitus-related plastic changes.

5.4.2 Delta oscillations

This experiment was approached with a strong expectation that delta and/or theta oscillations would be a strong correlate of tinnitus, in that they would be stronger in tinnitus than control groups, and would positively correlate with subjective tinnitus loudness. This was motivated by relatively consistent observations, reported in the literature, of a positive relationship between the strength of these oscillations and the presence and intensity of tinnitus. Specifically, that these low frequency oscillations are increased in tinnitus patients compared to controls (Llinás et al., 1999; Weisz et al., 2005a, 2007; Moazami-Goudarzi et al., 2010), that they are reduced in tinnitus patients following a successful course of treatment (Tass et al., 2012), that they are reduced by transient abolition of tinnitus through electrical stimulation (De Ridder et al., 2011b), and that they are transiently reduced along with tinnitus reduction in RI or tinnitus masking (Kahlbrock and Weisz, 2008; Adjamian et al., 2012; Sedley et al., 2012a). However, as with gamma oscillations, the resting-state MEG study best-controlled for hearing loss (Adjamian et al., 2012) only found a significant increase in delta oscillations in the tinnitus with hearing loss

group compared to the control without hearing loss group, as opposed to a main effect of tinnitus. In the present results, a correlation with hearing loss was not observed in either the tinnitus or control group, making the results of the studies not quite equivalent. Nonetheless, both studies were well-controlled for hearing loss, unlike previous resting-state studies, and neither found group-level delta/theta power changes specifically attributable to the presence of tinnitus. Furthermore, a recent animal study searched for, but did not find, altered delta/theta oscillations accompanying behavioural evidence of tinnitus (Noreña et al., 2010). However, the present results did indicate a positive relationship between perceived tinnitus loudness and the strength of delta oscillations, which is consistent with most of the literature and part of the hypothesis. On balance, available evidence suggests that low-frequency delta/theta oscillations play an important role in promoting the development and/or perception of tinnitus, but are not essential for its development. Mechanistically, delta oscillations accompany deafferentation, including functional deafferentation due to internally-directed attention (Harmony, 2013) or sleep (Steriade et al., 1993), and physical deafferentation due to sensory organ damage or disconnection below the level of cortex. In tinnitus a prominent model for cortical delta/theta oscillations, TCD, is based on the observation of delta-frequency bursting in the deafferented non-specific thalamus (Jeanmonod et al., 1996) and cortex (Llinás et al., 1999), with a hypothesised causal link between the two. However, it has also been demonstrated that deafferented cortex develops coherent delta oscillations even when disconnected from the thalamus. Thus while TCD may help to explain part of the mechanisms of tinnitus, it appears neither necessary nor sufficient to explain tinnitus as a whole.

In recent years there has been a lot of interest in delta/theta oscillations as a means of organising and modulating other forms of brain activity. Initial, and repeatedly-confirmed, observations found that gamma power is linked to the phase of theta oscillations (Canolty et al., 2006), such that bursts of gamma activity occur preferentially during a certain phase of the theta cycle. Further evidence has found that low frequency phase tracks the envelope of speech stimuli, and this effect is enhanced by comprehension (Peelle et al., 2013), and that the phase of theta oscillations when a stimulus is presented predict the speed with which that stimulus is processed (Stefanics et al., 2010). Taken together, these observations point to a role for low frequency oscillations in optimising sensory responses through organising higher frequency oscillations into discrete time windows optimised to the

stimulus, which may be generic as opposed to specific for speech (Arnal and Giraud, 2012). Increased delta/theta phase to gamma amplitude coupling has recently been identified in tinnitus patients compared to controls, with reversion towards the control level following successful tinnitus treatment (Adamchic et al., 2014). This follows previous observations of abnormal delta/theta amplitude to beta/gamma amplitude coupling in tinnitus patients (Llinás et al., 1999; De Ridder et al., 2011b; Vanneste et al., 2013a). It has been proposed that delta/theta oscillations have a role in predictive timing in tinnitus (De Ridder et al., 2012), similar to what has been proposed for timing in general (Arnal and Giraud, 2012). However, tinnitus rarely has a time-varying quality to its percept (and when present the periodicity is generally slower than the delta frequency range), so it is rather unclear what predictive timing means in the context of tinnitus. The intracranial tinnitus results (Chapter 4) found that delta oscillations showed widespread tinnitus-linked coherence throughout and beyond AC, which is consistent with EEG source reconstructions finding the spatial extent of delta changes in tinnitus to be similarly large (Tass et al., 2012). Based on the intracranial results, it was argued that the delta oscillations represented a driving or coordinating network that allowed synchronous communication between parts of the tinnitus network. As the phase lags inherent in the delta coupling were very short, this meant that different parts of the tinnitus network were in approximately the same phase of the theta cycle at any given time. Given the role of low-frequency phase in delineating temporal windows for processing through higher frequency oscillations, the effect of such widespread delta synchrony would be to synchronise sensory processing across a wide area of cortex. This might allow onward connections from these cortical areas to simultaneously stimulate their target brain areas, increasing the consequent depolarisation of neurons in these target areas and thus strengthening the effect on them. In this capacity, increased strength or coherence of delta/theta oscillations may therefore act to increase the impact of tinnitus-related activity on AC on global brain networks responsible for conscious perception, thus increasing its perceptual salience.

5.4.3 Alpha oscillations

Alpha oscillations in posterior parieto-occipital regions are the most prominent type of brain oscillation in the awake state, particularly during relaxation and/or rest. Less prominent resting-state alpha oscillations are found in AC, which are reduced during attention and acoustic stimulation. Alpha power findings in tinnitus are somewhat

inconsistent; while some studies have found reduced AC alpha power in tinnitus patients (Weisz et al., 2005a; Tass et al., 2012), and alpha power reductions have been associated with the presence of illusory percepts in normal subjects (Müller et al., 2013; Leske et al., 2014), while other group level studies have found no alpha power changes (Adjamian et al., 2012) or alpha power increases in tinnitus (Moazami-Goudarzi et al., 2010). The intracranial tinnitus data (Chapter 4) found alpha decreases in auditory and other cortical regions coinciding with suppression of tinnitus. Thus a clear relationship with tinnitus is not apparent. Recent proposals for the role of alpha in tinnitus include signalling the status quo (which is the presence of sound in tinnitus patients, compared to silence in controls), or that in some instances it represents 'high theta' oscillations, rather than what is typically called 'alpha' (De Ridder et al., 2015b). In the present results, alpha power changes appeared to localise to inferior parietal lobe, which forms part of GPNs and appears to be important for tinnitus perception. It may therefore be the case that alpha power here does signal the status quo, i.e. the presence of a tinnitus sound, and that stronger alpha power is associated with an increasingly strong baseline percept of tinnitus. Thus, while overall tinnitus loudness may be influenced by delta/theta synchrony across AC, day to day variations may be due to the influence of AC tinnitus brain activity on (GPNs).

Chapter 6. Auditory cortex neurochemical correlates of tinnitus

This experiment was performed at the Newcastle Magnetic Resonance Centre (NMRC). Significant assistance was provided by a postdoctoral magnetic resonance physicist at the NMRC, Dr Jehill Parikh. Dr Parikh implemented the MRI scanner sequences necessary for the acquisition of the magnetic resonance spectra (MRS), analysed the non-GABA neurochemical estimates, and set up the analysis tools for GABA spectrum estimation. A scanner patch and data processing tools were provided by Dr Richard Edden. The scans themselves were performed by radiographers at the NMRC. Limited patient recruitment was performed by Valerie Tait, a clinical audiologist at the Freeman Hospital, Newcastle upon Tyne. My roles were to conceive and design the study, plan and conduct screening and phenomenological assessments, recruit subjects, position the voxels used for MRS acquisition in each subject, analyse all data except the non-GABA metabolite concentrations, perform statistical analyses, interpret results and produce figures. This work has been submitted for publication.

6.1 Aims

Inhibitory neurotransmission is of considerable interest in tinnitus, as deficiency of inhibition could underlie or exacerbate tinnitus, and augmentation of inhibition could prove a viable treatment. GABA systems are of considerable interest in tinnitus, as discussed in Section 1.3.4, with deficient levels and action of GABA identified in the auditory pathway of animals with behavioural evidence of tinnitus (Brozoski et al., 2012). However, dramatic changes in excitatory and inhibitory neurotransmission occur as direct consequences of peripheral auditory insults (Gold and Bajo, 2014), so it is difficult to know how these findings relate specifically to tinnitus as opposed to other consequences of underlying auditory deafferentation. The main aim was therefore to establish whether GABA concentrations in AC are altered in patients with tinnitus once other factors such as hearing loss are controlled for.

The role of the cholinergic system in tinnitus has received less attention, though a recent model links persistent overactivation of auditory attention, mediated by the BF cholinergic system, to the presence and/or severity of tinnitus (Roberts et al., 2013). Furthermore, both ACh, and the membrane phospholipid parts of the cholinergic system, are likely to be

linked to neuronal plasticity, which has received considerable attention in tinnitus. Thus a secondary aim was to establish whether total choline concentrations correlated with the presence or perceived loudness of tinnitus.
Observed findings could help to identify which neurotransmitter systems might be most fruitfully targeted in the treatment of tinnitus, and the way in which they might best be targeted.

6.2 Methods

6.2.1 Subjects

Fourteen subjects with entirely or predominantly unilateral tinnitus (8 left) were recruited through a combination of referral from a local audiology clinic and advertisement on local research mailing lists and in the magazine of the British Tinnitus Association, 'Quiet'. Inclusion criteria were chronic subjective tinnitus that was at least predominantly lateralised to one ear and had been present for at least 6 months, and age 18 years or over. Exclusion criteria included contraindications to MRI, a neurological disorder other than tinnitus, the use of sedating medications, benzodiazepines, antiepileptic drugs or tricyclic antidepressants. Subjects were recruited in such a way that half of the group had hearing loss, defined as mean threshold between 0.25 and 8 kHz > 20 dB, more than two frequencies in a single ear having thresholds > 20 dB, or any single frequency having a threshold of > 30 dB. The groups were not formally stratified for hearing loss, but the intention was to obtain a good range of levels of hearing loss, and to include subjects with normal hearing. Once each tinnitus subject had been studied, a control subject was sought who matched for sex, age and pattern/degree of hearing loss. Control subjects without hearing loss were recruited through a local mailing list for volunteers interested in research studies. Control subjects with hearing loss were also recruited through this mailing list, and through word of mouth via existing participants, but by specifically requesting individuals with formally documented mild to moderate hearing loss, or who believed that they had hearing loss. These individuals then attended a pre-screening session, which included a pure-tone audiogram as detailed in section 5.2.2. Screened controls who were the closest matches specific tinnitus subjects were then invited to take part in the full study.

6.2.2 Phenomenological assessment

Subjects who had not already had pure tone audiometry had this performed, as described in Section 5.2.2. Tinnitus spectra were also measured as described in Section 5.2.2, with the exception that frequencies 0.25 to 8 kHz in octave steps, with the addition of 6 kHz, comprised the spectra. All subjects completed the following questionnaires: the HQ (Khalfa et al., 2002), HADS, PHQ-15. Tinnitus subjects also completed the THI (Newman et al., 1996), and gave VAS ratings of their tinnitus loudness and associated distress. For each VAS rating, subjects gave four responses: 1) the rating applicable to an average or typical day; 2/3) the lowest and highest ratings applicable at any point over the past 3 months; 4) the rating applicable at the time of the experiment. The 'average/typical' rating is referred to as the 'overall' loudness of distress. The rating applicable to the time of the experiment was converted into a 'current' loudness or distress rating, ranging from 0 to 10. This was done by interpolation, such that the lowest 3-month rating corresponded to 0, the average rating to 5, and the highest 3-month rating to 10. The rationale for distinguishing overall from current loudness and distress was to be able to make a distinction between static and dynamic tinnitus correlates (if one exists), which might help make a 'state-trait' distinction.

6.2.3 Magnetic resonance spectroscopy (MRS) acquisition

Data were acquired using a Philips Achieva 3 Tesla (3T) whole body MRI scanner, using an 8-channel head coil. To limit the potential influence of diurnal variation in metabolite concentrations, scans were all performed in the first half of the morning. As scanner heating and cooling, leading to frequency drifts, can affect spectroscopic measurements, no scans were performed after any sequences that lead to increased heating of the scanner magnets. First, a structural T1-weighted brain image was acquired. Subjects listened to music or radio of their choice before, during and after this scan, but this was stopped prior to the MRS sequences, in case current auditory environment had any impact on AC metabolite concentrations. MR spectra were acquired from left (LAC) and right (RAC) AC, in random order. The acquisition volumes were configured, through pilot experiments, so as to yield robust spectra while limiting the amount of non-auditory brain tissue sampled. These measured 45 (anterior-posterior), by 32 (right-left) by 20 (inferior-superior) mm. Volumes were positioned by first adjusting the pitch (rotation in the saggital plane) until they were parallel with the Sylvian fissure. Next they were positioned with their upper edge aligned with the Sylvian fissure, but with as little sampling of parietal

cortex as possible while still encompassing the superior temporal plane. In the axial plane, the centre of the volume was aligned with Heschl's sulcus (or the most anterior Heschl's sulcus if HG was duplicated), and moved as far anterolaterally as could be achieved with all of the volume remaining within the boundaries of the cortical convexity. This volume included A1, almost all of HG, much of the STG, planum temporale, superior temporal sulcus, planum polare, and some parts of MTG and insula. See Figure 12A for an example of RAC volume placement in one example subject.

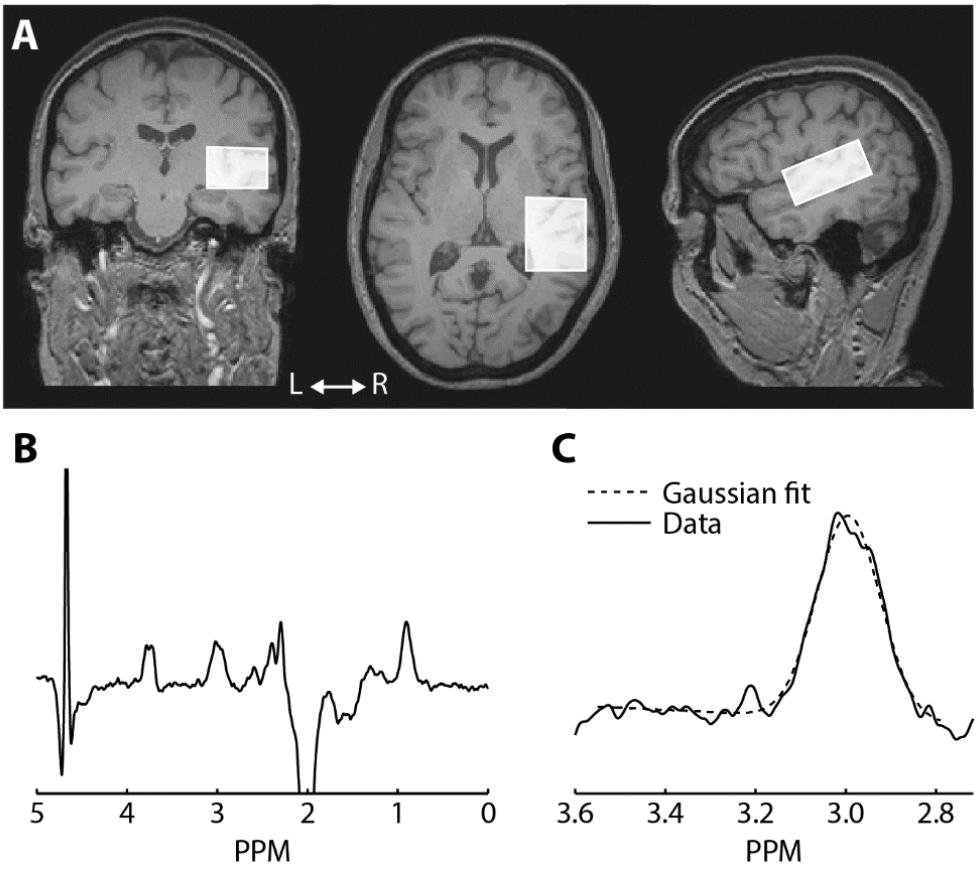

Figure 12: Volume placement and associated GABA spectrum from one representative subject
A: Coronal (left), axial (middle) and saggital (right) sections from the subject's T1 weighted MRI scan. The MRS volume is superimposed in white. The brain image is displayed in neurological convention (i.e. left on the left). B: GABA spectrum, obtained by contrasting averaged edited and non-edited spectral acquisitions from the volume illustrated in A. Note the artefact at 2 PPM due to the editing pulse. C: Zoomed view of part of B including the GABA peak at 3 PPM (solid), and the optimal Gaussian fit to that peak (dashed). The Gaussian fits to the 3 PPM peaks formed the basis of GABA quantification.

Once the volumes of interest had been specified, these were used for the acquisition of magnetic resonance (MR) spectra. Similarly to the basis for MRI, when hydrogen nuclei (protons) are exposed to a strong magnetic field they align to the direction of the field. The addition of an appropriate radiofrequency pulse causes the protons to be displaced from this alignment, and then to oscillate as they return to an aligned state. The frequency of oscillation of a given proton depends on its immediate chemical environment (i.e. the molecule in which it exists), and thus each molecule exhibits a characteristic frequency profile (i.e. spectrum). The resulting spectra can then be decomposed into the contributions of major metabolites, based on their known spectral shapes and frequencies.

GABA has three peaks in its MR spectrum (close to 2, 3 and 4 parts per million [PPM] on the scanner presently used). All of these peaks coincide with the far larger peaks of more abundant metabolites, for instance N-acetylaspartate (NAA) at 2 PPM. Therefore quantifying GABA directly is not feasible. Several techniques exist for measuring GABA spectra, and the approach used here is known as Mescher-Garwood proton resolved spectroscopy (MEGA-PRESS) (Mescher et al., 1998). In this technique, each spectral acquisition is paired with a radiofrequency pulse coinciding with the frequency of the GABA peak that coincides with the NAA peak (1.9 PPM here). This is known as an 'editing' pulse, and acts to remove the contribution of molecules at that frequency from the MR spectrum. Though the pulse is applied at the frequency of just one of the GABA peaks, it disrupts all three of them. Thus, subtraction of edited from non-edited spectra isolates the contribution of GABA, and allows it to be quantified. Is bears mention that GABA is not strictly the only metabolite quantified with this method, but there are also macromolecules with similar resonance properties which are also quantified. Thus the measurement made is more correctly termed 'GABA+' to reflect this contribution. While techniques exist to suppress macromolecules, they incur a significant loss of SNR, and are therefore not usually used (Edden et al., 2012). In the present experiment, the specific acquisition parameters were as follows: TR 2000ms; TE 68ms; 320 averages; acquisition bandwidth 1000Hz; scan duration 11 mins; sinc Gaussian editing pulse applied at 1.9 ppm (during EDIT-ON scans) and 7.5ppm (during EDIT-OFF scans); voxel size 45 (AP) x 32 (RL) x 20 (FH) mm for both LAC and RAC; VAPOR water suppression (Tkác et al., 1999). Non-water-suppressed spectra were also obtained from each AC (PRESS, TE=68ms, TR: 2000ms, 10 averages). Prior T1-weighted structural scans (3D MPRAGE, sagittal acquisition aligned with the AC-PC line, 1 mm isotropic resolution, matrix 240 x 240 x

180, TR = 9.6 ms, TE = 4.6 ms, flip angle = 8o, SENSE factor 2) were acquired to aid positioning of the MRS voxels.

6.2.4 Metabolite concentration estimation

GABA spectra were quantified using the Gannet toolbox for Matlab (Edden et al., 2014). The steps involved included correction of drift in creatine frequency (used as a reference point) across acquisitions, identifying and rejecting bad acquisitions, subtracting edited from non-edited spectra, averaging these subtractions, and fitting a Gaussian function in order to quantify the GABA peak at 3 PPM. Figure 12B/C shows an example GABA spectrum (subtraction of edited from non-edited spectra), and a zoomed view of the 3 PPM GABA peak along with the optimal Gaussian fit. These analysis steps were performed while the subject was still in the scanner, so that the scan could be repeated if, for any reason, a poor quality spectrum was obtained. Offline, further processing was performed as follows. Each subject's T1 weighted structural image was segmented into GM, WM and CSF using the SPM12 toolbox for Matlab. The proportions of each of these tissue types within the volumes of interest (tissue fractions) were then calculated. GABA measurements were converted to concentrations (in mM), based on a previously published correction equation incorporating the GABA measurement, water concentration and tissue fractions (Gao et al., 2015). Creatine, Choline and NAA spectra were quantified using the AMRES fitting algorithm in jMRUI software. Similarly to with GABA, these were converted into tissue concentrations.

6.2.5 Statistical analysis

Non-parametric statistics were used, namely the Friedman test for main effects of group, Wilcoxon rank sum tests for post-hoc group differences in individual hemispheres, and Spearman rank correlation coefficients for correlations. GABA and choline were treated as primary outcome measures, and therefore not subjected to multiple comparison penalties. Creatine and NAA measurements were treated as exploratory, and thus subjected to Bonferroni correction. Metabolite concentrations were compared between tinnitus and control groups, and regressed against key tinnitus measures of interest, and hearing loss.

6.3 Results

6.3.1 Subject characteristics

Fourteen tinnitus patients and an equal number of matched controls were studied. No significant differences were present between groups in terms of age, hearing loss in either ear or hyperacusis. There was one extra female subject in the control group compared to the tinnitus group. Mean tinnitus duration was 9.4 years (range 2 to 29). Eight of the tinnitus patients had left-ear-predominant tinnitus compared to 6 right-ear. Table 2 summarises the group characteristics, and Figure 13A the group hearing thresholds.

	Control	Tinnitus	Difference (p)
Group size (n)	14	14	
Age (years)	55.7 (10.6)	53.7 (15.1)	0.87
Sex (n female)	7/14	6/14	
Mean HL L (dB)	19.4 (14.4)	18.8 (15.3)	0.91
Mean HL R (dB)	17.4 (11.5)	18.0 (20.2)	0.58
Hyperacusis (HQ)	11.6 (5.7)	13.6 (6.4)	0.30
T duration (years)		9.4 (7.6)	
Laterality (n left)		8/14	
THI		26.7 (13.2)	
Overall loudness		3.9 (1.8)	
Current loudness		4.3 (2.3)	
Overall distress		3.1 (1.6)	
Current distress		3.9 (2.2)	

Table 2: Subject characteristics of tinnitus and control groups.
Non-bracketed and bracketed numbers indicate mean and SD respectively. p = p value between tinnitus and control groups, based on Wilcoxon rank sum statistic. HQ = Hyperacusis Questionnaire score. THI = Tinnitus Handicap Inventory.

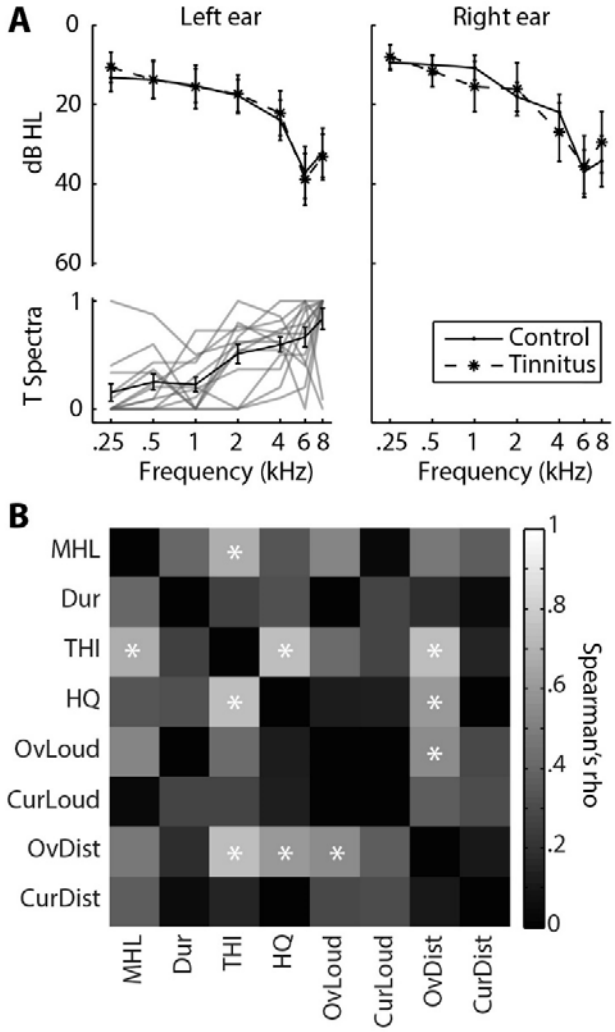

Figure 13: Group audiometric assessments, and correlations between tinnitus variables

A: Mean pure tone hearing thresholds of tinnitus and control groups. Error bars represent standard error of the mean. Below the left ear plot is the individual (grey) and group mean (black) tinnitus spectra from the tinnitus group. Error bars indicate standard error of the mean. The values 0 and 1 represent the lowest and highest (respectively) tinnitus likeness ratings given by each subject. The spectrum is omitted from one subject, who gave a 0/10 rating for all pure tones. B: Positive non-parametric correlations between hearing and tinnitus measures within tinnitus group. Significant ($p < 0.05$ uncorrected) correlations are denoted by asterisks. No negative correlations close to significance were observed, hence only positive correlations are shown. MHL = mean hearing loss (dB; across all frequencies shown in A). Dur = tinnitus duration (years). THI = Tinnitus Handicap Inventory. HQ = Hyperacusis Questionnaire. OvLoud = 'overall' VAS loudness. CurLoud = 'current' VAS loudness. 'OvDist' = 'overall' VAS tinnitus distress. 'CurDist' = 'current' VAS tinnitus distress. VAS = visual analogue scale.

There were significant positive correlations between certain tinnitus measures, as illustrated in Figure 13B. Most notably, THI score correlated with hearing loss and

hyperacusis, and VAS overall tinnitus distress score correlated positively with HQ, THI and VAS overall tinnitus loudness scores. Based on these correlations, and the prior relative interest in certain measures above others, hyperacusis and overall VAS distress were eliminated from further analysis.

6.3.2 Tissue fractions (structural brain changes)

There were no (uncorrected) significant differences in any of the tissue fractions (GM, WM or CSF), in either hemisphere, between tinnitus patients and controls (Figure 14A). However, within the subject group as a whole, GM fraction correlated negatively with both age (LAC: rho = -0.57, p = 0.0016; RAC: rho = -0.48, p = 0.009) and hearing loss (LAC: rho = -0.59, p = 0.001; RAC: rho = -0.49, p = 0.0078), and CSF fraction correlated positively with age (LAC: rho = 0.52, p = 0.0047; RAC: rho = 0.56, p = 0.0019) and hearing loss (LAC: rho = 0.25, p = 0.20; RAC: rho = 0.40, p = 0.033). These results are shown in Figure 14B.

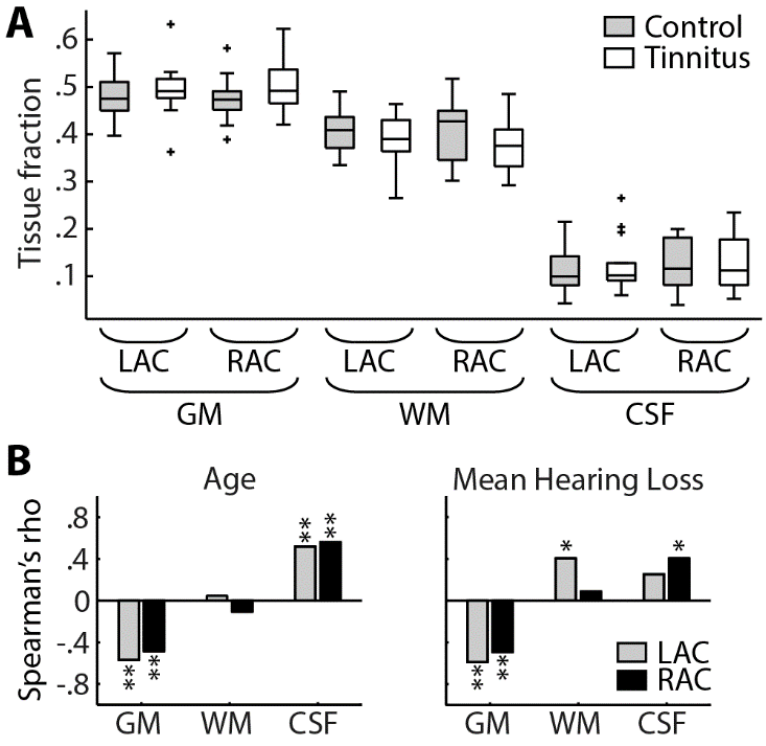

Figure 14: Auditory cortex tissue fractions related to tinnitus and other factors. A: Grey matter (GM), white matter (WM) and cerebrospinal fluid (CSF) fractions from left (LAC) and right (RAC) auditory cortex voxels used for spectroscopy, in tinnitus and control subjects. No significant differences were present. Boxes indicate interquartile range, with horizontal line at the median, whiskers indicate full range, barring outliers

which are indicated with '+' signs. B: Non-parametric correlations between tissue fractions, and age (left) and mean hearing loss (right). * = $p < 0.05$. ** = $p < 0.01$.

6.3.3 GABA spectroscopy

Compared to controls, the tinnitus group showed GABA decreases in LAC (median 0.99 vs. 1.08 mM/L) and RAC (median 1.12 vs. 1.28 mM/L). Friedman's test showed a significant main effect of subject group ($p = 0.015$), and Wilcoxon rank sum tests found the difference to be significant in RAC ($p = 0.018$) but not LAC ($p = 0.30$). These results are shown in Table 3 and Figure 15. There was no significant difference in RAC GABA concentration between the left and right ear tinnitus patients ($p = 0.85$). GABA concentrations showed no significant correlation with age, sex, hearing loss, hyperacusis, or any of the tinnitus severity measures.

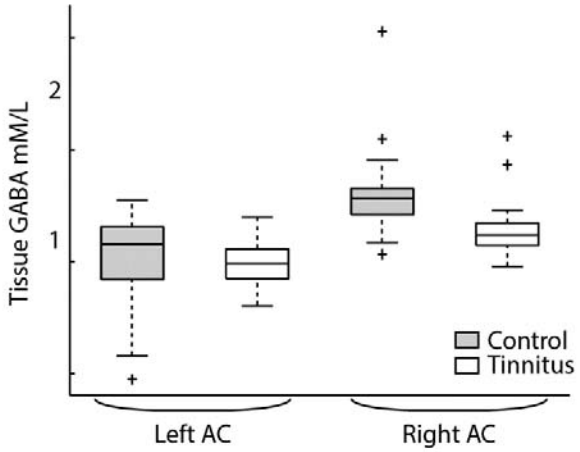

Figure 15: Auditory cortex GABA concentrations in tinnitus and control groups. AC = auditory cortex. Boxes indicate interquartile range, with horizontal line at the median, whiskers indicate full range, barring outliers which are indicated with '+' signs. GABA was significantly reduced ($p < 0.05$) as a main effect of subject group (tinnitus vs. control) and in RAC. Results displayed here are also tabulated in Table 3.

	Left AC			Right AC			
	Control (mM/L)	Tinnitus (mM/L)	p =	Control (mM/L)	Tinnitus (mM/L)	p =	Combined p =
GABA	1.08 (0.24)	0.99 (0.13)	0.30	1.28 (0.12)	1.12 (0.10)	**0.018**	**0.015**
Choline	2.72 (0.60)	2.60 (0.38)		3.43 (0.82)	3.23 (0.71)		0.15
NAA	13.5 (2.17)	13.7 (1.64)		15.2 (2.22)	15.3 (1.47)		0.67
Creatine	8.03 (2.36)	7.76 (1.48)		9.75 (2.13)	9.61 (4.22)		0.21

Table 3: Metabolite concentrations for tinnitus and control groups.
Where applicable, non-bracketed and bracketed numbers correspond to median and interquartile range respectively. Combined p values are uncorrected (though GABA represents a primary hypothesis), and are based on Friedman's test, treating hemisphere as a blocking variable. Where these are significant, p values are shown for left and right AC, which are based on Wilcoxon rank sum tests. Significant group differences are shown in bold.

6.3.4 Choline spectroscopy

Choline concentration was not significantly different between tinnitus and control groups (see Table 3). RAC choline correlated with overall VAS tinnitus loudness (rho = 0.050, p = 0.069 uncorrected), THI score (rho = 0.73, p = 0.034 corrected for all choline comparisons made), hearing loss in the subject group as a whole (rho = 0.62, p = 0.0055 corrected), hearing loss in the tinnitus group (rho = 0.81, p = 0.0078 corrected), and hearing loss in the control group (rho = 0.41, p = 0.14 uncorrected). These correlations are illustrated in Figure 16. As choline is present in higher concentrations in WM than GM (Rae, 2014), and tissue composition correlated with age and hearing loss, significant correlation analyses were repeated after partialling out age, hearing loss and all tissue fractions from both RAC choline concentration and the subject variable of interest. It should be borne in mind that such extensive partialisation removes a lot of variance from the data, therefore the same strength of correlation cannot be expected. Nonetheless, these partial analyses showed that the correlation between hearing loss and choline in the whole subject group remained

significant (rho = 0.39, p = 0.040 uncorrected) and the majority of the correlation between choline and THI score remained (rho = 0.41, p = 0.15 uncorrected).

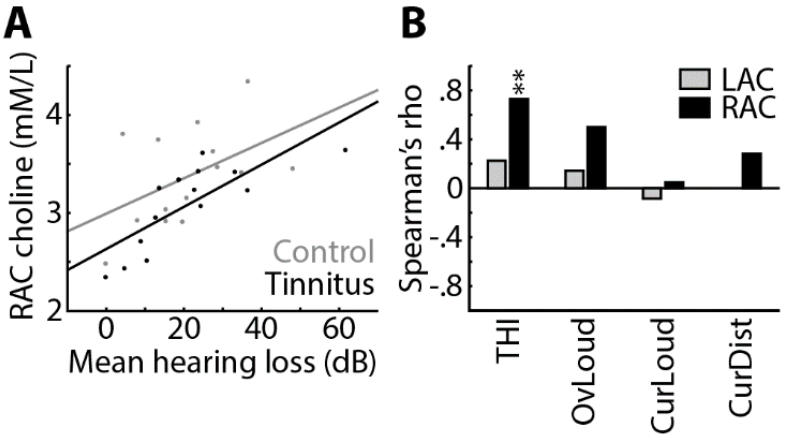

Figure 16: Correlations between choline concentration and subject variables
A: Relationship between mean hearing loss and right auditory cortex (RAC) choline concentration in control (grey) and tinnitus (black) groups. Dots denote individual subjects, and lines represent least squares best linear fits. B: Spearman's rank correlation coefficients (rho) between choline and subjective tinnitus variables in bilateral auditory cortices, within the tinnitus group. THI = Tinnitus Handicap Inventory. OvLoud = VAS overall tinnitus loudness. CurLoud = VAS current tinnitus loudness. CurDist = VAS current tinnitus distress. VAS = visual analogue scale. ** = $p < 0.01$ uncorrected.

6.3.5 NAA and creatine spectroscopy

There were no group level differences between tinnitus and control groups for NAA or creatine, in either AC, even before Bonferroni correction. Choline and NAA both reflect neuronal density (Miller et al., 1996), therefore testing was performed to see whether similar correlations existed with hearing loss and THI scores with NAA, as there were for choline, which might indicate a structural basis to observed changes. NAA did not correlate significantly with either mean hearing loss (p = 0.95 uncorrected) or THI score (p = 0.76 uncorrected).

6.4 Discussion

This study featured a group of tinnitus patients and controls matched for age, sex, hearing loss and hyperacusis, thus observed differences can reasonably be inferred to relate to tinnitus as opposed to any of these confounding factors. As macromolecule suppression was not performed, for reasons of preserving SNR and allowing greater robustness to subject motion, all GABA results should be considered as indicating 'GABA+' (i.e. GABA

plus macromolecules). MRS measurements were made from a large voxel spanning almost all of AC, encompassing primary and association areas, and including some areas of surrounding non-auditory cortex. Such a large sampling area has the advantage of providing a robust GABA measurement, and is likely to be appropriate in tinnitus, where ongoing abnormal neurophysiological signals have been found to occur across a correspondingly large anatomical area as opposed to just circumscribed parts of AC (Chapter 4). However, the exact size and position of the voxel used could influence the sensitivity for detecting changes in other factors that might correlate with neurotransmitter concentrations in more localised parts of AC. Such a voxel size and placement issue might explain a relationship was not observed between GABA concentration and hearing loss, as was recently reported in association with age-related hearing loss (Gao et al., 2015). However, the present study had other methodological differences to this one, including studying undifferentiated hearing loss as opposed to specifically the age-related type. For all significant results, there were qualitatively similar findings in LAC as in RAC, but the findings were much stronger, and only significant in, RAC. The 20% loss of signal observed in LAC can be potentially explained by spatial effects influencing GABA MRS measurements (Edden and Barker, 2007). Specifically, there are small deviations between specified voxel position and 'actual' voxel volume from which measurements are made, and it is likely that asymmetry in these deviations resulted in diminished signal from LAC. Thus, it is possible that in reality the observed neurochemical correlates of tinnitus are bilateral. However, direct evidence must be obtained before any conclusion can be made that this is the case. While there was a slight excess of left ear-predominant tinnitus subjects (8 vs. 6), there were no significant differences between left and right ear tinnitus even after markedly relaxing statistical thresholds, making tinnitus laterality a very unlikely explanation for hemispheric differences.

6.4.1 GABA in tinnitus

This study demonstrates, for the first time, an AC GABA deficit in human tinnitus subjects. Given the tight matching of the control group for age and hearing loss, this deficit can be specifically attributed to tinnitus itself. Presently the implications of this finding for understanding tinnitus pathophysiology as a whole are uncertain, though in light of findings in animal tinnitus models (Middleton et al., 2011; Llano et al., 2012) it is likely that this GABA deficiency is responsible for excessive magnitude and lateral spread of

cortical responses to thalamic stimulation. Therefore, GABA deficiency may underlie excessive sound-evoked (Gu et al., 2010) activity that has previously been observed in tinnitus in humans, even after matching for hearing loss and hyperacusis, and excessive amplification or synchrony of SA that is believed to contribute to tinnitus. It is possible that GABA deficiency is a primary cause of tinnitus that, in conjunction with hearing loss, removes the necessary inhibition to prevent SA in the auditory system from being perceived as tinnitus. It is also plausible that it is the direct consequence of chronic stimulation (by tinnitus or its precursors originating subcortically) of the auditory cortex, but there is a lack of evidence about the effect of chronic sensory stimulation on cortical GABA concentration that could address this possibility. It is also uncertain whether this GABA deficit is a cause or consequence of tinnitus. While there was not a relationship between tinnitus duration and GABA concentration, which would have favoured the GABA deficit being a consequence of tinnitus, this question remains open. Regardless of the exact origin and role of cortical GABA in tinnitus, it seems probable that it is a significant positive force in its pathogenesis, as reduced GABA concentration most likely indicates reduced GABA-ergic inhibition and therefore a relative excess of excitation in the auditory system. While there is still the need for understanding other aspects of GABA systems in tinnitus such as receptor density, which presently only has limited evidence in humans, from a study lacking clear controls (Shulman et al., 2000), the current evidence suggests that drugs acting to increase GABA concentrations could be an effective way of modulating GABA-ergic inhibition in tinnitus. As well as replicating the present findings, future studies of GABA systems in humans might involve combining GABA measurements using MRS with GABA receptor measurements using positron emission tomography (PET). In animals, a number of additional measures, such as GAD expression and GABA receptor behaviour, might also be simultaneously measured. Studies might also examine acute, as well as chronic, tinnitus to establish the temporal order of tinnitus phenomenology and GABA changes, and also the effect of chronic physiological auditory stimulation on GABA systems.

6.4.2 Choline in tinnitus

These results indicate that auditory cortex choline concentration correlates positively with both tinnitus severity (in terms of distress, and possibly loudness also) and hearing loss (particularly in the tinnitus group). Choline is strongly influenced by neuronal density

(Miller et al., 1996), and GM loss (hence increased WM to GM ratio) was found to increase with hearing loss, as previously reported (Husain et al., 2011). However, given the relative persistence of observed findings after statistically adjusting for the influence of GM and WM tissue fractions, it seems probable that choline relates directly to hearing loss and tinnitus. As choline measured by MRS reflects increased neuronal membrane turnover (Rae, 2014), which may relate to plasticity (Gutiérrez-Fernández et al., 2012), and (though ACh barely contributes to the choline signal) correlates strongly with local concentration of ACh (Wang et al., 2008), it cannot presently be determined which of these factors is perturbed as a function of hearing loss and tinnitus severity. Further work to directly measure neuronal plasticity and ACh is required to understand the relationship between choline and tinnitus.

6.4.3 Conclusions

In summary, this study has specifically related the presence and severity of tinnitus, after eliminating confounding factors, to non-invasively measured metabolite concentrations in AC. The finding of a GABA deficit in tinnitus patients is beyond a homeostatic response to hearing loss, and underscores the importance of GABA systems in the pathophysiology of tinnitus and may help to direct future treatments. The correlation of choline with tinnitus severity is a novel and exciting finding, which requires further study.

Chapter 7. EEG auditory steady state responses (ASSRs) in tinnitus

This study was performed on the same subjects who participated in the MRS experiment (Chapter 6), barring two who did not complete this stage of the experiments. Aside from the limited assistance with recruitment mentioned previously, all aspects of this experiment were performed by me.

7.1 Aims

This study aimed to quantify 40 Hz ASSRs, recorded with EEG, in tinnitus and matched control patients, in order to try and gain insight into abnormal auditory gain and inhibition mechanisms associated with tinnitus, particularly ones that might relate to AC neurochemical measurements. However, the relationship between the presence of tinnitus and ASSR amplitudes, at any frequency, is not consistent in the literature (as discussed previously), with studies variably finding decreases, no change, or increases associated with tinnitus. A number of methodological differences might have been responsible for the inconsistent findings, including matching of control subjects for hearing loss, loudness of AM tones used, method of determining AM tone loudness, and the presence of hyperacusis. With regard to loudness, different results are likely to be obtained by using a fixed sound pressure level (SPL; which would lead to smaller responses with increasing hearing loss), a fixed sensation level (SL, = SPL – hearing threshold; which would lead to increased responses with hearing loss, due to loudness recruitment), and psychophysical matching to a normal-hearing frequency (which would be influenced inversely to the degree of hyperacusis). A single study found that in control subjects presentation of multiple carrier tones with slightly different modulation frequencies reduced the amplitude of the ASSRs compared to individual modulated tones, whereas in tinnitus subjects the same condition led to increased ASSR amplitudes (Diesch et al., 2010) in the ‘edge’ tones, and less suppression of the ‘central’ tone. These findings were interpreted as evidence of reduced lateral/surround inhibition in tinnitus, and/or with increased lateral/surround summation. The present experiment aimed to address three questions:

1) How ASSR magnitudes vary between tinnitus and control subjects, once hearing loss, hyperacusis and loudness recruitment are controlled for.

2) Establish whether the finding of reduced ASSR inhibition during multiple AM tone presentations could be replicated and generalised.

3) Whether the magnitude of ASSRs, or the extent of lateral/surround inhibition would correlate with AC GABA or choline concentration.

7.2 Methods

7.2.1 Subjects

The subjects, and recruitment procedure, have been described in Section 6.2.1.

7.2.2 Phenomenological assessment

Phenomenological assessment procedures have been described in Section 6.2.2.

7.2.3 EEG data acquisition

Subjects' heads were individually measured, and markings were made at 21 electrode sites from the 10-20 system. At each location, the scalp was gently cleaned and abraded, and an AgCl electrode was attached with electroconductive paste. These were attached to a Neuroscan SynAmps 64 channel amplifier (Neuroscan, Compumedics Ltd., Abbotsford, Victoria, Australia), operated with standard Neuroscan Acquire software. Cz was used as a reference, and impedances were kept under 5 kΩ. Recordings were made with participants seated comfortably in a dimply-lit sound-proof chamber. To maintain alertness, subjects watched a cartoon film without the sound, and were instructed to remain awake, with their eyes open, and to maintain a state of physical muscle relaxation. Subject wakefulness was monitored via live EEG data and a video feed. Stimuli were pure tones of 12 s duration, with carrier frequencies of 1 or 4 kHz (below and generally within the tinnitus spectrum, respectively), and a sinusoidal amplitude modulation (AM) of 40 Hz with 100% modulation depth. For each carrier frequency, two conditions were included: one with just the individual AM tone, and another with two additional AM tones present. The additional AM tones had carrier frequencies one octave above and below the carrier frequency of the main tone, and modulation rates of 38 and 42 Hz respectively. The spacing of one octave was chosen because it has been shown to result in inhibition of 40 Hz ASSRs - generated at the level of A1 - but not of ASSRs with higher modulation rates – generated subcortically (John et al., 1998). Thus, it was anticipated that this stimulus configuration

would specifically address lateral/surround inhibition within A1. Thus four stimulus conditions were tested: 1 kHz and 4 kHz carriers, each in isolation and with additional AM tones. Each stimulus was 12 s long, and a total of 50 repetitions of each stimulus were presented in random order. Each AM tone was scaled to a loudness of 60 'phon' in each ear (i.e. the perceptual loudness experienced by a subject with pure tone thresholds of zero in response to a stimulus presentation at 60 dB SPL), using the following dB to phon conversion method, using an algorithm to predict loudness recruitment based on the subject's audiogram (Moore and Glasberg, 2004). Estimation of loudness recruitment was performed using a freely available application developed by the authors of this study, which takes account of the stimulus power spectrum and the subject's audiogram. To try and avoid subjects with cochlear dead regions, which can influence loudness recruitment estimation, only subjects with mild to moderate (or no) hearing loss were included. As the loudness recruitment estimation algorithm does not have an easily-implementable inverse, the correction was performed by an iterative cycle of estimated loudness recruitment for a particular stimulus, then adjusting the stimulus loudness, until the output loudness matched the desired loudness. Simuli were presented diotically, with a fixed inter-stimulus interval of 1 s. Sound delivery was through Sennheiser HD 380 pro headphones, and prior calibration was performed using a Bruel and Kjaer artificial ear type 4153, with pressure field microphone type 4192, and sound level meter type 4231 to ensure delivery at the appropriate sound pressure level. Mean SPLs (dB), to achieve these 60 phon estimated loudnesses, for the 1 kHz stimuli were 64.4 (left) and 63.3 (right), and ranges were 56.9-79.6 (left) and 60.0-74.2 (right). Mean SPLs for the 4 kHz stimuli were 73.5 (left) and 71.4 (right), with ranges 57.8-97.8 (left) and 59.1-101.8 (right). Stimulus sensation levels (SLs; defined as SPL minus hearing threshold) for the 1 kHz stimuli were mean 50.3 and 53.6 (left and right ears respectively), and for the 4 kHz stimuli were mean 50.1 in both ears.

7.2.4 EEG data processing

EEG data were rearranged into epochs of 1 s duration, with the middle 10 epochs used for each stimulus and the first/last epochs discarded. Epochs were manually inspected for muscle or other artefacts, and artefact-containing epochs discarded. Eye movements and blinks were allowed to remain, as these were removed subsequently using ICA, which was performed after rejection of bad epochs, and was performed using the FieldTrip toolbox for Matlab. Components containing significant line noise, ocular or cardiac artefact were

removed from the data. Epochs were then averaged within each stimulus condition, and Fourier transformed. Analysis was performed in sensor space, as accurate co-registration with individual subjects' MRI scans was not possible. To determine the electrode pair with the highest SNR, contrasts of Fourier transformed data were performed between every possible combination of electrodes. For each pair, the absolute value of the spectrum was taken. 'Signal' was quantified as the value at 40 Hz, and 'noise' the average value between 30 and 50 Hz, excluding 38, 40 and 42 Hz. In nearly all individual subjects, and in the group as a whole, the channel pair Cz/Oz gave the highest SNR, and was therefore used as the basis for further analysis. Although the use of this pair did not allow distinction of the ASSRs in the left and right hemispheres, it was judged that the increased SNR was more important than this distinction, which was not necessary for addressing the aims of the study. For each condition in each subject, the 'signal' value in the channel pair Cz/Oz was used as the basis for statistical analysis. The analysis just described provides a frequency resolution of 1 Hz. For the purpose of displaying ASSR spectra, 1 s epochs were concatenated into blocks of 25 s prior to Fourier transformation, thus producing a 0.04 Hz frequency resolution. An example of one subject's ASSR spectra for the four conditions is shown in Figure 17A/B.

7.2.5 Statistical analysis

ASSR amplitudes for each stimulus condition were compared between tinnitus and control groups using a Student's T test. As there was a prior hypothesis that 4 kHz ASSRs would differ between groups, no penalty for multiple comparisons was made here. Other comparisons were subject to Bonferroni correction. The same applied to the 4 kHz response as part of the multiple AM tone presentation condition. Pearson product moment correlation coefficients were also calculated between ASSR amplitudes and metabolite concentrations as measured in Chapter 6.

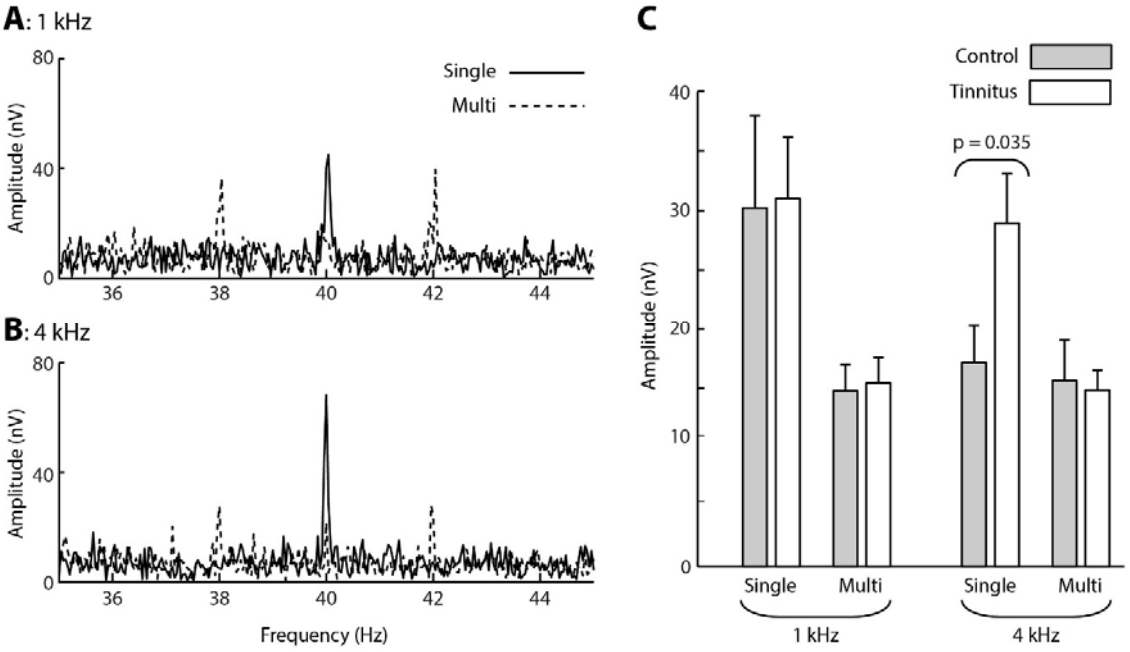

Figure 17: EEG auditory steady state responses (ASSRs) to amplitude modulated (AM) pure tones presented at 60 phon
A and B: ASSR frequency spectra, from one tinnitus subject, to 1 and 4 kHz carrier tones (respectively), with (solid) and without (dashed) the addition of additional AM tones with carrier frequencies one octave above and below, and modulation rates 2 Hz above and below. C: Group ASSR amplitudes for the 40 Hz AM tone in the four stimulus conditions, expressed as mean and standard error, for the control (grey) and tinnitus (white) groups. 'Single' = AM tone presented in isolation. 'Multi' = AM tone presented with additional AM tones.

7.3 Results

Figure 17C summarises the group level results for the four stimulus conditions. Tinnitus subjects showed significantly higher amplitude ASSRs to 4 kHz tones presented in isolation ($p = 0.035$), but not to 1 kHz tones. The addition of octave-separated AM tones reduced the amplitude of ASSRs to both 1 kHz and 4 kHz carriers, in both tinnitus and control subjects. No differences between subject groups were found in the amplitude of ASSRs in the conditions where additional AM tones were present, but notably the amplitude reduction in the multiple presentation mode was so great that responses were close to the noise floor, and therefore may not have been reliably quantified. There were no significant correlations between ASSR amplitudes in any stimulus condition and cortical concentrations of GABA or choline, even before Bonferroni correction.

7.4 Discussion

The finding that 40 Hz ASSR amplitudes to AM tones in the tinnitus spectrum (here 4 kHz) needs to be interpreted in the context of a disparate literature. While increased ASSR magnitudes have been reported in tinnitus patients compared to non-hearing matched controls (Wienbruch et al., 2006), in tinnitus compared to non-tinnitus frequencies (Diesch et al., 2004), and to correlate with tinnitus-related distress (Diesch et al., 2004), other studies have found no differences between tinnitus patients and controls (Paul et al., 2014), and decreased amplitudes at the tinnitus frequency (Roberts et al., 2015). As discussed in Section 7.1, methodological differences, particularly differences in hearing loss, hyperacusis and the method of loudness matching, may have played a part in these differences. The present finding of increased ASSR magnitudes at the tinnitus frequency was derived from a study involving tight matching for age and hearing loss, no differences in hyperacusis (as quantified by HQ score), and the novel use (in this context) of a loudness recruitment prediction algorithm to set loudness levels. The downside to the use of this algorithm is that is cannot be validated in a patient group, as there is no gold standard. However, the lack of a gold standard is part and parcel of the flaws inherent in other methods, as discussed earlier, and a non-subjective method equally applicable across all subjects has the advantage of not being confounded by any hyperacusis over and above 'adaptive' loudness recruitment, which has been demonstrated in tinnitus patients (Hébert et al., 2013). Though the present study may offer some methodological improvements over previous ones, it is just one study using a small group. Therefore its findings must be interpreted with due caution. That said, the finding of increased ASSR amplification is consistent with increased sound response magnitudes present subcortically in ABRs (Schaette and McAlpine, 2011; Gu et al., 2012), and cortically in fMRI responses (Gu et al., 2010), whereas reduced ASSR magnitudes would have been somewhat paradoxical.

In general, ASSR amplitudes are known to increase with attention, and it has recently been found that this effect is absent in tinnitus patients for tones in the tinnitus frequency range (Paul et al., 2014). In the present experiment, attention should not have differed between stimulus conditions, meaning a different explanation must be sought. The abolition of the tinnitus-related increase in ASSR amplitude by the addition of competing AM tones suggests that lateral interactions in the auditory pathway may be responsible for the tinnitus-related increase in amplitude, because modification of lateral interactions (via competing stimuli) appears to remove the effect, however due to the poor SNR of

responses in the presence of competing AM tones this assertion cannot be made confidently. Evidence of increased lateral spread of cortical responses to thalamic stimulation have been found in an animal model of tinnitus (Llano et al., 2012), which appeared to be related to GABA-ergic deficiency. A similar increase in lateral spread of ASSRs in tinnitus patients would entrain a larger area of cortex into the 40 Hz rhythm, and therefore increase the magnitude of the response. Addition of additional AM tones at nearby frequencies would be expected to prevent this additional spread by competing for the same areas of cortex. While this is a different explanation for the ASSR increase in tinnitus to enhancement by tonotopically-specific attention, the two explanations might not be mutually exclusive; increased attention may operate by increasing the gain of excitatory neurons and broadening receptive fields, hence increasing the lateral extent of AC responding to a particular AM tone. Also, if GABA-ergic deficiency were responsible for increased ASSR amplitudes, one might have expected to see a correlation between ASSRs and cortical GABA concentrations, which were not observed. However, this might have been due to relatively small subject numbers, low SNR of GABA measurements, or due to the influence of other parts of GABA systems besides total GABA concentration.

Chapter 8. Explicit neural codes of sensory inference in pitch perception

The recordings for this study took place in the Human Brain Research Laboratory in the University of Iowa, and were performed in epileptic patients undergoing invasive electrode monitoring for seizure localisation. I had no role in subject recruitment or electrode implantation, and the experimental scripts were actually run by Dr Phillip Gander. In all other respects, the experiment was fully conceived, designed, coded, analysed and interpreted by me. This work has been submitted for publication.

8.1 Aims

Bayesian accounts of perception such as predictive coding are growing in popularity and, as well as having face validity, appear to more parsimoniously explain the range of empirical brain data across the literature than other models. Explicit links between computational processes involved in such models and empirical brain responses have recently been proposed, and in limited cases these are supported by empirical evidence. In particular, gamma oscillations are proposed to encode prediction errors, beta oscillations changes to predictions, and delta/theta oscillations to predict timing by orchestrating temporal windows for processing via higher frequency oscillations (Arnal and Giraud, 2012; Bastos et al., 2012). In light of these proposed associations, initial attempts have been made to use abnormalities of neural oscillations associated with tinnitus to infer the computational processes underlying its generation. However, not all of these associations are supported by direct evidence, and the evidence that exists is not that specific about exactly what computational quantities are represented. For instance, gamma oscillation magnitude correlates with the unexpectedness of a sensory event (Arnal et al., 2011; Brodski et al., 2015), but it is not clear whether what is being represented is prediction error (difference between the mean of the prediction and the sensory event) or surprise (which also takes into account the precision of the prediction), and whether it is also affected by the precision of the sensory information (as in ‘precision-weighted prediction errors’). A link between beta oscillations and changes to predictions is hypothesised (Arnal and Giraud, 2012), but proving the association requires knowing exactly how much predictions are being changed at any given moment, which has not so far been achieved experimentally. Finally, while there is an established link between delta/theta oscillations

and predictive timing (Calderone et al., 2014), their role is far less understood in prediction 'what' rather than 'when', which is the aspect of their function that is potentially most relevant to tinnitus. In light of these unknowns, this study aimed to quantitatively and explicitly correlate the computational processes involved in predictive coding with observed associated oscillatory brain activity. Specifically, to achieve this through a paradigm where these computational quantities could be explicitly controlled in order to associate them with measured neuronal oscillations. Figure 18 shows a schematic of the theoretically distinct quantities of predictive coding with respect to the presentation of a single auditory stimulus of a given fundamental frequency (usually 'f0', but here referred to as 'f' for clarity). This experiment was approached with hypotheses that gamma oscillations would relate to surprise (to a greater extent than prediction error), and the beta oscillations would relate to changes in predictions.

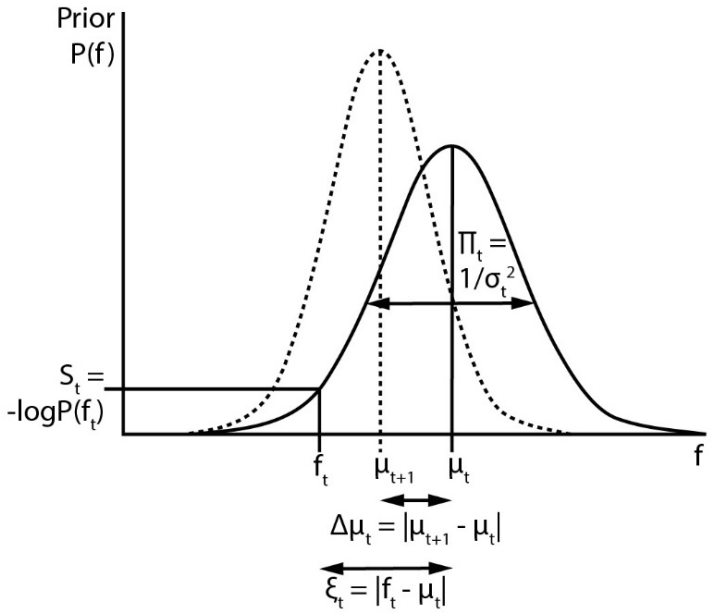

Figure 18: Computational quantities involved in predictive coding
The graph displays a schematic probability distribution representing the prior prediction about the fundamental frequency (f) of an upcoming auditory stimulus (f_t), where t simply refers to the number or position of the stimulus within a sequence. This prior is characterised by its mean (μ_t) and precision (Π_t), which is the inverse of its variance (σ^2). The incongruence between the actual f_t and the prior can be expressed either as a (non-precision-weighted) prediction error (ξ_t), i.e. the absolute difference from the prior mean, or as surprise (S_t), i.e. the negative log probability of the actual f_t value according to the prior distribution. As a result of a mismatch with bottom up sensory information, the prior changes (new prior distribution illustrated by dashed line). The change to the prediction ($\Delta\mu_t$) is calculated simply as the absolute difference between the old (μ_t) and new (μ_{t+1}) prior means.

8.2 Methods

8.2.1 Subjects

In principle, there was a relatively open choice about the recording modality to use for this experiment. However, indirect measures of neural activity, such as functional MRI, would clearly have been unsuitable, as they do not permit the distinction of different frequency bands of neural oscillations. Potentially EEG, MEG or iEEG would have been suitable. As gamma oscillations were of paramount importance, it was important to have sufficient SNR in the recordings to be able to resolve these. From previous work conducted, it is clear that resolving auditory gamma oscillations at all with EEG is extremely difficult. With MEG, auditory gamma oscillations can be resolved accurately (Sedley et al., 2012b), but with inter-individual variability in the ability to resolve them, and only ever with large numbers of trials of highly salient stimuli. Therefore iEEG was the only feasible option, and has the further advantage of being able to confidently distinguish different divisions of AC and examine local connectivity.

The subjects were three patients undergoing invasive electrode monitoring for the localisation of medically refractory epilepsy. Subjects were all awake and alert at the time of the experiment, though two out of three were relatively somnolent due to their recent surgery. No subject had a history of any hearing deficit. Figure 19 displays 3D anatomical reconstructions of the subjects' brains, along with the locations of electrodes featured in the analysis. The procedure for determining which electrodes to include in the analyses is described later.

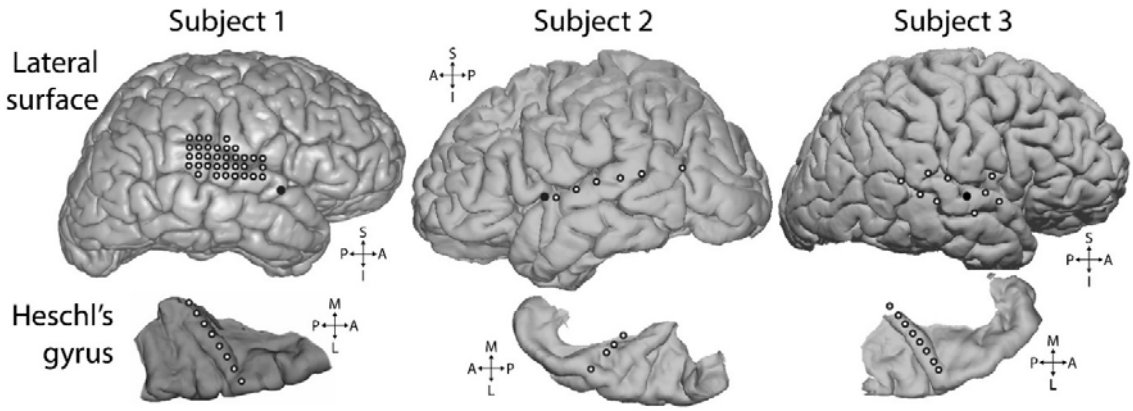

Figure 19: Positions of electrodes used for analysis
White-filled circles each indicate one electrode. All electrodes shown were included in the presented analyses, and were selected based on showing significant responses to the experimental stimulus, as described in the Methods section. Top row: lateral surface of the cerebral hemisphere recorded from. Solid black circles mark the insertion point for the Heschl's gyrus (HG) depth electrode. Bottom row: depth electrode contacts used for analysis (white-filled circles), shown in the context of the surface of the superior temporal plane. Depth electrode contacts were positioned along the axis of HG. S = superior, I = inferior, A = anterior, P = posterior, M = medial, L = lateral.

8.2.3 Data recording setup

The data recording setup was as described in Section 4.2.2. Recordings were made from one hemisphere in each subject (Subjects 1 and 3: right, Subject 2: left). All subjects had an 8-contact depth electrode placed along the axis of HG, including anatomically and physiologically-defined A1, and a subdural grid overlying STG. LFP data were downsampled to 1 kHz, and electrical noise was filtered out.

8.2.3 Paradigm

The basis of the experiment was an algorithm in which stimulus segments varied across only one perceptual dimension, and values were drawn randomly from populations, i.e. Gaussian distributions, each characterised by its mean (μ) and standard deviation (σ). These populations constituted hidden states, not directly observable but with inferable parameters. The populations were randomly changed according to simple rules, such that subjects could be expected to unconsciously learn these rules in order to minimise uncertainty about upcoming stimuli. The rules were that for each stimulus segment, there was a 7/8 chance that its value would be drawn from the existing population, and a 1/8 chance that a new population would come into effect. Once a new population came into

effect, it became the 'existing' population. Each population had its μ and σ drawn randomly from uniform distributions. See Figure 20A for a schematic of the paradigm. The algorithm was implemented in the auditory domain, with stimuli taking the form of harmonic complexes, containing only unresolved harmonics (by high-pass filtering from 1.8 kHz). Each harmonic had a random phase offset, which was preserved across all segments, stimuli and subjects. The variable dimension was fundamental frequency (f0; hereafter just 'f' for simplicity), which is the major determinant of perceived pitch. Population μ was limited to the range 120-140 Hz, and σ to the range 1/128-1/16 octaves. Stimulus segments were 300 ms in duration, and were smoothly concatenated to avoid any transients at the transitions between segments. This was achieved by defining instantaneous frequency at every point in the stimulus, calculating the cumulative sum of this, and then creating harmonics individually in the time domain as follows in Equation 1:

$$a_T = \sin(2\pi r + 2\pi h \frac{1}{s} \sum_{t=1}^{T} f_t)$$

Where a is the amplitude of the waveform, T is the current time point (measured in samples), t is all previous time points, r is the random phase offset for the harmonic, h is the number of the harmonic, s is the sampling rate and f is the instantaneous frequency. This procedure was repeated for every harmonic, from below the high-pass to above the Nyquist frequency. To prevent aliasing, the stimulus was generated at 88.2 kHz sampling rate, then downsampled to 44.1 kHz. The segment duration of 300 ms was chosen as the minimum duration that would capture most of the transient response to the onset of pitch within a stimulus, based on previous work (Griffiths et al., 2010). Stimuli were 2,000 segments long; 4 different stimuli were created, and used for each subject (i.e. 8,000 segments per subject). See Figure 20B for an example section of the auditory stimulus. Stimuli were presented diotically, via insert earphones (ER4B; Etymotic Research, Elk Grove Village, IL) through moulds fitted to the subject's ear, at the loudest comfortable volume. During the experiments, subjects engaged in an irrelevant auditory task to maintain attention, but a specific performance on this task was not required. This task involved detecting a change to the timbre of individual stimulus segments (64 targets over 8,000 segments), which was unrelated to their frequencies or underlying population parameters. Subject 1 performed well on the task, and subjects 2 and 3 performed poorly,

with high false alarm rates. The first 100 stimulus segments, and 10 segments following each target, were removed from analysis.

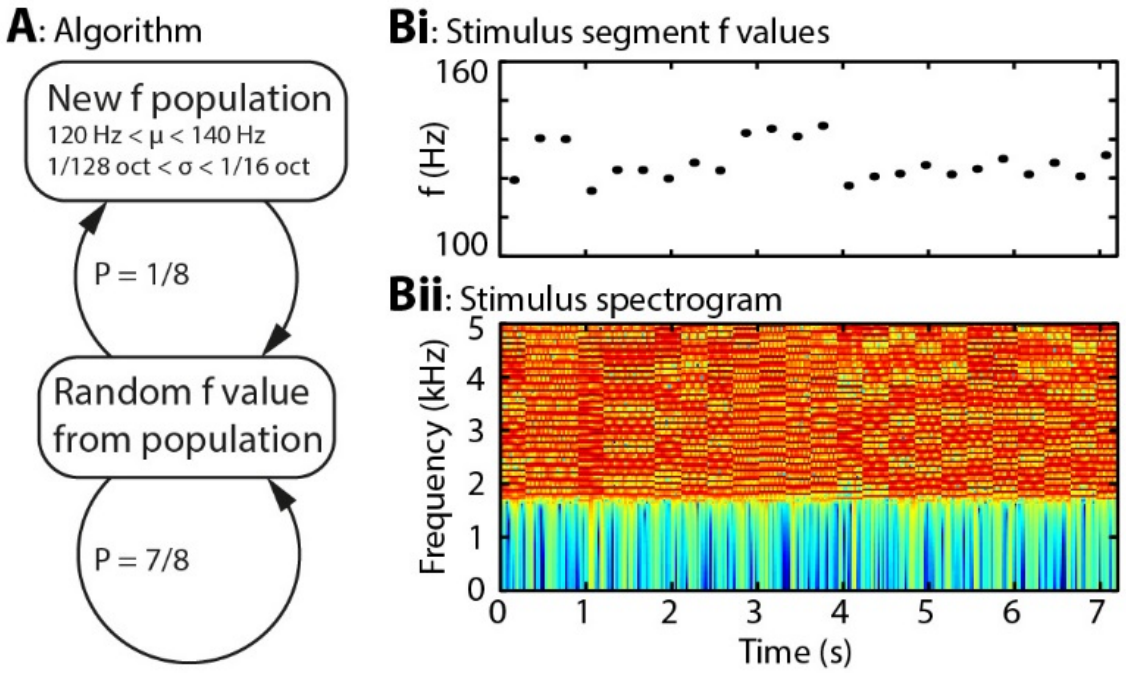

Figure 20: Algorithm and example stimulus
A: The stimulus is composed of a series of concatenated segments, differing only in fundamental frequency (f). At any time, a given f population is in effect, characterised by its mean (μ) and standard deviation (σ). For each successive segment, there is a 7/8 chance that that segment's f value will be drawn from the present population, and a 1/8 chance that the present population will be replaced, with new μ and σ values drawn from uniform distributions. B: Example section of stimulus. Bi: Dots indicate the f values of individual stimulus segments, of 300 ms duration each. Four population changes are apparent. Bii: Spectrogram of the corresponding stimulus, up to 5 kHz, on a colour scale of -60 to 0 dB relative to the maximum power value. The stimulus power spectrum does not change between segments, and the only difference is the spacing of the harmonics.

8.2.4 Modelling of computational quantities

The analyses performed so far have been based on the assumption that each subject modelled the hidden population states in an approximately optimal fashion. Previous evidence suggests that subjects tend to make Bayes optimal sensory inferences based on available information (Ernst and Banks, 2002; Körding and Wolpert, 2004). It does not matter if subjects' inference of the hidden states was not actually optimal (as this would just reduce the strength of the results), as long as it was not either orthogonal or in any way opposite to the modelled 'ideal' inference.

It is important to emphasise that it is impossible to infer the parameters of the hidden states (i.e. the mean and SD of the populations) with complete accuracy. However, there exists an upper bound on the certainty with which these parameters can be modelled. This idealised inference assumes full knowledge of the rules of the paradigm, the range of values from which population parameters can be drawn, and the probability of a population changing at any given segment. Obviously the subjects could not have started the paradigm with this knowledge, and modelling the learning process was far beyond the scope of the study, hence the discarding of the first arbitrary number of trials, namely 100. Once these rules and parameter ranges are known, Bayes optimal estimates of the population parameters over time can be made, in a process that amounts to inversion of the forward model that is the experimental paradigm. Following this, the parameter estimates can be used, in conjunction with the forward model, in order to generate predictions at each segment about the f value of the following segment. These predictions can be specified by their mean and SD, which correspond to the *predictions* and their *precision*. The f value of the subsequent segment then has an associated *prediction error* (difference, in octaves, between the prediction mean and the segment's actual value), and also a *surprise* (the negative log probability of the segment's value, based on the prediction's probability distribution). The procedure used to generate these predictions is illustrated in Figure 21, and was performed as follows:

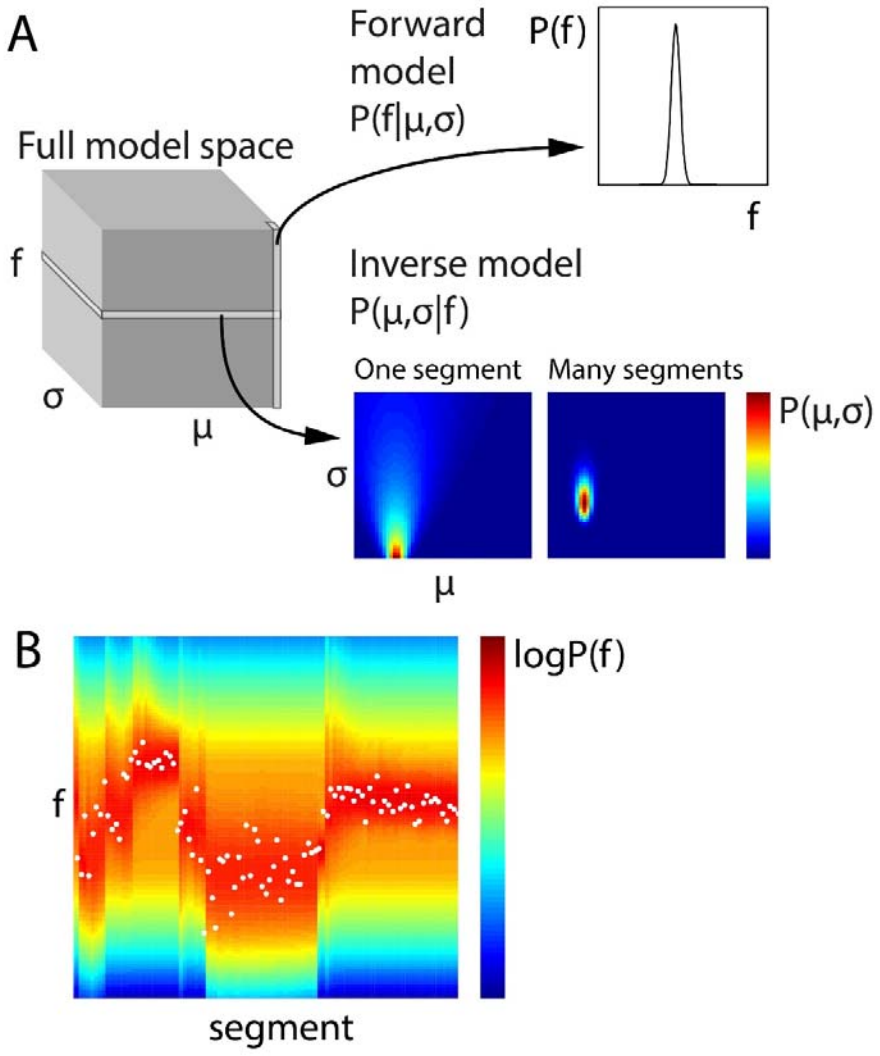

Figure 21: Generative model and inversion scheme used for data analysis
A: Schematic of the full 3-dimensional model space, with dimensions indicating population mean (σ), population standard deviation (σ) and stimulus fundamental frequency (f). To ease computational demands, the model space was discretised. Each point in model space corresponds to the probability of a particular f, given a specific μ and σ, i.e. P(f|μ,σ). Therefore each column (along the f dimension) gives the probability distribution P(f|μ,σ), and corresponds to the forward model. The planes of the model space, conversely, indicate the probability of each given combination of μ and σ, given a particular f value, i.e. P(μ,σ|f), or in other words the inverse model. To generate priors based on a series of observed f values, the scalar product of the planes for each of these f values is taken, and the resulting plane scaled to a sum of 1. This plane represents the estimates of the hidden states μ and σ, and is then used to weight the columns of the model space. The weighted model space is averaged into a single column (forward model), and scaled to a sum of 1, thus providing optimal priors on the assumption that the f population does not change. The priors assuming a population change are derived from the same procedure, but with uniform weighting across the model space. The change and no change priors are then weighted according to the probability of a population change, and then

summed. The only part of the process not illustrated here is the inference of population changes, determining how many preceding f values form part of the model inversion, which is explained in Equations 2 and 3. B: Observed f values from a section of the stimulus (white dots), overlaid on prior predictions (colour scale) based on previous observations of f, using the model inversion scheme described in A.

1) A discrete three-dimensional model space was generated (represented as a three-dimensional matrix), with dimensions corresponding to population μ, population σ, and f value. Any given value in the matrix indicates $P(f|\mu,\sigma)$, i.e. the probability of a given frequency given a particular μ and σ. The columns (all f values for a given μ and σ combination) thus constitute the forward model (by which stimuli are generated), and the planes (all combinations of μ and σ for a given f value) constitute the inverse model (by which hidden parameters can be estimated from observed f values).

2) For each segment, the model was inverted for its particular f value, yielding a two-dimensional probability distribution for the hidden parameters.

3) These probability distributions, for each segment subsequent to the most recent estimated population change (as defined later), were multiplied together, and scaled to a sum of 1. The resulting probability distribution thus reflects parameter probabilities taking into account all relevant f values.

4) This combined parameter probability distribution was then scalar multiplied with the full model space, in order to weight each of the forward model columns (each corresponding to a particular parameter combination) by the probability of that parameter combination being in effect. The resulting weighted model space was then averaged across parameter dimensions, to yield a one-dimensional (forward) probability distribution, constituting an optimal prediction about the f value of the next stimulus segment, provided a population change did not occur before then. A probability distribution applicable if a population change were to occur was calculated the same way, but without weighting the forward model columns (so as to encompass every possible parameter combination).

5) To infer population changes, for each segment the probability of observing the present f value was compared for the two probability distributions (the distribution assuming a population change, and the distribution assuming no change), i.e. P(f|c) and P(f|~c) respectively, with c denoting a population change. The probabilities were compared, in conjunction with the known prior probability of a population change (1/8), using Bayes' rule, as stated in Equation 2:

$$P(c|f) = \frac{P(f|c)P(c)}{P(f)}$$

Here, P(c|f) is the chance that a population change occurred at that particular time. Given that P(c) is known to be 1/8, and P(f), the total probability of the observed f value, can be rewritten P(f|c)P(c)+P(f|~c)(1-P(c)), the above equation can be rewritten as Equation 3:

$$P(c|f) = \frac{1}{1 + \frac{7P(f|\sim c)}{P(f|c)}}$$

6) For each segment, the above calculation of P(c|f) was made not only with respect to the immediately preceding segment, but also a number of segments preceding that, up to a maximum of 4. Therefore, for segment t, it was possible to conclude that a population change had occurred immediately prior to t, t-1, t-2, t-3, or none of the above. A population change was judged to have occurred at the time point with the highest value of P(c|f), provided this value was greater than 0.5. While truly ideal inference would have kept track of every possible location the last population change could have occurred (right back to the beginning of the stimulus), this would have been computationally unfeasible. Importantly, using more than 4 lags did not appreciably alter the estimates obtained by model inversion.

7) Once the population change positions were estimated, and therefore optimal prior predictions were generated for each stimulus segment, these predictions were used to calculate the predictive coding quantities of interest. Predictions themselves were summarised by their mean (μ) and precision (1/variance). Changes to predictions (Δμ) were calculated as the absolute change (in octaves) in μ from one prediction to the next. Surprise (S) was calculated as the negative log probability of the observed f value given the prior prediction, and prediction error (irrespective of prediction precision) was

calculated as the absolute difference (in octaves) between the observed f value and the mean of the prior prediction. Finally, Δf was calculated as the absolute difference between the current and preceding value of f.

As the regressors (the quantities calculated above) were highly correlated with each other, both instantaneously and over neighbouring segments (Figure 22), these were partialised with respect to each of the other regressors, and the preceding and subsequent two values of both the other regressors and themselves. This conservative approach removed a lot of explanatory power from these regressors, but was necessary to be able to uniquely attribute observed neural correlates to a specific process.

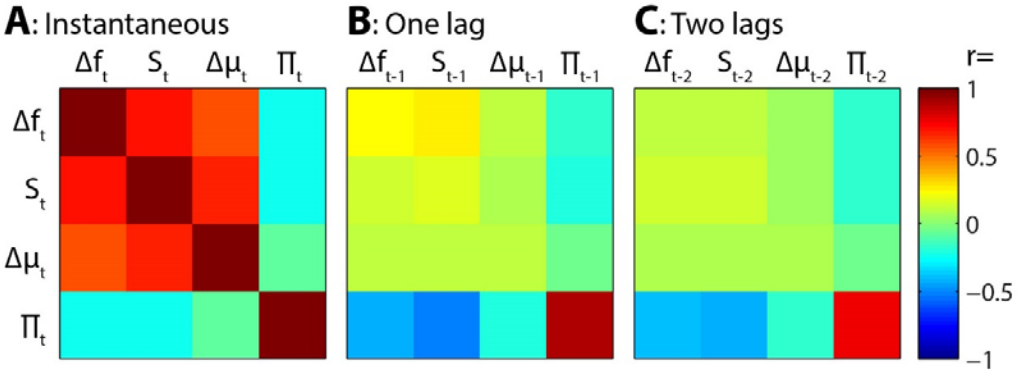

Figure 22: Correlations between predictive coding quantities
Correlation matrices between instantaneous (A) and time-lagged (B, C) values of the main regressors. Note the strong instantaneous mutual positive correlations between Δf, S and Δμ, and the negative correlations between Π and preceding values of Δf, S and Δμ.

8.2.5 iEEG data processing

iEEG data from AC electrodes HG and over STG were rearranged into epochs spanning from 0 to 600 ms with respect to the onset of a given segment (i.e. all of that segment and the subsequent one). Spectrotemporal decomposition was performed in the EEGlab (Swartz Center for Computational Neuroscience, University of California San Diego) toolbox for Matlab, with Morlet wavelet convolution, oversampled at 2 Hz frequency resolution and 10 ms time resolution, in the time range 0-600 ms from segment onset (i.e. spanning current and subsequent stimulus segments) and frequency range 2-100 Hz. The upper frequency bound was limited to 100 Hz in light of previous observations of a lack of qualitative response difference to pitch stimuli between the 80-100 Hz range and higher frequencies (Griffiths et al., 2010). The number of cycles per wavelet increased linearly

from 1 cycle at 2 Hz to 10 cycles at 100 Hz. The absolute value (i.e. amplitude) of the wavelet coefficients was calculated for artefact rejection purposes, and these were normalised for each frequency (i.e. shifted/scaled to mean 0 and standard deviation 1). The largest of each of these values in any channel was then taken, and histograms plotted of the resulting trial values. Threshold for epoch rejection were specified based on inspection of these histograms, corresponding to the upper bound of the normal distribution shape, beyond which individual values appeared to be outliers. Epochs exceeding either the maximum or average amplitude value threshold were discarded. Also, as mentioned previously, the first 100 epochs were discarded. 10 epochs after each target segment were also discarded. After removal of segments at the start of the experiment, following target segments, and with outlying amplitude values, 89, 86 and 87% of segments remained, for the three subjects respectively. Data were initially processed for all electrodes either in HG or over STG, and electrodes were selected for further analysis if they showed a statistically significant response to the stimulus as a whole. To determine significant overall stimulus responses, a permutation approach was set up (Maris and Oostenveld, 2007), using 100 permutations. In each of these a 300 ms window was taken, which was randomly displaced by up to +/- 300 ms for each segment. The normalised amplitude values within these windows were then averaged across trials, and the largest absolute mean value occurring at any electrode-time-frequency combination was added to a null distribution. The actual data were analysed in the same way, but without randomly displacing each segment in time, and an electrode was considered to significantly respond to the stimulus if it contained one or more time-frequency points where the mean amplitude exceeded the 5th largest value in the null distribution (corresponding to $p < 0.05$ corrected). The electrodes selected using this procedure are displayed in Figure 19. In all subjects, electrodes were included from both A1 and non-primary AC.

8.2.6 Correlational analysis

For each partialised regressor, complex time-frequency data were subject to a two-stage regression approach. First, the complex data for every electrode-time-frequency combination were regressed against it to yield a pair (real and imaginary) of Pearson product moment correlation coefficients (r). The modulus of these constituted the evoked (time-locked) response. To calculate the induced response, the residuals from this regression were converted to amplitude (by taking their absolute value), and the regression

was performed again. The result was a pair (evoked and induced) of time-frequency correlation images for each electrode for each regressor. Inspection of these responses found no qualitative differences between the responses observed in different divisions of AC, hence the correlations were averaged over electrodes for further analysis. To quantify the distribution of correlation strengths, the pattern, across time and frequency, of induced correlation coefficients for each regressor was averaged across electrodes and subjects. This pattern was used as a filter, in that it was scalar multiplied with the correlation coefficient pattern for each electrode for each subject, then averaged across time and frequency to yield a single correlation value for that electrode/subject combination. These values, for each regressor, for each subject, were divided by the largest absolute correlation value for that regressor, in order to represent relative correlation strengths on a scale of -1 to 1. These correlation values are displayed in Figure 23, and show no systematic dissociation between the anatomical distributions of the correlations for the different regressors.

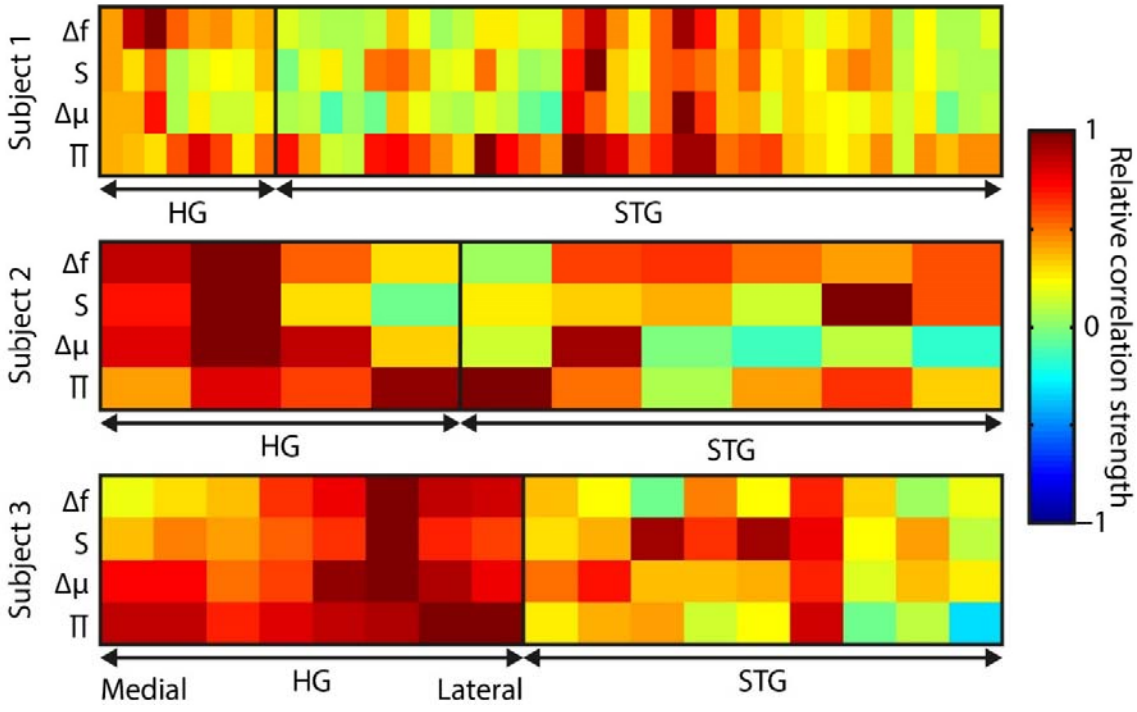

Figure 23: Anatomical distribution of regressor correlations
Each coloured plot represents one subject. Within each plot, the columns represent individual electrodes (positions displayed in Figure 19), with the vertical line separating Heschl's gyrus (HG) from superior temporal gyrus (STG) electrodes. HG electrodes are arranged medial (left) to lateral (right). Rows indicate the four main partial regressors. Colour values indicate the relative similarity between the correlation pattern for that

subject/electrode combination and the mean correlation pattern across electrodes and subjects (range -1 to 1). Δf = absolute change in f value (octaves) compared to previous, S = surprise, $\Delta\mu$ = absolute change in prediction mean (octaves), Π = precision of prediction.

8.2.7 Statistical analysis

To compare surprise and prediction error, for each of these regressors, the mean of the induced correlation coefficients (across time, frequency, electrode and subject) was calculated within the time window 90-500 ms from segment onset and the frequency window 30- 100 Hz. This was performed once with the regressors partialised as previously described (i.e. for current and adjacent values of Δf, Π and $\Delta\mu$), and again with additional partialisation of each regressor with respect to the other. This latter analysis measures the unique contribution of each regressor in explaining the observed data over and above the other, and was the analysis subjected to statistical analysis. For statistical testing, a permutation approach was used, with 100 permutations (and shuffled trial order in each), and each was quantified in the way just described.

For the main correlation analysis, a permutation approach of 100 permutations was also used. For each permutation, the trial order was randomly shuffled, and the analysis was repeated otherwise identically. For each permutation, the correlation values were averaged across the three subjects, and the largest absolute mean correlation coefficient (at any time-frequency point, for any regressor) was added to the null distribution. For the actual data, points in time-frequency space were considered significant if the absolute value of the average across subjects exceeded the 5th largest value of the null distribution (corresponding to $p < 0.05$ corrected). Due to the strong prior hypothesis about gamma oscillations correlating with surprise or prediction error, the statistical analysis was repeated for these regressors but with only frequencies in the gamma range (30-100 Hz) being included in the analysis.

8.3 Results

8.3.1 Surprise (S) versus prediction error (ξ)

In keeping with prior hypotheses, both surprise and prediction error (the latter not taking into account the precision of predictions) were associated with significant gamma band responses in the LFP. First, it was established which of these quantities explained the LFP data better. Figure 24 shows the strong correlation between these quantities (A), the

explanatory power of each with respect to the LFP data (B), and the unique explanatory power of each after partialling out the other quantity (C). Both quantities correlated positively with gamma magnitude, but surprise showed a stronger correlation in all three subjects. In the partial analysis (C), residual surprise (after partialling out prediction error) correlated positively with gamma magnitude, whereas residual prediction error (after partialling out surprise) showed only a weak negative correlation in two subjects, and no correlation in one subject. These correlations were significantly different to each other at $p < 0.05$ corrected, thus it was concluded that the better correlate of gamma magnitude was surprise, which was therefore used for further analysis.

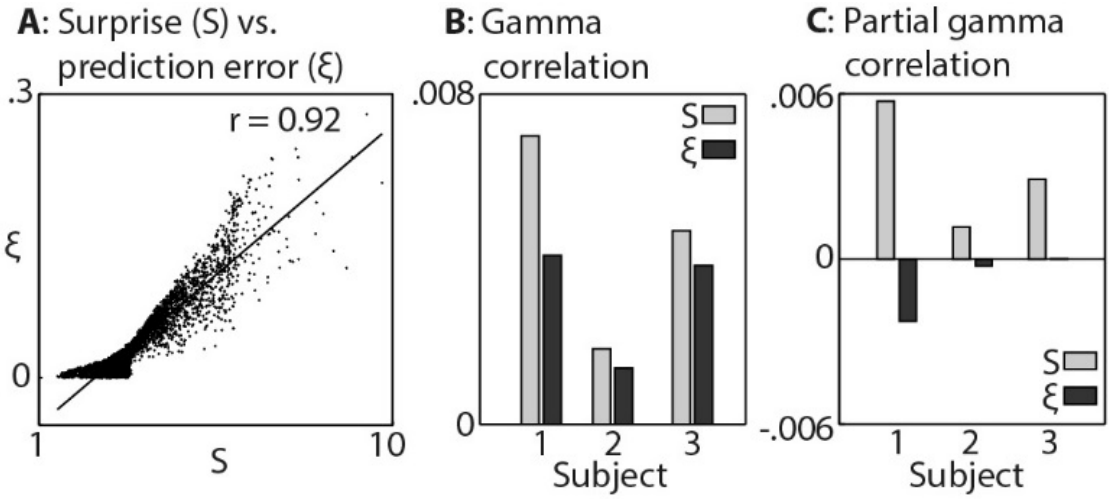

Figure 24: Comparison between surprise and prediction error
A: Correlation between surprise (S) and non-precision-weighted prediction error (ξ), with each dot indicating an individual stimulus segment and the line indicating a linear regression fit. B/C: Mean Pearson product moment correlation coefficients (r) between S_t or ξ_t, and gamma oscillation magnitude (30-100 Hz) in the 90-500 ms period following the onset of stimulus segment t. Regression coefficients were calculated for each time-frequency point, after partialling out the influences of current and preceding/subsequent values of all other regressors. In C, the influence of S on ξ, and ξ on S, was also partialled out, thus exposing the unique contribution of each quantity to explaining the observed neural response. Regression coefficients were then averaged across time and frequency. Partial S showed a higher mean correlation, across subjects, with gamma magnitude than partial ξ ($p < 0.05$).

8.3.2 Induced oscillatory profiles of predictive coding quantities

Figure 25 shows the induced oscillations uniquely explained by each of the three quantities of interest: surprise (S), change in prediction mean (Δμ), precision of predictions (Π), as well as the change in f value from one stimulus to the next (Δf). These are shown for each

subject, and areas of significant correlation across the three subjects are outlined in white. In accordance with the prior hypothesis, S correlated positively with gamma oscillations, beginning at around 100 ms from segment onset, and this was significant across subjects from 200 ms. Two of the subjects also showed an early positive beta response to surprise (around 100 ms), and two showed a late negative low frequency (beta or delta-theta-alpha) response, (from around 350 ms) but these were not significant. Also in accordance with prior hypotheses, $\Delta\mu$ correlated positively with beta oscillations coinciding with the onset of the subsequent stimulus segment (about 100 ms after), which again was significant. Π correlated positively with delta-alpha (2-12 Hz) frequency oscillations (for most of the 0-300 ms period from segment onset) in all three subjects, though this was only significant in the alpha frequency range, and fell slightly below significance in the delta-theta range. Given the strong negative correlation between Π and the preceding Δf value, it seemed likely that the low-frequency correlates of these were being mutually attenuated by the partialisation process. The analyses were therefore repeated, with only the contemporaneous value of Δf being partialled out (Figure 26). This analysis found highly significant correlates of Π in the full delta-alpha range, but could not attribute the delta-theta component to Π with absolute confidence.

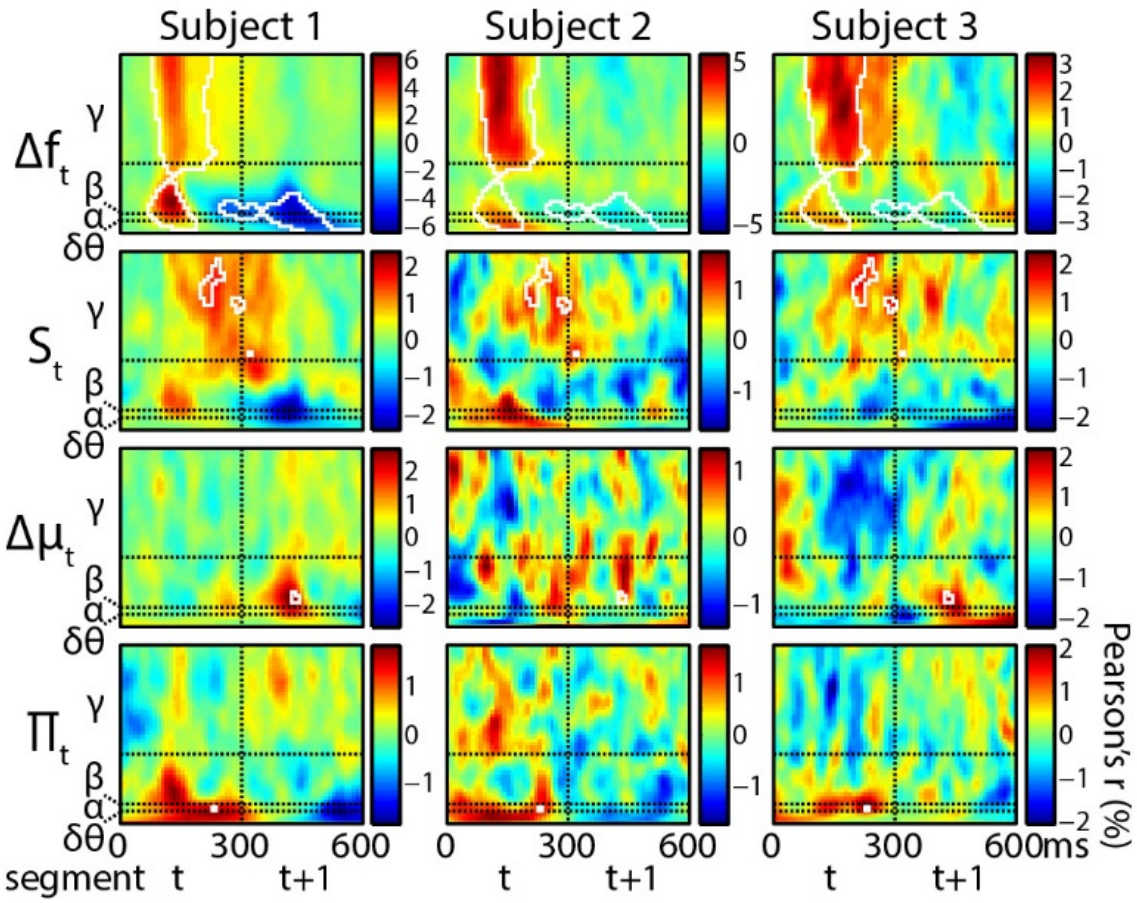

Figure 25: Induced spectrotemporal profiles of computational quantities in predictive coding

Each plot shows the time (x axis) – frequency (y axis) correlates of the quantity of interest, expressed as Pearson product moment correlation coefficients ('r'). Vertical dashed lines separate the current (left) and subsequent (right) segments with respect to the segment to which the quantity of interest is applicable. In the case of change in prior mean, this refers to the change occurring as a result of the current segment. Greek letters on the frequency axes indicate the different frequency bands, with are separated by horizontal dashed lines. Rows of plots indicate different quantities of interest, and columns indicate different subjects. δ = delta (2-4 Hz), θ = theta (4-8 Hz), α = alpha (8-12 Hz), β = beta (12-30 Hz), γ = gamma (>30 Hz).

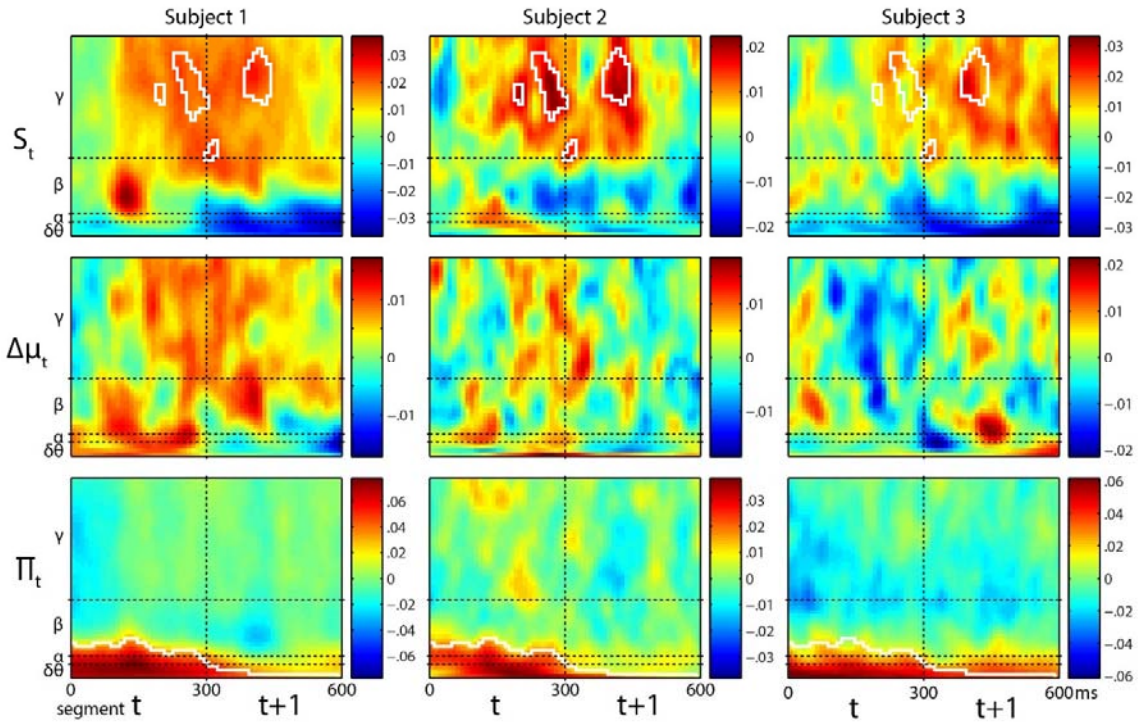

Figure 26: Induced spectrotemporal profiles of key predictive coding quantities, without mutual partialisation

Layout and notation of this figure is as for Figure 25, except that the Δf regressor is not included. Also, colour scales indicate Pearson's r as a proportion (i.e. 0-1) as opposed to a percentage. The difference between the figures is that in the present case, regressors were partialised only with respect to the contemporaneous Δf value (for clarity of display). As such, overlap territory between the regressors (with and without time lags) is retained, and thus results cannot be uniquely attributed to any one particular statistical quantity. In particular (see Figure 22), there is positive overlap between contemporaneous S and Δμ values (resulting in increased gamma, and attenuated beta, responses to Δμ in the non-partialled), and between Π values and the preceding values of Δf, S and Δμ (revealing strong delta/theta/alpha correlates, which are positive in the 0-300 ms range with respect to Π, and negative in the 300-600 ms range with respect to S).

8.3.3 Evoked spectrotemporal profiles of predictive coding quantities

Evoked results are shown in Figure 27. These were variably present in association with the quantities of interest, but unlike the induced results, there was no qualitative distinction between the timing or frequency profiles of the different quantities. The only significant evoked responses were to Δf and Δμ, and not to S or Π.

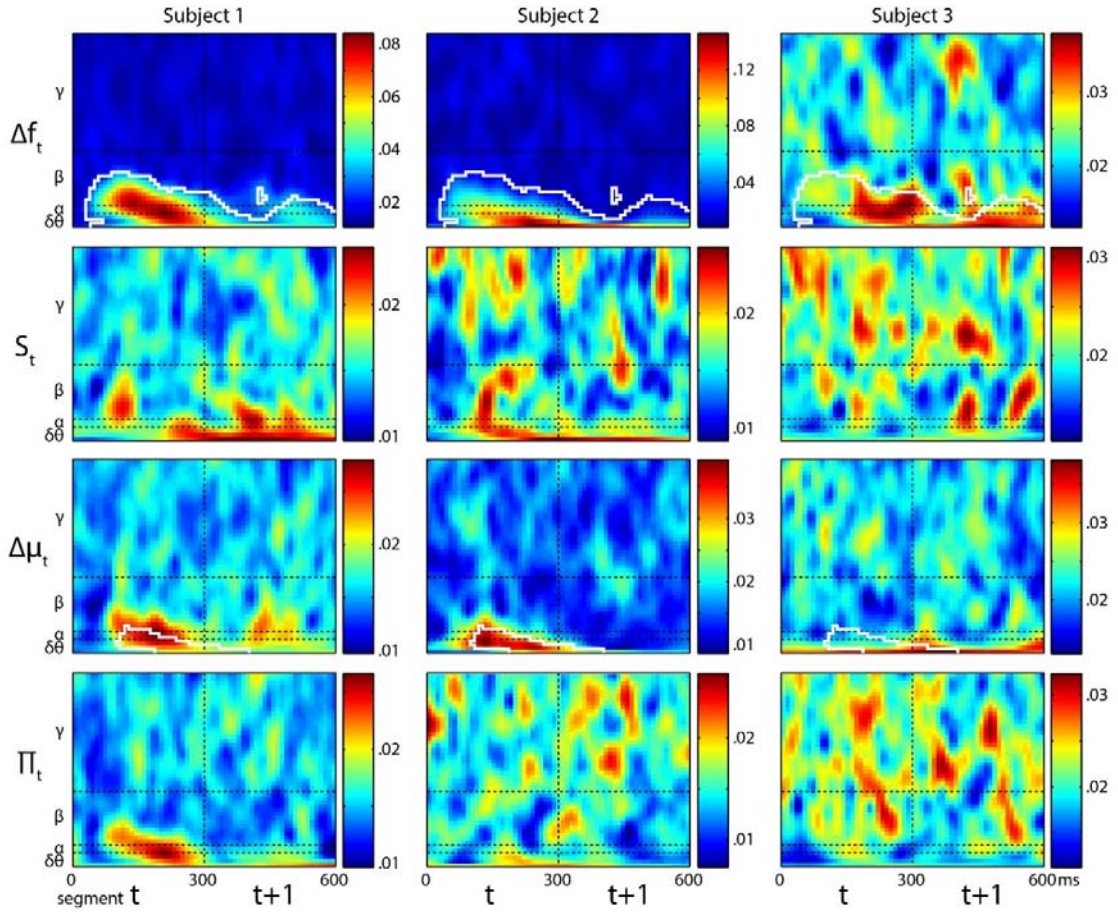

Figure 27: Evoked spectrotemporal correlates of computational quantities in predictive coding
Organisation and notation of the figure is as for Figure 25. Colour scales represent the absolute value of the complex-valued correlation coefficient hence values can only be positive. Also, colour scales indicate Pearson's r as a proportion (i.e. 0-1) as opposed to a percentage.

8.4 Discussion

The finding that gamma oscillations correlated positively with violations of predictions was in accordance with prior evidence and theory (Fujioka et al., 2009; Arnal and Giraud, 2012; Bastos et al., 2012, Brodski et al., 2015). However, previously it has not been established whether they represent a correlate of prediction error *per se*, or the related quantity of surprise, which is influenced by the precision of the prediction being violated. The present results strongly favour gamma as a correlate of surprise. Current theory proposes that beta oscillations are the correlates of changes to predictions (Arnal and Giraud, 2012; Bastos et al., 2012), however directly supportive evidence has so far been lacking. The present findings strongly support this theory, and provide the first direct

empirical confirmation. Theta oscillations, and neighbouring frequency bands (delta and alpha), have been linked to predictive timing, via their role in establishing temporal windows for processing of sensory inference with higher-frequency oscillations (Arnal and Giraud, 2012; Calderone et al., 2014). However a role of these oscillations in predictive *coding* (predicting *what* rather than *when*) has not previously been apparent. The present findings suggest that these low frequency oscillations, via their amplitude (rather than phase) have a role in encoding the precision of predictions. The most relevant existing evidence is that alpha oscillation magnitude has been found to correlate with the estimated probability of a change in an ongoing visual stimulus will occur at a particular time point (Bauer et al., 2014). In the context of alpha oscillations, it has been proposed that as their magnitude increases the temporal windows in which gamma activity is facilitated become shorter, and hence the overall gamma amplitude decreases (Jensen and Mazaheri, 2010). More recent evidence from spontaneous layer-resolved cortical recordings in macaques directly supports this hypothesis (Spaak et al., 2012). It is entirely possible that the same applies to theta oscillations, which similarly organise higher frequency oscillations (Canolty et al., 2006), particularly in the context of the present results, where alpha and theta appear to similarly correlate with prior precision. Thus, taking into account the present findings, it appears that more precise predictions are associated with higher theta/alpha power, which may narrow the temporal window in which gamma-mediated prediction errors can occur. However, what is more difficult to reconcile is the theory that increased theta/alpha reduces the magnitude of gamma responses, with the present observation that gamma oscillations reflect surprise; i.e. a given prediction error gives a stronger gamma response if the precision of the prediction which it violates (encoded by theta/alpha power) is higher. Put another way, existing theory and evidence expects theta/alpha power to negatively correlate with gamma power, while the present findings suggest that gamma responses to a given event are stronger when theta/alpha power is stronger. That said, the present findings concern dynamics varying on a short timescale around discrete events, rather than spontaneous brain activity in coarse epochs, so the same correlations need not necessarily apply. For instance, sensory systems may generally alternate between states of relatively stable perception (characterised by high theta/alpha power and low gamma power) and changing perception (associated with elevated gamma power and reduced theta/alpha power), but these might be linked by brief transition periods in which both types of activity are elevated (e.g. when an unexpected sensory change

occurs during stable perception). Also, even if theta/alpha amplitude causes an overall reduction in gamma amplitude, the overall impact on the onward effect of gamma oscillations might not be negative; the concentration of gamma activity into narrower temporal windows would be expected to increase the temporal coincidence of post-synaptic potentials generated on target neurons, and hence increase their summative effect. Furthermore, it is possible that the negative spontaneous amplitude correlation between high and low frequencies is caused by high frequency amplitude changes causing low frequency changes, as well as or instead of low frequencies driving high frequencies. The finding (in 2 out of 3 subjects) of a late negative low frequency response to surprise, following the preceding positive gamma response, is in keeping with this possibility, and may therefore reveal something about the dynamic interplay between these frequency bands. Overall, as the findings relating theta/alpha oscillations to precision are so new, some caution is required with regard to interpretation until further evidence is available.

8.4.1 Further work on the subject

As well as just the spectrotemporal profile of the statistical quantities of interest, it is also of interest to examine communication between cortical areas, along with communication between frequency bands, in order to gain a clearer understanding of the dynamics of the system as a whole, and the anatomical hierarchy involved. Such analyses have recently been applied to the analysis of normal speech perception data (Fontolan et al., 2014). So far, analyses of the present dataset have been restricted to using idealised inference about hidden states, hence idealised predictions. It will also be of interest to use different models of inference, in order to provide the best possible fit to the iEEG data, and identify which methods of inference the different subjects were using. Further experiments might pursue various lines of investigation, including transposing the paradigm to different hierarchical levels of pitch processing, different auditory attributes besides pitch (e.g. loudness, which is of particular relevance to tinnitus), and also examining the effects of attention, and the precision of sensory information.

Chapter 9. Discussion

The experimental work described in Chapters 4-8 has yielded several novel findings, all of which are relevant to current understanding of the brain mechanisms of tinnitus. Section 9.1 provides a brief summary of the key positive and negative findings of this work, and Section 9.2 uses these findings, along with the key points highlighted in the introduction, and components from existing models, to propose a new and comprehensive model of tinnitus that can potentially explain the current paradoxes in tinnitus neuroscience.

9.1 Summary of findings

As this summary of findings serves as an introduction to Section 9.2 which presents a new model of tinnitus, the chapter summaries below are ordered to produce a coherent narrative, rather than in ascending numerical order.

9.1.1 Group-level MEG correlates of tinnitus

The MEG study of spontaneous brain oscillations in tinnitus found that there were no significant difference in source-space oscillation magnitudes, within or outside of AC, between tinnitus patients and age/sex/hearing-matched controls. However, the degree of hearing loss (particularly in the tinnitus group) correlated strongly with right AC gamma power. This finding was entirely concordant with a previous study (Ortmann et al., 2011) finding isolated increases in right AC gamma power in amateur musicians with transient hearing loss and tinnitus, which appeared to relate more to the hearing loss than tinnitus. The lack of group oscillatory power differences also mirrors the same finding in a recent similar study that was well-matched for hearing loss (Adjamian et al., 2012). Previous studies reporting increased resting-state gamma power in tinnitus patients versus controls (Llinás et al., 1999; Ashton et al., 2007; Weisz et al., 2007) must therefore be considered to be reporting differences due to hearing loss, not tinnitus, unless proven otherwise.
The study did, however, find a correlation between delta oscillation magnitude and overall ('trait') tinnitus loudness, the relevance of which is discussed below, in the context of dynamic delta changes.

9.1.2 Direct neurophysiological recordings of core tinnitus processes

Despite tinnitus not being associated with group-level oscillatory power changes, as discussed above, the intracranial study of RI in tinnitus found that even small dynamic changes in tinnitus are accompanied by substantial and widespread changes in oscillatory magnitude and coherence. Taken together, these observations suggest that certain neural oscillatory processes may be linked to the perceived loudness of tinnitus, but none in isolation is sufficient or necessary to determine whether tinnitus occurs in the first place. Delta/theta oscillations appear particularly relevant to the loudness of tinnitus, as they tracked it in this experiment, and correlated with it in the MEG experiment, but also have been linked to short-term (Kahlbrock and Weisz, 2008; Adjamian et al., 2012; Sedley et al., 2012a) and long-term (Tass et al., 2012) suppression of tinnitus loudness. These oscillations also appear to be heavily responsible for long-range communication within AC and between it and other cortical regions. High frequency (gamma) oscillations were also highlighted by this study but, as shown previously during short-term tinnitus manipulations (Sedley et al., 2012a) have a variable direction of association with tinnitus loudness. Despite relating heavily to hearing loss, gamma oscillations also have been found to relate to perceived tinnitus loudness in a large study corrected for hearing loss (De Ridder et al., 2015a), albeit only on a ROI analysis (which, in the context of such a well-powered study, suggests a weak effect). Ultimately, the relationship of gamma oscillations to tinnitus is not a straightforward one. Finally, gamma oscillations were observed throughout AC and adjacent cortical areas, strongly suggesting that they cannot be explained as an 'edge effect' of abnormal thalamocortical inputs, as underpins the TCD model of tinnitus (Llinás et al., 2005; De Ridder et al., 2015b).

9.1.3 Explicit neural codes of sensory inference in pitch perception

The intracranial study of predictive coding found that gamma oscillations, in normal perception, are a correlate of surprise, i.e. the incongruence of sensory input with prior prediction, scaled by the precision of the prior prediction. This specific association may be able to explain the paradoxical relationship of gamma oscillations with hearing loss and tinnitus. AC beta oscillations feature little in studies of tinnitus. The finding that these oscillations encode changes to predictions may explain this lack of observed differences, as tinnitus is generally a steady-state phenomenon without dynamically changing predictions. However, beta increases were observed during tinnitus suppression in the intracranial study

of RI (Chapter 4), and this may have indicated changing predictions accompanying changes in tinnitus intensity. Finally, low-frequency (delta, theta and alpha) oscillations were found to indicate the precision of sensory predictions. Given the hierarchical organisation of predictive coding systems, with the inferred sensation at one level constituting the prediction for the level below (albeit often via a nonlinear linking function (Friston, 2008)), it may be that relationships between delta-alpha magnitude and tinnitus intensity (as seen in the MEG and intracranial studies of tinnitus) are mediated by the precision of auditory cortical representations of SA. This possibility warrants further study, but is not mutually exclusive with respect to other roles of low-frequency oscillations, such as mediating long-range communication or phase-amplitude cross-frequency coupling (each may in effect entail the other).

9.1.4 Auditory cortex neurochemical correlates of tinnitus

The MRS study of tinnitus found that tinnitus patients, compared to tightly-matched controls, have reduced cortical GABA concentrations. This finding indicates a deficit in cortical-level inhibition, which may be responsible for excessive amplification of SA that may underlie tinnitus, and concords with models of tinnitus based on excessive gain, particularly at a cortical level. The finding of a positive correlation between choline concentration and tinnitus loudness is of uncertain significance. Choline might relate to plasticity, or to activity of the cholinergic neuromodulatory system. Both are highly relevant to tinnitus.

9.1.5 EEG auditory steady state responses (ASSRs) in tinnitus

The EEG study of ASSR magnitudes, in tinnitus patients compared to controls, found selectively increased responses to tinnitus-frequency tones with a 40 Hz amplitude modulation, which reflects the level of early processing in A1. This finding is indicative of excessive cortical and/or subcortical gain in the tinnitus frequency range. The lack of a correlation between ASSR magnitude and GABA concentration could indicate insufficient SNR of one or both measurements, or subject numbers, to expose such a relationship, or could indicate that the mechanism responsible for this amplification is reflected in other factors than cortical GABA concentration (such as receptor density/binding, other neurotransmitter systems, or subcortical changes).

9.2 A ‘comprehensive’ model of tinnitus

This section introduces a novel model of tinnitus. Crucially, this model explains tinnitus as arising from a combination of processes, any number of which may be present in individuals without tinnitus. The factors themselves predispose towards, or exacerbate, tinnitus, but what determines whether or not tinnitus actually develops is a synergy between these processes, leading to an attractor state that causes the persistence of tinnitus even after a reversal of the precipitating factors. The lack of measurable differences in spontaneous neural activity between tinnitus patients and matched controls reflects the fact that the predisposing factors, individually, are not necessarily any different at group level to those in matched controls, but rather it is the synergy between them that precipitates tinnitus. Furthermore, the attractor state aspect to the model means that even if there are increases in one or more predisposing factors at the time of onset, once tinnitus is established these may well return to baseline levels. The model itself is centred on a predictive coding account of perception, and present knowledge about its underpinning neurobiology. While just one perceptual dimension is described (loudness), the same framework can be applied to other dimensions such as timbre and pitch, and potentially even affective and cognitive appraisal of the tinnitus. A further aspect of the model is that it describes a reduction in the inferred loudness or strength of the tinnitus representation (or its precursor) with increasing hierarchical level. This ‘hierarchical descent’ on salience occurs due to a lack of behavioural, affective, cognitive and perceptual relevance of the SA (as it is noisy, relatively constant, and relates to nothing of relevance in the internal or external environment), and as such forms part of an adaptive system to filter irrelevant sensations out of higher perceptual networks and conscious awareness. Tinnitus is usually not perceived due to the success of this filtering mechanism. While in reality the specified mechanisms may operate across multiple hierarchical levels, the present model description just illustrates interactions within just one pair of hierarchical levels for clarity. The hierarchical descent on salience is also driven by the low precision of spontaneous auditory activity (low *estimated* precision due to behavioural irrelevance, and low *actual* precision due to its lack of an intrinsic temporal structure), compared with the relatively greater precision of higher predictions (the default being ‘silence’). For tinnitus to be perceived, the precision of spontaneous auditory activity must become sufficiently high to bias perception away from the prediction, such that a threshold for conscious perception is crossed. Some further parts of the model are not unique, but have already been proposed in

other models of tinnitus. One of these is amplification through attention (Roberts et al., 2013), whereby stimulus-driven (i.e. by SA) and/or volitionally-directed ('top-down') attention further increase the precision of the tinnitus signal, leading to further increases in its loudness. Another is re-setting of the 'default' prediction from 'silence' to 'tinnitus' (De Ridder et al., 2015b). This re-setting constitutes establishment of the attractor state, such that even if precision of SA reverts to its previous level, the salience of the representation no longer gets attenuated to the same degree by the higher prediction, and is still perceived as tinnitus. Unlike this existing account of prediction resetting, the new model involves the default prediction only shifting part-way towards the spontaneous auditory activity. The reason for this is that even if tinnitus is perceived, many of the factors limiting its behavioural relevance remain. This important distinction means that, at least in most cases of tinnitus, a hierarchical descent on salience still persists, which is necessary to explain certain phenomenological and electrophysiological observations. A further advantage of this model is that it does not require a distinction between peripherally-driven and centrally-generated SA in the auditory pathway, as both are eventually relayed to AC where the process of sensory inference begins. The model incorporates a diverse array of factors shown to be related to tinnitus by illustrating how they, individually or in combination, act to increase the precision of spontaneous auditory activity. A brief conceptual schematic of the model is shown in Figure 28, while the model's anatomical and functional architecture are illustrated in full in Figure 29, and explained in its detailed legend.

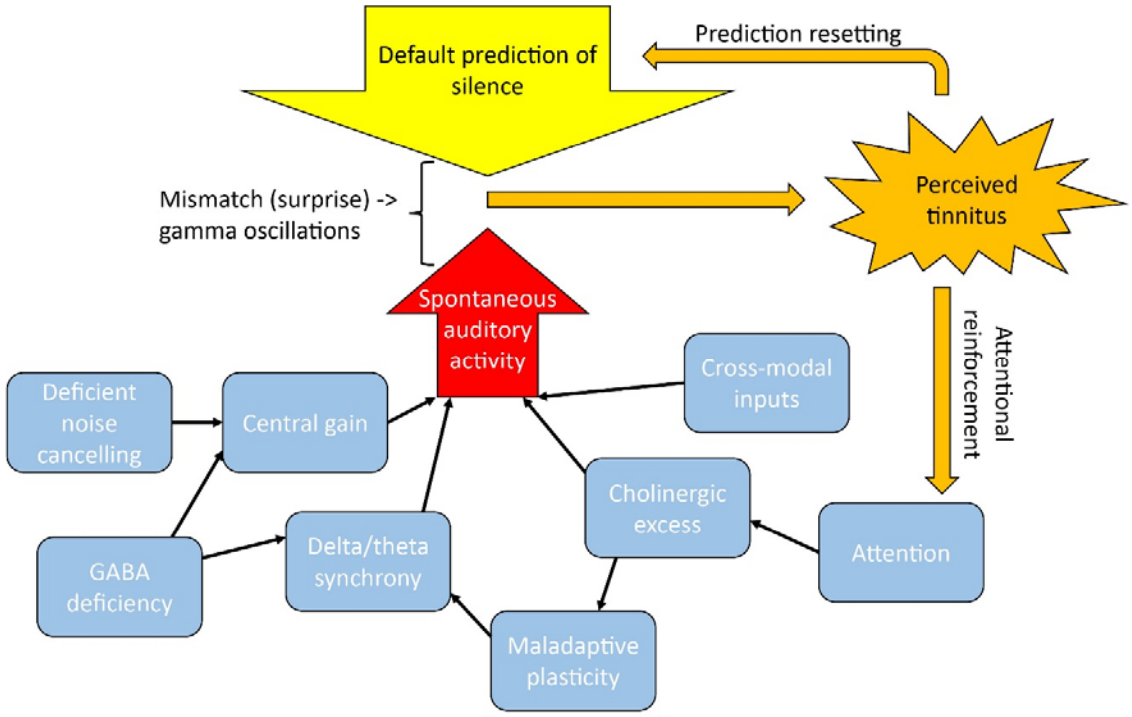

Figure 28: Schematic overview of the model
The core of the model is that, in all individuals, there is spontaneous activity in auditory cortex (red arrow), which may have a subcortical origin, and a higher 'default' prediction (yellow arrow) that is in conflict with this across one or more perceptual dimensions. Here, just the dimension of loudness is considered. Each of these opposing entities is weighted by its *precision* (here denoted by arrow width). Gamma oscillations reflect *precision-weighted surprise*, which loosely equates to (prediction precision) x (spontaneous activity precision) x (mismatch between spontaneous activity and prediction). As such, they provide a window into the workings of tinnitus perception, but are not yoked in magnitude to any particular part of the perceptual experience. The relative precision of each entity determines how much it influences overall perception; fundamental to the model is that the precision of spontaneous activity is significantly lower than that of the prediction, and also that the higher prediction is of a less loud sound than is encoded by the spontaneous activity. Given that the default prediction is initially of 'nothing' or 'silence', for tinnitus to occur, the precision of spontaneous activity must become sufficiently high for the overall inference (or percept; orange) to cross a threshold necessary for conscious perception. In blue are a number of factors which are proposed to act individually or synergistically to increase the precision of spontaneous activity, and the interdependencies between these. Once the precision is increased sufficiently to cause perceptible tinnitus, two processes of self-reinforcement occur (orange); attention paid towards tinnitus increases acetylcholine release which further boosts precision, and over time the default prediction switches from silence to one encompassing tinnitus.

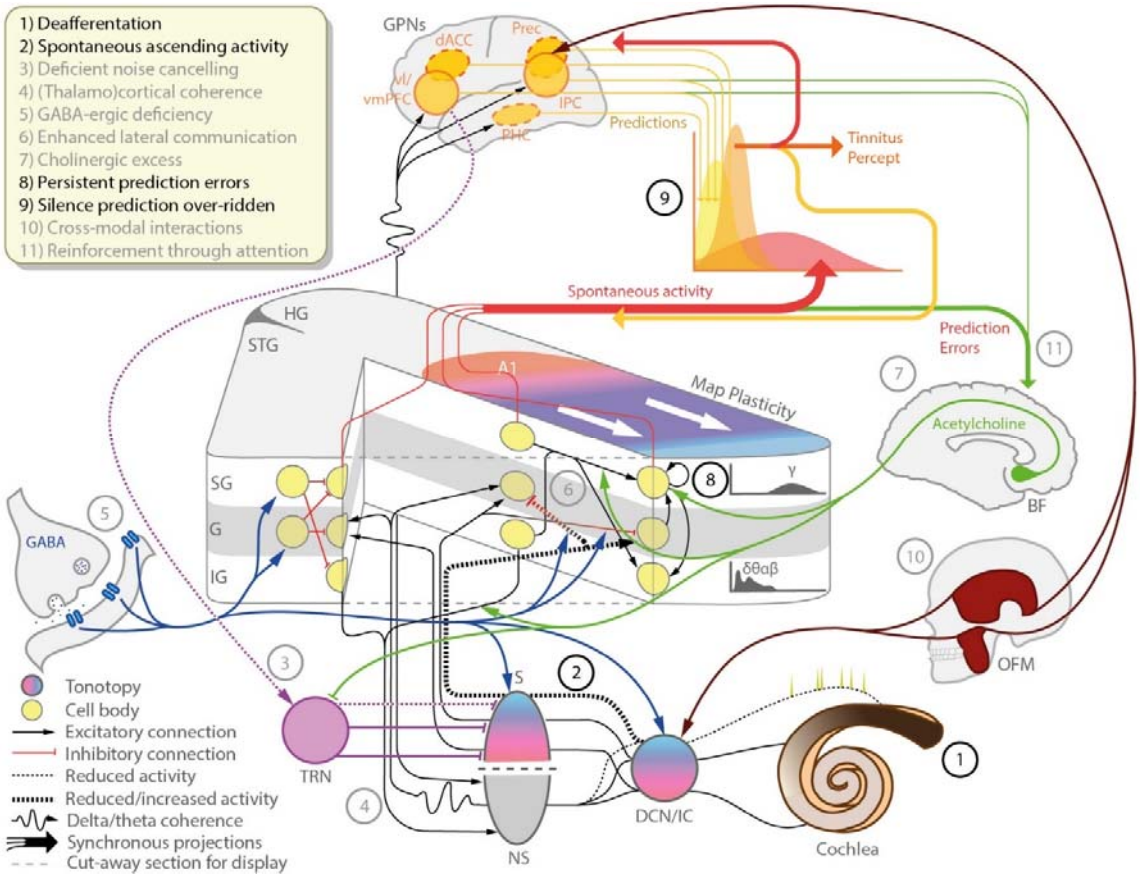

Figure 29: Schematic of factors promoting or exacerbating tinnitus
The culmination of the illustrated factors is a process of Bayesian inference (9) in which spontaneous activity (SA) in AC (red; AC = auditory cortex) is compared against prior predictions (yellow) generated by higher perceptual centres, resulting in an overall perceptual inference (orange). The process of how this Bayesian inference scheme leads to perceived tinnitus is illustrated in Figure 30, and in this the key factor that determines the emergence of tinnitus, and its loudness, is the precision of SA in AC (height/narrowness of red distribution in the Bayesian inference plot). Ordinarily, the precision of SA is so low as to preclude conscious perception. However, underlying tinnitus is the influence of one or more factors, which synergise to increase the precision of this SA. Because precision is determined by a multifactorial synergy, none of the individual processes (nor its neural correlates) needs to show group-level differences in tinnitus patients vs. controls. These factors are numbered, with black numbers indicating processes mandatory for the perception of most clinically-significant cases of tinnitus, and grey numbers indicating optional processes that may predispose to tinnitus or increase its severity. The central portion of the figure depicts AC, including A1, other parts of Heschl's gyrus (HG) and superior temporal gyrus (STG). Other divisions of AC not illustrated might also be similarly involved. The three cortical layers featured are based on the Haeusler and Maass canonical microcircuit model, and comprise the granular layer (G) which receives forward connections, the supragranular layer (SG) which sends forward connections and receives backward connections, and the infragranular layer (IG) which sends backward connections. Lateral connections are based on the Felleman and van Essen model, and project from non-

granular layers to non-granular layers. Three example cortical columns are illustrated, two in primary A1 and one in STG. In the latter, inhibitory interneurons are also included whereas in the other columns they are omitted for clarity. The right-most column includes the main intrinsic excitatory connections, and to the right of this column are example oscillatory power spectra associated with the SG and IG layers; the SG layer principally generates gamma oscillations, whereas the IG layer generates lower frequency oscillations. Other parts of the figure illustrate other brain areas, functional processes and/or neurochemical influences relevant to tinnitus. Clockwise from top, these comprise: global perceptual networks (GPNs), including (but not necessarily limited to) precuneus (Prec), inferior parietal cortex (IPC), parahippocampal cortex (PHC), ventrolateral/medial prefrontal cortex (vl/vmPFC) and dorsal anterior cingulate cortex (dACC); Bayesian perceptual inference based on weighted contributions from GPNs and AC; cholinergic projections to AC from the basal forebrain (BF) cholinergic system; the influence of orofacial movements (OFMs) on both the subcortical auditory pathway and GPNs; the cochlea; the subcortical central auditory pathway, including dorsal cochlear nucleus (DCN) and inferior colliculus (IC), which are grouped together as it is not necessary to separate them in this model, and both specific (S) and non-specific (NS) divisions of the auditory thalamus (Medial Geniculate Body; MGB), along with the thalamic reticular nucleus (TRN); the action of the inhibitory neurotransmitter gamma-aminobutyric acid (GABA) on AC and the subcortical pathway.

The numbered tinnitus-related processes/factors are as follows:

1) A degree of peripheral deafferentation, usually high-frequency, is typically required, in the form of cochlear damage and/or auditory nerve damage. The de-afferented frequency region therefore sends reduced input to the central auditory pathway, depicted by the dashed line, initially at the level of the cochlear nuclei. However, transient tinnitus, and chronic tinnitus at its onset, may be driven by spontaneous firing from the cochlea, depicted by yellow spikes.

2) To maintain mean firing rates in the deafferented tonotopic regions, gain is increased at the level of the DCN/IC (and higher auditory centres in principle), which amplifies both peripheral input and internal noise (the latter constituting an essential tinnitus precursor). The result is reduced (i.e. not fully compensated) responses to external sounds, and increased spontaneous ascending activity, with the thick dashed line representing this dichotomy. This abnormal pattern of activity is relayed through the specific MGB, to multiple divisions of AC.

3) The TRN exerts a tonic inhibitory influence on thalamic activity, and inhibition (or reduced activation) of relevant neuronal populations in the TRN (e.g. by subcallosal cortical regions, and/or BF cholinergic inputs) leads to further amplification of ascending activity.

4) Optionally, particularly in cases with more marked deafferentation, deprivation of input to the non-specific MGB (not tonotopically organised) causes hyperpolarisataion, which leads to spontaneous neuronal bursting in the delta/theta frequency range (depicted by the oscillating lines). This induces delta/theta oscillations in AC, which are coherent across auditory regions (and thus strongly detectable extracranially). AC projects back to non-specific thalamus, thus forming a reciprocal loop. Deafferented cortex is also capable of generating delta oscillations independently of thalamic connections, so additional mechanisms of delta/theta cortico-cortical coherence might also apply. Delta/theta oscillations also project widely to non-auditory cortical regions comprising GPNs that are relevant to tinnitus. Because delta/theta oscillations control the temporal windows in which bursts of higher frequency (beta and gamma) oscillations occur, the effect of widespread

delta/theta coherence is that high frequency activity occurs in temporally coincident bursts (represented by coalescence of forward connections from AC), which increases the summation of excitatory post-synaptic potentials generated by onward connections. However, as the phase of the high frequency oscillations orchestrated by the delta/theta rhythm is not necessarily coherent across cortical areas, this need not be accompanied by increased magnitude of high frequency oscillations.
5) Deficiency of GABA-ergic activity (tissue concentration, receptor affinity, and/or receptor density) reduces one or more of: tonic inhibition, forward inhibition (both affecting gain on bottom-up connections), or lateral/surround inhibition (affecting spread of activity across cortex). This therefore increases the gain of spontaneous ascending activity, and/or the spread and synchrony of this activity across neighbouring cortical columns.
6) Both increased lateral connections and decreased lateral inhibition (due to GABA-ergic deficiency, deafferentation and/or neuronal plasticity) have the effect of synchronising neural activity across a wider than normal extent of cortex. In the context of responses to external auditory stimuli, this is manifest as tonotopic map plasticity, increased evoked response magnitude and/or hyperacusis. In the context of spontaneous ascending activity, the result is increased synchrony of neural activity along the tonotopic axis.
7) Cholinergic projections from the BF act in multiple ways, particularly promoting plasticity that drives neuronal synchrony between cortical columns (either directly or via cortico-thalamo-cortical connections), and increasing the gain of superficial pyramidal cells. BF projections may also inhibit relevant parts of the TRN and thereby increase subcortical gain.
8) Spontaneous ascending activity is inherently noisy (i.e. temporally irregular and unpredictable), and therefore generates a persistent prediction error signal, manifest as gamma oscillations within supragranular pyramidal cells. This signal should arise simply due to the presence of any spontaneous ascending activity (hence, to a certain extent it is a normal process), but the processes just described that increase its magnitude (3, 5 and 7), inter-columnar synchrony (4, 5, 6 and 7) or align the timing of gamma bursts across auditory regions (4) all have the effect of increasing the influence of the prediction error signal on its target neuronal populations, i.e. they increase the precision of SA.
9) Ordinarily, the prediction error signal (which constitutes an auditory representation) is over-ridden by a prediction in higher cortical areas (i.e. those comprising GPNs) that predicts no auditory percept (i.e. silence). Note that higher predictions can also encompass auditory memory, particularly in PHC, and also mechanisms for the cancellation/suppression of unpleasant or irrelevant stimuli. The substantially higher precision of the prediction than the prediction error (driven by the spontaneous activity) results in a sensory inference that is too weak to be perceived. However, if the precision of the prediction error becomes sufficiently strong then the sensory percept deviates from the higher prediction, and a spontaneous, ongoing auditory percept (i.e. tinnitus) occurs. Once a tinnitus percept is established, the higher prediction changes to one of tinnitus, rather than silence, and thereafter tinnitus will always persist, unless the processes underlying the SA itself can be reversed, or the prediction can be abolished. See Figure 30 for further details of the sensory inference processes proposed to underlie tinnitus.
10) OFMs, and other craniocervical somatomotor inputs, increase gain within the DCN (and possibly higher centres in the auditory pathway), particularly in the context of deafferentation, thus increasing the magnitude of SA. Voluntary OFMs also influence activity in GPNs, as they relate to task-related behaviour, motor planning and the multi-model perceptual consequences of the OFMs. This may mean that OFMs induce a

temporal correlation between the magnitude of SA underlying tinnitus, and behaviourally-relevant representations in GPNs, thereby increasing the behavioural relevance of the SA and thus the estimated precision attributed to it by these higher networks.
11) Selective attention, via the BF system, causes the release of acetylcholine in AC, which acts to further increase the precision of spontaneous prediction errors in the ways described in 8, and therefore increase the perceived loudness and clarity of tinnitus. It may also operate via inhibition of the TRN (3). Attention may be driven through voluntary attention to the tinnitus percept ('top-down'; via higher centres such as the prefrontal cortex), or automatically ('bottom-up'), by the mismatch between prediction and ascending sensory activity (i.e. the persistence of a prediction error). Increased attention may also be the initial event that raises the precision of the prediction error sufficiently for a tinnitus percept to occur.

It is apparent that this model can account for a number of paradoxes present in the tinnitus literature, including: the lack of a single reliable neural correlate showing group-level differences between tinnitus patients and matched controls; the shift from peripheral to central origin of the activity underlying tinnitus; that only a certain proportion of individuals with hearing loss develop tinnitus; and that a certain degree of tinnitus is present, or can be induced by OFMs, in most individuals in the right conditions. The model also brings together a number of disparate accounts of tinnitus generation, including increased gain, plasticity, reduced inhibition, deficient noise cancelling, somatomotor influences, thalamocortical rhythms, attentional reinforcement and Bayesian inference. In doing so, it allows all these account to work together without any conflict between them, and rectifies the insufficiencies inherent in using any model in isolation or in its previously-proposed context. However, what has not been previously proposed in the context of tinnitus, even in part, is the concept of the hierarchical descent on salience. This is crucial for explaining how tinnitus actually arises in the Bayesian inference framework (which has not been specified in existing models), and for explaining a number of aspects of tinnitus phenomenology, such as initial emergence of tinnitus, enhancement by attention, attractor state behaviour, habituation, and RI/RE. These processes are illustrated and explained in Figure 30.

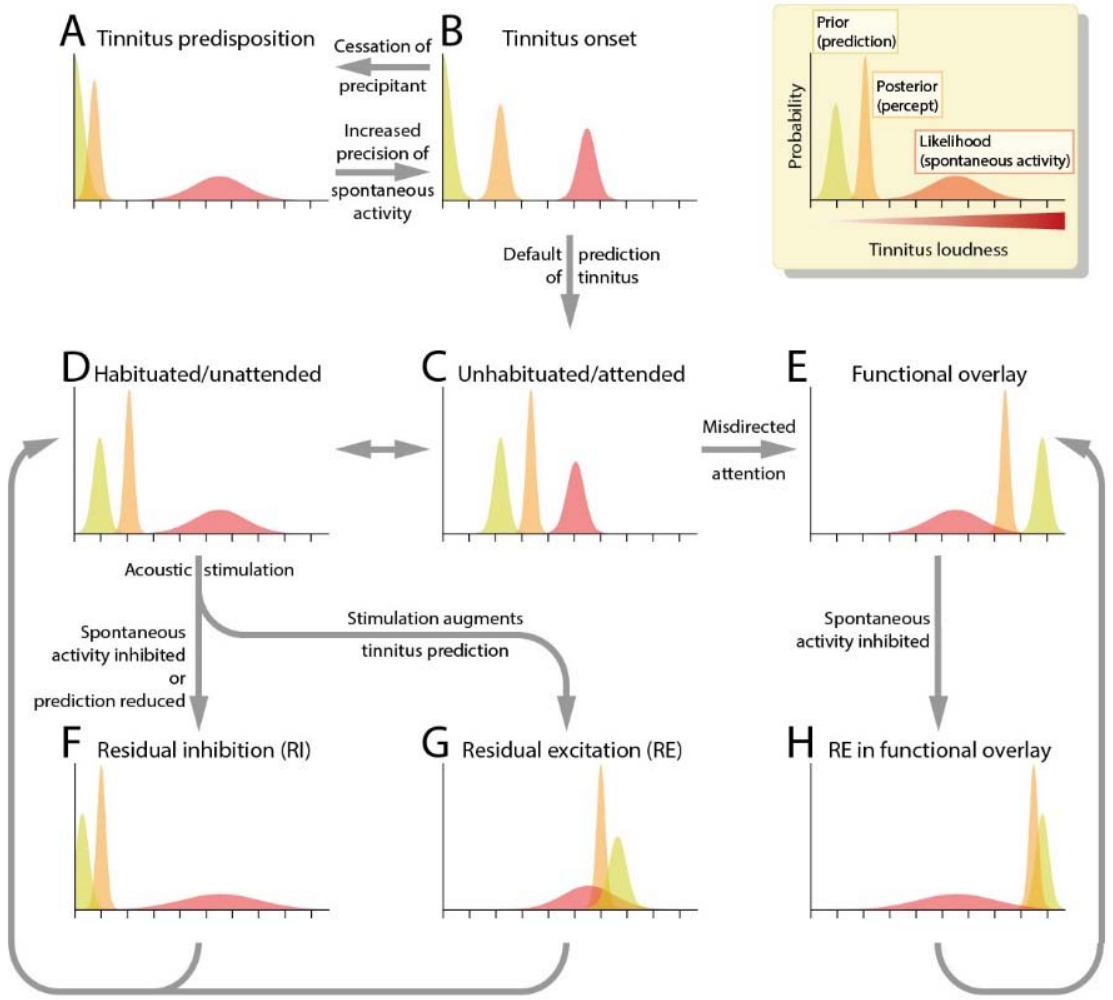

Figure 30: Schematic of proposed Bayesian inference underlying tinnitus
The inset illustrates the notation used in this figure. The graph shows three probability distributions, with the abscissa indicating a particular perceptual dimension (here the loudness of tinnitus, with the origin representing silence), and the ordinate representing the probability of each particular value. The yellow distribution is the prior, i.e. the existing (top-down) prediction about the percept. The red distribution is the likelihood, i.e. the (bottom-up) sensory representation (here the direct consequence of spontaneous activity; SA). The orange distribution is the posterior, i.e. the overall inference (here the perceived tinnitus loudness) based on an optimally weighted combination of the prior and the likelihood. The width of each distribution indicates its precision (defined as inverse variance), which reflects the level of confidence or certainty attributed to it. Surprise refers to the prediction error (the mismatch between the mean of the prior and the mean of the likelihood), weighted by the precision of the prior, such that a more precise prior leads to greater surprise for a given mismatch. Surprise is encoded by gamma band oscillations, the magnitude of which may also be related to the precision of the likelihood. Ordinarily, during stable perception, the prior is quickly adjusted to match the likelihood, so as to minimise surprise. Conversely, a fundamental part of this model is that there is a persistent mismatch between the prior and likelihood. The mismatch is maintained because higher cognitive appraisal of the SA reveals it to be of limited (if any relevance), due to its lack of

correlation with events in any other sensory modality (or, generally, within the auditory modality), lack of any cognitive or behavioural relevance, and its low precision. Thus, a 'hierarchical descent' on salience is present. The low precision may be related to low amplitude, but is principally due to a lack of temporal structure (which forms the basis of most higher audition) on account of its origin being in random neuronal firing. The lettered panels of the main figure illustrate various time points in the onset and evolution of tinnitus.

A: The predisposition to tinnitus exists because there is SA in the ascending auditory pathway (red). This has very low precision, compared to a relatively precise prediction of silence (yellow). Therefore the inferred loudness (orange) is biased strongly towards silence, and is below the threshold for conscious perception, except perhaps during focused attention in a silent environment (note that around 50% of all adults experience mild tinnitus in these conditions).

B: One or more precipitating events (such as increased deafferentation, focused attention, increased arousal, and/or altered contextual factors) cause the precision of the SA (red) to be increased. This increase in precision causes the posterior inference (orange) to become sufficiently strong to result in an auditory percept (tinnitus). At this stage, the prior prediction (yellow) has not been altered, and therefore a cessation of the precipitant leads to a cessation of perceived tinnitus.

C/D: Once the prior prediction becomes altered to reflect the tinnitus percept (i.e. the 'attractor state' is established), the posterior tinnitus loudness is always sufficiently strong to be consciously perceived (except during distraction or masking).

C: Attention towards tinnitus (such as occurs in unhabituated patients) increases the precision of the likelihood, and therefore increases its influence on overall inference, making the tinnitus percept louder.

D: In unattended or habituated conditions, the precision of the likelihood is reduced back to pre-tinnitus levels. However, the prior has been altered, and therefore the overall inference is still over the threshold for conscious perception, though not as strong as in attended or unhabituated conditions.

E: Ordinarily, even during attention and when unhabituated, the prior prediction remains weaker than the likelihood, as the tinnitus has limited cognitive/behavioural/affective relevance. However, if the tinnitus is attributed high levels of importance in these regards then the prior can reach anywhere up to the same level as the likelihood. It is also possible for the prior to exceed the likelihood; usually attention towards a percept increases precision of the likelihood and therefore biases perception towards its value, however a recent concept is the misdirection of attention (towards the cognitive/affective/behavioural consequences of the symptom, rather than the sensation itself), by which increased attention can amplify a symptom well beyond the likelihood, or even generate a symptom from only normal SA. In tinnitus, this model proposes that that this type of process may exacerbate tinnitus dramatically, rather than be its sole cause, thus constituting a functional overlay.

F: After a masking stimulus has been presented, gain in the ascending auditory pathway is reduced (due to temporary reversal of deafferentation, which is therefore accompanied by reduced delta/theta oscillations), and thus the precision of the likelihood is reduced. This results in the perception of tinnitus being more influenced by the prior, and therefore becoming quieter (i.e. residual inhibition; RI). The mismatch between the prior and the likelihood remains the same, but the reduced precision of the likelihood reduces the magnitude of gamma oscillations. Alternatively (or additionally), RI can be caused by a temporary change in the prior prediction (towards silence). In this case, surprise is actually

increased (hence gamma oscillations increase), but the tinnitus percept becomes weaker. If both mechanisms coexist then the net change in gamma oscillation magnitude may be close to zero.
G: After presentation of a stimulus closely matched to the tinnitus frequency, there is no significant change in the likelihood, but the prior prediction related to the tinnitus percept has been influenced by the masker stimulus, and therefore starts from a loudness representing that of the preceding stimulus (i.e. louder than its usual level). During the period while the prior prediction returns to its baseline, the tinnitus percept is strengthened, but surprise is substantially reduced, due to the prior being relatively concordant with the likelihood. Thus an increase in tinnitus loudness is accompanied by a drop in gamma oscillation magnitude.
H: This model predicts that in patients with a functional overlay, and very loud/severe tinnitus, the prior prediction exceeds the loudness of the likelihood. Therefore, conditions that suppress spontaneous auditory activity, and hence normally cause RI, lead to the tinnitus percept being biased towards the prior prediction, which in these patients means getting louder. Hence, these patients should experience RE instead of RI. This RE should be associated with a reduction in gamma power, but also a reduction in delta/theta power (i.e. should have the same neural correlates as typical RI).

9.2.1 Predictions made by the model

The model proposed above has a certain face validity, in that it offers the most complete and parsimonious reconciliation of known abnormalities in tinnitus with the known functional properties and anatomical architecture of sensory systems. However, the model also may be tested through a number of predictions it implicitly makes about the results of hypothetical experiments. If correct, these would provide further support to the model, and if incorrect would prompt reconsideration or revision of the model.

Transient increases in tinnitus precursors precipitating onset

The model posits that tinnitus is initially precipitated by factors increasing the precision of SA in the AC, aspects of which are manifest as delta/theta and gamma oscillations, but that the precipitants often revert to normal subsequently. Therefore it predicts that tinnitus patients, around the time of tinnitus onset, should show increased levels of delta/theta and/or gamma oscillations compared to preceding and subsequent times.

Window of reversibility at tinnitus onset

Although a window of reversibility is suggested based on animal studies showing abolition of behavioural evidence of tinnitus using furosemide to inhibit cochlear activity, this window coincides with the period immediately following the auditory insult. The present model, is compatible with these findings, but also suggests a different type of window of

reversibility, at the time when tinnitus first develops perceptually. This window is based on the time period between perceptual onset of tinnitus and establishment of the attractor state through re-setting of the default prediction. Though this window sometimes coincides with the auditory insult, at other times it occurs much later. In such instances, the model predicts that suppression of the cortical or subcortical drive to tinnitus (e.g. through acoustic or pharmacological therapies) should result in lasting cessation of perceived tinnitus, provided they are effective in the short term. Of course, tinnitus could become re-precipitated at a later date, in which case an equivalent window of reversibility would apply then also.

Correlates of 'residual inhibition' in control subjects with hearing loss

The model explains the predominant type of RI as forward inhibition of the subcortical and cortical SA driving tinnitus, which is manifest as delta/theta and/or gamma oscillations. It also proposes that the magnitudes of these oscillations reflect tinnitus precursor processes, and therefore are approximately equally present in matched control populations. Therefore these control populations (e.g. subjects with hearing loss but no tinnitus) should show neurophysiological evidence of 'RI' after equivalent stimuli, manifest as reduced delta/theta oscillations. They should also show reduced gamma oscillations, as the gain on prediction errors would be reduced. While a minority of tinnitus patients show RI associated with increased gamma oscillations, the model predicts that this operates by weakening of the tinnitus prediction. As tinnitus-predisposed controls would not have a tinnitus prediction, this mechanism of 'RI' should not be applicable to them, and therefore they should only show gamma decreases with 'RI', and never increases.

Residual excitation, not inhibition, in functional overlay patients

As explained in the legend to Figure 30, the model predicts that RI generally operates by reducing the precision of spontaneous auditory activity, thus biasing perception towards the tinnitus prediction. In most patients the prediction is of a quieter sound than that encoded by the SA, so tinnitus perception is reduced. In the hypothesised functional overlay patients, the prediction is of louder tinnitus than encoded by SA, and therefore tinnitus perception is increased by conditions that would normally be associated with RI. This type of 'RE' in functional overlay patients should be associated with the typical correlates of RI in most tinnitus patients (i.e. reduced delta/theta and gamma power).

Findings in 'pseudo-tinnitus' produced by chronic acoustic stimulation

The Bayesian inference (predictive coding) framework that features in the model is not unique to tinnitus, but could apply equally to any chronic percept that is noisy, information-poor, unchanging, and unrelated to any motor actions or stimuli in any sensory domain. This could be achieved by presenting an ambient stimulus in animal studies, or with chronically headphone-delivered stimuli in human studies (though care would need to be taken to dissociate the onset of the stimulus from the putting on of the headphones and other subject-identifiable events). Under the right conditions, the model would predict that some individuals would 'tune out' this stimulus from conscious perception, though they would probably perceive it during directed attention in quiet environments. Other subjects would develop a default prediction of a sound, though as in tinnitus there should be a hierarchical descent on salience. This would be expected to result in phenomena such as enhancement by attention, plus phenomena of RI (by reducing the loudness or precision of the stimulus, or simply by applying an additional masker stimulus as in tinnitus patients) or excitation (by superimposing a frequency-matched stimulus that is louder and/or has higher precision).

Cholinergic influences in tinnitus

A prediction of the model is that in most tinnitus patients (except those with functional overlay), ACh acts to bias perception towards the spontaneous auditory activity, thereby increasing the perceived loudness or salience of tinnitus. Therefore, administration of drugs with a cholinergic agonist or potentiating action should increase tinnitus loudness or awareness in these patients. A further point of study might be genetic variation associated with the high-affinity choline uptake transporter (CHT), which is a limiting factor in cholinergic neurotransmission (Sarter and Parikh, 2005). Genetic variants associated with reduced CHT function have been linked to poorer attentional performance (Berry et al., 2013). Conversely, in tinnitus the model would predict that this genotype is associated with less severe tinnitus, and possibly a lower chance of developing tinnitus. Functional overlay patients should experience reduced tinnitus loudness with increased cholinergic action, and therefore show the opposite relationship with ACh-related factors.

Relationship of cortical to subcortical activity

The model predicts that spontaneous cortical, and thalamic activity, are driven by subcortical activity, and from the periphery in some cases. Therefore simultaneous recordings, in animal models of noise trauma and tinnitus, should reveal that the time courses of activity at various levels of the auditory pathway should be correlated with each other. Purely thalamic/cortical models of tinnitus, conversely, would predict a lack of correlation, or an inverse correlation (i.e. thalamic/cortical hyperactivity would be driven by deafferentation, so spontaneous increases in subcortical/subthalamic activity would reduce this).

9.3 Conclusions

This body of work comprises a literature review on neural bases for tinnitus, a discussion of the inconsistencies and paradoxes in the tinnitus literature unaccounted for by existing models, five original research studies investigating cortical neurophysiological and neurochemical processes associated with tinnitus and directly-related normal perceptual processes, and the specification of a new model to address existing paradoxes, built upon aspects of existing models, the reviewed literature and novel experimental findings. The new model is built upon the framework of predictive coding, and centrally features sensory precision as the synergistic result of diverse precursor processes, which allows spontaneous activity to cross a threshold for conscious perception as tinnitus. Finally, a set of testable predictions generated by this model are proposed, which may help to direct future work in this field.

References

Adamchic I, Langguth B, Hauptmann C, Tass PA. (2014) Abnormal cross-frequency coupling in the tinnitus network. Front Neurosci 8:1–11

Adjamian P, Barnes GR, Holliday IE (2008) Induced Gamma activity in primary visual cortex is related to luminance and not color contrast : An MEG study. J Vis 8:1–7.

Adjamian P, Holliday IE, Barnes GR, Hillebrand A, Hadjipapas A, Singh KD (2004) Induced visual illusions and gamma oscillations in human primary visual cortex. Eur J Neurosci 20:587–592

Adjamian P, Sereda M, Zobay O, Hall DA, Palmer AR (2012) Neuromagnetic indicators of tinnitus and tinnitus masking in patients with and without hearing loss. J Assoc Res Otolaryngol 13:715–731

Argence M, Saez I, Sassu R, Vassias I, Vidal PP, de Waele C (2006) Modulation of inhibitory and excitatory synaptic transmission in rat inferior colliculus after unilateral cochleectomy: an in situ and immunofluorescence study. Neuroscience 141:1193–1207

Arnal LH, Giraud A-L (2012) Cortical oscillations and sensory predictions. Trends Cogn Sci 16:390–398

Arnal LH, Wyart V, Giraud A-L (2011) Transitions in neural oscillations reflect prediction errors generated in audiovisual speech. Nat Neurosci 14:797–801

Ashburner J, Friston KJ (2000) Voxel-based morphometry--the methods. Neuroimage 11:805–821

Ashton H, Reid K, Marsh R, Johnson I, Alter K, Griffiths TD (2007) High frequency localised “hot spots” in temporal lobes of patients with intractable tinnitus: a quantitative electroencephalographic (QEEG) study. Neurosci Lett 426:23–28

Attias J, Urbach D, Gold S, Shemesh Z (1993) Auditory event related potentials in chronic tinnitus patients with noise induced hearing loss. Hear Res 71:106–113

Axelsson A, Ringdahl A (1989) Tinnitus--a study of its prevalence and characteristics. Br J Audiol 23:53–62

Baldo P, Doree C, Molin P, McFerran D, Cecco S (2006) Antidepressants for patients with tinnitus. Cochrane Libr

Balkenhol T, Wallhäusser-Franke E, Delb W (2013) Psychoacoustic tinnitus loudness and tinnitus-related distress show different associations with oscillatory brain activity. PLoS One 8:e53180

Banay-Schwartz M, Lajtha A, Palkovits M (1989) Changes with aging in the levels of amino acids in rat CNS structural elements. I. Glutamate and related amino acids. Neurochem Res 14:555–562

Bastos AM, Usrey WM, Adams RA, Mangun GR, Fries P, Friston KJ (2012) Canonical microcircuits for predictive coding. Neuron 76:695–711

Bauer C, Brozoski T (2001) Assessing Tinnitus and Prospective Tinnitus Therapeutics Using a Psychophysical Animal Model. J Assoc Res Otolaryngol 2:54–64.

Bauer CA, Turner JG, Caspary DM, Myers KS, Brozoski TJ (2008) Tinnitus and inferior colliculus activity in chinchillas related to three distinct patterns of cochlear trauma. J Neurosci Res 86:2564–2578

Bauer M, Oostenveld R, Peeters M, Fries P (2006) Tactile spatial attention enhances gamma-band activity in somatosensory cortex and reduces low-frequency activity in parieto-occipital areas. J Neurosci 26:490–501

Bauer M, Stenner M-P, Friston KJ, Dolan RJ (2014) Attentional Modulation of Alpha/Beta and Gamma Oscillations Reflect Functionally Distinct Processes. J Neurosci 34:16117–16125

Beckmann CF, DeLuca M, Devlin JT, Smith SM (2005) Investigations into resting-state connectivity using independent component analysis. Philos Trans R Soc Lond B Biol Sci 360:1001–1013

Berry AS, Demeter E, Sabhapathy S, English BA, Blakely RD, Sarter M, Lustig C (2013) Disposed to Distraction : Genetic Variation in the Cholinergic System Influences Distractibility But Not Time-on-Task Effects. :1981–1991.

Biswal B, Yetkin FZ, Haughton VM, Hyde JS (1995) Functional connectivity in the motor cortex of resting human brain using echo-planar MRI. Magn Reson Med 34:537–541

Bitterman Y, Mukamel R, Malach R, Fried I, Nelken I (2008) Ultra-fine frequency tuning revealed in single neurons of human auditory cortex. Nature 451:197–201

Boyen K, Kleine E De, Dijk P Van, Langers DRM (2014) Tinnitus-related dissociation between cortical and subcortical neural activity in humans with mild to moderate sensorineural hearing loss. Hear Res 312:48–59

Boyen K, Langers DRM, de Kleine E, van Dijk P (2013) Gray matter in the brain: differences associated with tinnitus and hearing loss. Hear Res 295:67–78

Brancucci A, Franciotti R, D'Anselmo A, Della Penna S, Tommasi L (2011) The sound of consciousness: neural underpinnings of auditory perception. J Neurosci 31:16611–16618

Brodski A, Paasch G-F, Helbling S, Wibral M (2015) The Faces of Predictive Coding. J Neurosci 35:8997–9006

Brozoski T, Odintsov B, Bauer C (2012) Gamma-aminobutyric acid and glutamic acid levels in the auditory pathway of rats with chronic tinnitus: a direct determination using high resolution point-resolved proton magnetic resonance spectroscopy (H-MRS). Front Syst Neurosci 6:9

Brozoski TJ, Bauer CA (2005) The effect of dorsal cochlear nucleus ablation on tinnitus in rats. Hear Res 206:227–236

Brozoski TJ, Bauer CA, Caspary DM (2002) Elevated fusiform cell activity in the dorsal cochlear nucleus of chinchillas with psychophysical evidence of tinnitus. J Neurosci 22:2383–2390

Brugge JF, Volkov IO, Oya H, Kawasaki H, Reale RA, Fenoy A, Steinschneider M, Howard M a (2008) Functional localization of auditory cortical fields of human: click-train stimulation. Hear Res 238:12–24

Burianova J, Ouda L, Profant O, Syka J (2009) Age-related changes in GAD levels in the central auditory system of the rat. Exp Gerontol 44:161–169

Burton H, Wineland A, Bhattacharya M, Nicklaus J, Garcia KS, Piccirillo JF (2012) Altered networks in bothersome tinnitus: a functional connectivity study. BMC Neurosci 13:3

Calderone DJ, Lakatos P, Butler PD, Castellanos FX (2014) Entrainment of neural oscillations as a modifiable substrate of attention. Trends Cogn Sci 18:300–309

Campolo J, Lobarinas E, Salvi R (2013) Does tinnitus “fill in” the silent gaps? Noise Heal 15.

Canolty RT, Edwards E, Dalal SS, Soltani M, Nagarajan SS, Kirsch HE, Berger MS, Barbaro NM, Knight RT (2006) High gamma power is phase-locked to theta oscillations in human neocortex. Science 313:1626–1628

Caspary DM, Raza A, Lawhorn Armour BA, Pippin J, Arnerić SP (1990) Immunocytochemical and neurochemical evidence for age-related loss of GABA in the inferior colliculus: implications for neural presbycusis. J Neurosci 10:2363–2372

Caspary DM, Schatteman TA, Hughes LF (2005) Age-related changes in the inhibitory response properties of dorsal cochlear nucleus output neurons: role of inhibitory inputs. J Neurosci 25:10952–10959

Cazals Y, Horner KC, Huang ZW (1998) Alterations in Average Spectrum of Cochleoneural Activity by Long-Term Salicylate Treatment in the Guinea Pig : A Plausible Index of Tinnitus. :2113–2120.

Chalk M, Herrero JL, Gieselmann M a, Delicato LS, Gotthardt S, Thiele A (2010) Attention reduces stimulus-driven gamma frequency oscillations and spike field coherence in V1. Neuron 66:114–125

Chen G, Jastreboff PJ (1995) Salicylate-induced abnormal activity in the inferior colliculus of rats. Hear Res 82:158–178

Chen G, Lee C, Sandridge S a, Butler HM, Manzoor NF, Kaltenbach JA (2013) Behavioral evidence for possible simultaneous induction of hyperacusis and tinnitus following intense sound exposure. J Assoc Res Otolaryngol 14:413–424

Chen Y-C, Xia W, Feng Y, Li X, Zhang J, Feng X, Wang C-X, Cai Y, Wang J, Salvi R, Teng G-J (2015) Altered interhemispheric functional coordination in chronic tinnitus patients. Biomed Res Int 2015:345647

Colding-Jørgensen E, Lauritzen M, Johnsen NJ, Mikkelsen KB, Saermark K (1992) On the evidence of auditory evoked magnetic fields as an objective measure of tinnitus. Electroencephalogr Clin Neurophysiol 83:322–327

Dauman R, Frederic B-F (2005) Assessment and amelioration of hyperacusis in tinnitus patients. Acta Otolaryngol 125:503–509.

David O, Kiebel SJ, Harrison LM, Mattout J, Kilner JM, Friston KJ (2006) Dynamic causal modeling of evoked responses in EEG and MEG. Neuroimage 30:1255–1272

Davies J, Gander PE, Andrews M, Hall DA (2014) Auditory network connectivity in tinnitus patients: a resting-state fMRI study. Int J Audiol 53:192–198

De Ridder D, Congedo M, Vanneste S (2015a) The neural correlates of subjectively perceived and passively matched loudness perception in auditory phantom perception. Brain Behav 5:e00331

De Ridder D, Elgoyhen AB, Romo R, Langguth B (2011a) Phantom percepts: tinnitus and pain as persisting aversive memory networks. Proc Natl Acad Sci U S A 108:8075–8080

De Ridder D, van der Loo E, Vanneste S, Gais S, Plazier M, Kovacs S, Sunaert S, Menovsky T, van de Heyning P (2011b) Theta-gamma dysrhythmia and auditory phantom perception. J Neurosurg 114:912–921

De Ridder D, Vanneste S, Engineer ND, Kilgard MP (2014) Safety and efficacy of vagus nerve stimulation paired with tones for the treatment of tinnitus: a case series. Neuromodulation 17:170–179

De Ridder D, Vanneste S, Freeman W (2012) The Bayesian brain: Phantom percepts resolve sensory uncertainty. Neurosci Biobehav Rev

De Ridder D, Vanneste S, Langguth B, Llinas R (2015b) Thalamocortical Dysrhythmia: A Theoretical Update in Tinnitus. Front Neurol 6:1–13

De Ridder D, Vanneste S, Weisz N, Londero A, Schlee W, Elgoyhen AB, Langguth B (2013) An integrative model of auditory phantom perception: Tinnitus as a unified percept of interacting separable subnetworks. Neurosci Biobehav Rev

Delb W, Strauss DJ, Low YF, Seidler H, Rheinschmitt A, Wobrock T, D'Amelio R (2008) Alterations in Event Related Potentials (ERP) associated with tinnitus distress and attention. Appl Psychophysiol Biofeedback 33:211–221

Diesch E, Andermann M, Flor H, Rupp A (2010) Interaction among the components of multiple auditory steady-state responses: enhancement in tinnitus patients, inhibition in controls. Neuroscience 167:540–553

Diesch E, Struve M, Rupp A, Ritter S, Hu M, Flor H (2004) Enhancement of steady-state auditory evoked magnetic fields in tinnitus. Eur J Neurosci 19:1093–1104.

Dohrmann K, Elbert T, Schlee W, Weisz N (2007) Tuning the tinnitus percept by modification of synchronous brain activity. Restor Neurol Neurosci 25:371–378.

Dong S, Rodger J, Mulders WHAM, Robertson D (2010) Tonotopic changes in GABA receptor expression in guinea pig inferior colliculus after partial unilateral hearing loss. Brain Res 1342:24–32

Edden RAE, Barker PB (2007) Spatial effects in the detection of gamma-aminobutyric acid: improved sensitivity at high fields using inner volume saturation. Magn Reson Med 58:1276–1282

Edden RAE, Puts NAJ, Barker PB (2012) Macromolecule-suppressed GABA-edited magnetic resonance spectroscopy at 3T. Magn Reson Med 68:657–661

Edden RAE, Puts NAJ, Harris AD, Barker PB, Evans CJ (2014) Gannet: A batch-processing tool for the quantitative analysis of gamma-aminobutyric acid–edited MR spectroscopy spectra. J Magn Reson Imaging 40:1445–1452

Edwards E, Soltani M, Deouell LY, Berger MS, Knight RT (2005) High gamma activity in response to deviant auditory stimuli recorded directly from human cortex. J Neurophysiol 94:4269–4280

Edwards MJ, Adams RA, Brown H, Pareés I, Friston KJ (2012) A Bayesian account of "hysteria". Brain 135:3495–3512

Eggermont JJ (2000) Sound-Induced Synchronization of Neural Activity Between and Within Three Auditory Cortical Areas. J Neurophysiol 83:2708–2722

Eggermont JJ (2012) The Neuroscience of Tinnitus, 1st ed. Oxford: Oxford University Press.

Eggermont JJ (2013) Hearing loss, hyperacusis, or tinnitus: what is modeled in animal research? Hear Res 295:140–149

Eggermont JJ, Kenmochi M (1998) Salicylate and quinine selectively increase spontaneous firing rates in secondary auditory cortex. Hear Res 117:149–160

Engineer ND, Riley JR, D SJ, Vrana WA, Shetake JA, Sudanagunta SP, Borland MS, Kilgard MP (2011) Reversing pathological neural activity using targeted plasticity. Nature 470:101–104.

Ernst MO, Banks MS (2002) Humans integrate visual and haptic information in a statistically optimal fashion. Nature 415:429–433

Finlayson PG, Kaltenbach JA (2009) Alterations in the spontaneous discharge patterns of single units in the dorsal cochlear nucleus following intense sound exposure. Hear Res 256:104–117

Fontolan L, Morillon B, Liegeois-Chauvel C, Giraud A-L (2014) The contribution of frequency-specific activity to hierarchical information processing in the human auditory cortex. Nat Commun 5:4694

Fournier P, Hébert S (2013) Gap detection deficits in humans with tinnitus as assessed with the acoustic startle paradigm: does tinnitus fill in the gap? Hear Res 295:16–23

Fries P, Reynolds JH, Rorie AE, Desimone R (2001) Modulation of oscillatory neuronal synchronization by selective visual attention. Science 291:1560–1563

Friston K (2005) A theory of cortical responses. Philos Trans R Soc Lond B Biol Sci 360:815–836

Friston K (2008) Hierarchical models in the brain. PLoS Comput Biol 4:e1000211

Friston K, Kiebel S (2009) Predictive coding under the free-energy principle. Philos Trans R Soc Lond B Biol Sci 364:1211–1221.

Friston K, Kilner J, Harrison L (2006) A free energy principle for the brain. J Physiol Paris 100:70–87

Friston KJ, Harrison L, Penny W (2003) Dynamic causal modelling. Neuroimage 19:1273–1302

Fritz J, Shamma S, Elhilali M, Klein D (2003) Rapid task-related plasticity of spectrotemporal receptive fields in primary auditory cortex. Nat Neurosci 6:1216–1223

Fujioka T, Trainor LJ, Large EW, Ross B (2009) Beta and gamma rhythms in human auditory cortex during musical beat processing. Ann N Y Acad Sci 1169:89–92

Galambos R, Makeig S, Talmachoff PJ (1981) A 40-Hz auditory potential recorded from the human scalp. Proc Natl Acad Sci U S A 78:2643–2647

Gander PE, Bosnyak DJ, Roberts LE (2010) Evidence for modality-specific but not frequency-specific modulation of human primary auditory cortex by attention. Hear Res 268:213–226

Gao F, Wang G, Ma W, Ren F, Li M, Dong Y, Liu C, Liu B, Bai X, Zhao B, Edden RAE (2015) Decreased auditory GABA+ concentrations in presbycusis demonstrated by edited magnetic resonance spectroscopy. Neuroimage 106:311–316

Garrido MI, Sahani M, Dolan RJ (2013) Outlier responses reflect sensitivity to statistical structure in the human brain. PLoS Comput Biol 9:e1002999

Gieselmann MA, Thiele A (2008) Comparison of spatial integration and surround suppression characteristics in spiking activity and the local field potential in macaque V1. Eur J Neurosci 28:447–459

Gold JR, Bajo VM (2014) Insult-induced adaptive plasticity of the auditory system. Front Neurosci 8:110

Gray CM, Konig P, Engel AK, Singer W (1989) Oscillatory responses in cat visual cortex exhibit inter-columnar synchronization which reflects global stimulus properties. Nature 338:334–338.

Greicius MD, Krasnow B, Reiss AL, Menon V (2002) Functional connectivity in the resting brain: A network analysis of the default mode hypothesis. Proc Natl Acad Sci 100:253–258

Griffiths TD, Kumar S, Sedley W, Nourski K V, Kawasaki H, Oya H, Patterson RD, Brugge JF, Howard MA (2010) Direct recordings of pitch responses from human auditory cortex. Curr Biol 20:1128–1132

Gross J, Kujala J, Hamalainen M, Timmermann L, Schnitzler A, Salmelin R (2001) Dynamic imaging of coherent sources: Studying neural interactions in the human brain. Proc Natl Acad Sci U S A 98:694–699

Gross J, Schnitzler A, Timmermann L, Ploner M (2007) Gamma oscillations in human primary somatosensory cortex reflect pain perception. PLoS Biol 5:e133

Gruber T, Müller MM, Keil A, Elbert T (1999) Selective visual-spatial attention alters induced gamma band responses in the human EEG. Clin Neurophysiol 110:2074–2085

Gu JW, Halpin CF, Nam E-C, Levine RA, Melcher JR (2010) Tinnitus, diminished sound-level tolerance, and elevated auditory activity in humans with clinically normal hearing sensitivity. J Neurophysiol 104:3361–3370

Gu JW, Herrmann BS, Levine R A, Melcher JR (2012) Brainstem Auditory Evoked Potentials Suggest a Role for the Ventral Cochlear Nucleus in Tinnitus. J Assoc Res Otolaryngol JARO 13:819–833

Gutiérrez-Fernández M, Rodríguez-Frutos B, Fuentes B, Vallejo-Cremades MT, Alvarez-Grech J, Expósito-Alcaide M, Díez-Tejedor E (2012) CDP-choline treatment induces brain plasticity markers expression in experimental animal stroke. Neurochem Int 60:310–317

Haeusler S, Maass W (2007) A statistical analysis of information-processing properties of lamina-specific cortical microcircuit models. Cereb Cortex 17:149–162

Hall DA, Haggard MP, Akeroyd MA, Summerfield AQ, Palmer AR, Elliott MR, Bowtell RW (2000) Modulation and task effects in auditory processing measured using fMRI. Hum Brain Mapp 10:107–119

Harmony T (2013) The functional significance of delta oscillations in cognitive processing. Front Integr Neurosci 7:83

Hartmann T, Lorenz I, Müller N, Langguth B, Weisz N (2014) The effects of neurofeedback on oscillatory processes related to tinnitus. Brain Topogr 27:149–157

Hasselmo ME, Sarter M (2011) Modes and models of forebrain cholinergic neuromodulation of cognition. Neuropsychopharmacology 36:52–73

Hébert S, Fournier P, Noreña A (2013) The Auditory Sensitivity is Increased in Tinnitus Ears. J Neurosci 33:2356–2364

Hébert S, Paiement P, Lupien SJ (2004) A physiological correlate for the intolerance to both internal and external sounds. Hear Res 190:1–9

Heffner H, Harrington I (2002) Tinnitus in hamsters following exposure to intense sound. Hear Res 170:83–95.

Herrmann CS, Munk MHJ, Engel AK (2004) Cognitive functions of gamma-band activity: memory match and utilization. Trends Cogn Sci 8:347–355

Hickox AE, Liberman MC (2014) Is noise-induced cochlear neuropathy key to the generation of hyperacusis or tinnitus? J Neurosci 111:552-564

Hiller W, Janca A, Burke KC (1997) Association between tinnitus and somatoform disorders. J Psychosom Res 43:613–624

Hilton M, Zimmermann E, Hunt W (2013) Ginkgo biloba for tinnitus. Cochrane Libr

Hipp JF, Engel AK, Siegel M (2011) Oscillatory synchronization in large-scale cortical networks predicts perception. Neuron 69:387–396

Hoare D, Edmondson-Jones M, Sereda M, Akeroyd M, Hall DA (2014) Amplification with hearing aids for patients with tinnitus and co-existing hearing loss. Cochrane Libr

Hobson J, Chisholm E, El Refaie A (2012) Sound therapy (masking) in the management of tinnitus in adults. Cochrane Libr

Hoekstra C, Rynja S, van Zanten G, Rovers M (2011) Anticonvulsants for tinnitus. Cochrane Libr

Hoffman P, Pobric G, Drakesmith M, Ralph MAL (2012) Posterior middle temporal gyrus is involved in verbal and non-verbal semantic cognition : Evidence from rTMS non-verbal semantic cognition : Evidence from rTMS. Aphasiology:37–41.

Hoke ES, Mühlnickel W, Ross B, Hoke M (1998) Tinnitus and event-related activity of the auditory cortex. Audiol Neurootol 3:300–331

Hoke M (1990) Objective evidence for tinnitus in auditory-evoked magnetic fields. Acta Otolaryngol Suppl 476:189–194

Hoogenboom N, Schoffelen J-M, Oostenveld R, Fries P (2010) Visually induced gamma-band activity predicts speed of change detection in humans. Neuroimage 51:1162–1167

Husain FT, Medina RE, Davis CW, Szymko-bennett Y, Simonyan K, Pajor NM, Horwitz B (2011) Neuroanatomical Changes due to Hearing Loss and Chronic Tinnitus: A Combined VBM and DTI Study. Brain Res 1369:74–88.

Jacobson GP, Ahmad BK, Moran J, Newman CW, Tepley N, Wharton J (1991) Auditory evoked cortical magnetic field (M100-M200) measurements in tinnitus and normal groups. Hear Res 56:44–52

Jacobson GP, McCaslin DL (2003) A reexamination of the long latency N1 response in patients with tinnitus. J Am Acad Audiol 14:393–400

Jastreboff PJ (1990) Phantom auditory perception (tinnitus): mechanisms of generation and perception. Neurosci Res 8:221–254

Jastreboff PJ, Brennan JF, Coleman JK, Sasaki CT (1988) Phantom auditory sensation in rats: an animal model for tinnitus. Behav Neurosci 102:811–822

Jeanmonod D, Magnin M, Morel A (1996) Low-threshold calcium spike bursts in the human thalamus. Common physiopathology for sensory, motor and limbic positive symptoms. Brain 119 (Pt 2):363–375

Jensen O, Mazaheri A (2010) Shaping functional architecture by oscillatory alpha activity: gating by inhibition. Front Hum Neurosci 4:186

Jia X, Tanabe S, Kohn A (2013) Gamma and the coordination of spiking activity in early visual cortex. Neuron 77:762–774

John MS, Lins OG, Boucher BL, Picton TW (1998) Multiple Auditory Steady-state Responses (MASTER): Stimulus and Recording Parameters. Audiology 37:59–82.

Kadner A, Viirre E, Wester DC, Walsh SF, Hestenes J, Vankov A, Pineda JA (2002) Lateral inhibition in the auditory cortex: an EEG index of tinnitus? Neuroreport 13:443–446

Kahlbrock N, Weisz N (2008) Transient reduction of tinnitus intensity is marked by concomitant reductions of delta band power. BMC Biol 6:4

Kalappa BI, Brozoski TJ, Turner JG, Caspary DM (2014) Single unit hyperactivity and bursting in the auditory thalamus of awake rats directly correlates with behavioural evidence of tinnitus. J Physiol 592:5065–5078

Kaltenbach JA, Zacharek MA, Zhang J, Frederick S (2004) Activity in the dorsal cochlear nucleus of hamsters previously tested for tinnitus following intense tone exposure. Neurosci Lett 355:121–125

Kenmochi M, Eggermont JJ (1997) Salicylate and quinine affect the central nervous system. Hear Res 113:110–116

Khalfa S, Dubal S, Veuillet E, Perez-Diaz F, Jouvent R, Collet L (2002) Psychometric Normalization of a Hyperacusis Questionnaire. Orl 64:436–442

Kim J, Kim Y, Lee S, Seo J-H, Song H-J, Cho JH, Chang Y (2012) Alteration of functional connectivity in tinnitus brain revealed by resting-state fMRI?: A pilot study. Int J Audiol 51:413–417

Körding KP, Wolpert DM (2004) Bayesian integration in sensorimotor learning. Nature 427:244–247

Lachaux J-P, George N, Tallon-Baudry C, Martinerie J, Hugueville L, Minotti L, Kahane P, Renault B (2005) The many faces of the gamma band response to complex visual stimuli. Neuroimage 25:491–501

Landgrebe M, Langguth B, Rosengarth K, Braun S, Koch A, Kleinjung T, May A, de Ridder D, Hajak G (2009) Structural brain changes in tinnitus: grey matter decrease in auditory and non-auditory brain areas. Neuroimage 46:213–218

Langers DRM, de Kleine E, van Dijk P (2012) Tinnitus does not require macroscopic tonotopic map reorganization. Front Syst Neurosci 6:2

Lanting CP, De Kleine E, Bartels H, Van Dijk P (2008) Functional imaging of unilateral tinnitus using fMRI. Acta Otolaryngol 128:415–421

Leaver AM, Renier L, Chevillet M a, Morgan S, Kim HJ, Rauschecker JP (2011) Dysregulation of limbic and auditory networks in tinnitus. Neuron 69:33–43

Leaver AM, Seydell-Greenwald A, Turesky TK, Morgan S, Kim HJ, Rauschecker JP (2012) Cortico-limbic morphology separates tinnitus from tinnitus distress. Front Syst Neurosci 6:21

Leske S, Tse A, Oosterhof NN, Hartmann T, Müller N, Keil J, Weisz N (2014) The strength of alpha and beta oscillations parametrically scale with the strength of an illusory auditory percept. Neuroimage 88C:69–78

Levine RA, Abel M, Cheng H (2003) CNS somatosensory-auditory interactions elicit or modulate tinnitus. Exp brain Res 153:643–648

Ling LL, Hughes LF, Caspary DM (2005) Age-related loss of the GABA synthetic enzyme glutamic acid decarboxylase in rat primary auditory cortex. Neuroscience 132:1103–1113

Llano DA, Turner J, Caspary DM (2012) Diminished cortical inhibition in an aging mouse model of chronic tinnitus. J Neurosci 32:16141–16148

Llinás R, Urbano FJ, Leznik E, Ramírez RR, van Marle HJF (2005) Rhythmic and dysrhythmic thalamocortical dynamics: GABA systems and the edge effect. Trends Neurosci 28:325–333

Llinás RR, Ribary U, Jeanmonod D, Kronberg E, Mitra PP (1999) Thalamocortical dysrhythmia: A neurological and neuropsychiatric syndrome characterized by magnetoencephalography. Proc Natl Acad Sci U S A 96:15222–15227

Lobarinas E, Hayes SH, Allman BL (2013) The gap-startle paradigm for tinnitus screening in animal models: limitations and optimization. Hear Res 295:150–160

Lobarinas E, Sun W, Cushing R, Salvi R (2004) A novel behavioral paradigm for assessing tinnitus using schedule-induced polydipsia avoidance conditioning (SIP-AC). Hear Res 190:109–114

Lockwood AH, Salvi RJ, Coad ML, Towsley ML, Wack DS, Murphy BW (1998) The functional neuroanatomy of tinnitus: evidence for limbic system links and neural plasticity. Neurology 50:114–120

Ma W-LD, Hidaka H, May BJ (2006) Spontaneous activity in the inferior colliculus of CBA/J mice after manipulations that induce tinnitus. Hear Res 212:9–21

Manabe Y, Yoshida S, Saito H, Oka H (1997) Effects of lidocaine on salicylate-induced discharge of neurons in the inferior colliculus of the guinea pig. Hear Res 103:192–198

Maris E, Oostenveld R (2007) Nonparametric statistical testing of EEG- and MEG-data. J Neurosci Methods 164:177–190

Martinez-Devesa P, Perera R, Theodoulou M, Waddell A (2007) Cognitive behavioural therapy for tinnitus. Cochrane Libr

Maudoux A, Lefebvre P, Cabay J-E, Demertzi A, Vanhaudenhuyse A, Laureys S, Soddu A (2012) Auditory Resting-State Network Connectivity in Tinnitus: A Functional MRI Study Draganski B, ed. PLoS One 7:e36222

Melcher JR, Knudson IM, Levine RA (2013) Subcallosal brain structure: correlation with hearing threshold at supra-clinical frequencies (>8 kHz), but not with tinnitus. Hear Res 295:79–86

Melcher JR, Levine RA, Bergevin C, Norris B (2009) The auditory midbrain of people with tinnitus: abnormal sound-evoked activity revisited. Hear Res 257:63–74

Melcher JR, Sigalovsky IS, Guinan JJ, Levine RA (2000) Lateralized Tinnitus Studied With Functional Magnetic Resonance Imaging : Abnormal Inferior Colliculus Activation. J Neurophysiol 83:1058-1072

Melloni L, Molina C, Pena M, Torres D, Singer W, Rodriguez E (2007) Synchronization of neural activity across cortical areas correlates with conscious perception. J Neurosci 27:2858–2865

Meng Z, Liu S, Zheng Y, Phillips J (2011) Repetitive transcranial magnetic stimulation for tinnitus. Cochrane Libr

Merker B (2013) Cortical gamma oscillations: the functional key is activation, not cognition. Neurosci Biobehav Rev 37:401–417

Mescher M, Merkle H, Kirsch J, Garwood M, Gruetter R (1998) Simultaneous in vivo spectral editing and water suppression. NMR Biomed 11:266–272

Metherate R, Ashe JH (1993) Nucleus basalis stimulation facilitates thalamocortical synaptic transmission in the rat auditory cortex. Synapse 14:132–143

Middleton JW, Kiritani T, Pedersen C, Turner JG, Shepherd GMG, Tzounopoulos T (2011) Mice with behavioral evidence of tinnitus exhibit dorsal cochlear nucleus hyperactivity because of decreased GABAergic inhibition. Proc Natl Acad Sci U S A 108:7601–7606

Miller BL, Chang L, Booth R, Ernst T, Cornford M, Nikas D, McBride D, Jenden DJ (1996) In Vivo 1H MRS Choline: Correlation with in vitro chemistry/histology. Life Sci 58:1929–1935.

Mirz F, Gjedde A, Ishizu K, Pedersen CB (2000) Cortical networks subserving the perception of tinnitus--a PET study. Acta Otolaryngol Suppl 543:241–243

Moazami-Goudarzi M, Michels L, Weisz N, Jeanmonod D (2010) Temporo-insular enhancement of EEG low and high frequencies in patients with chronic tinnitus. QEEG study of chronic tinnitus patients. BMC Neurosci 11:40

Moller AR (2007 Neural generators for auditory brainstem evoked potentials. In: Auditory evoked potentials (Burkard RF, Don M, Eggermont JJ, eds), pp 336.354. Baltimore: Lippincott Williams and Wilkins.

Moore BCJ, Glasberg BR (2004) A revised model of loudness perception applied to cochlear hearing loss. Hear Res 188:70–88

Moran RJ, Campo P, Symmonds M, Stephan KE, Dolan J, Friston KJ (2014) Free energy , precision and learning : the role of cholinergic neuromodulation. 33:8227–8236.

Mühlau M, Rauschecker JP, Oestreicher E, Gaser C, Röttinger M, Wohlschläger AM, Simon F, Etgen T, Conrad B, Sander D (2006) Structural brain changes in tinnitus. Cereb Cortex 16:1283–1288

Mühlnickel W, Elbert T, Taub E, Flor H (1998) Reorganization of auditory cortex in tinnitus. Proc Natl Acad Sci U S A 95:10340–10343

Mulders WHAM, Barry KM, Robertson D (2014) Effects of furosemide on cochlear neural activity, central hyperactivity and behavioural tinnitus after cochlear trauma in guinea pig. PLoS One 9:e97948

Mulders WHAM, Robertson D (2009) Hyperactivity in the auditory midbrain after acoustic trauma: dependence on cochlear activity. Neuroscience 164:733–746

Müller N, Keil J, Obleser J, Schulz H, Grunwald T, Bernays R, Huppertz H, Weisz N (2013) NeuroImage You can't stop the music : Reduced auditory alpha power and coupling between auditory and memory regions facilitate the illusory perception of music during noise. Neuroimage 79:383–393

Newman CW, Jacobson GP, Spitzer JB (1996) Development of the Tinnitus Handicap Inventory. Arch Otolaryngol - Head Neck Surg 122:143–148

Noreña A, Cransac H, Che S (1999) Towards an objective classification of tinnitus. Clin Neurophysiol 110:666–675

Noreña A, Micheyl C, Chery-Croze S, Collet L (2002) Psychoacoustic characterization of the tinnitus spectrum: implications for the underlying mechanisms of tinnitus. Audiol Neurootol 7:358–369.

Noreña AJ (2011) An integrative model of tinnitus based on a central gain controlling neural sensitivity. Neurosci Biobehav Rev 35:1089–1109

Noreña AJ, Eggermont JJ (2003) Changes in spontaneous neural activity immediately after an acoustic trauma: implications for neural correlates of tinnitus. Hear Res 183:137–153

Norena AJ, Eggermont JJ (2005) Enriched Acoustic Environment after Noise Trauma Reduces Hearing Loss and Prevents Cortical Map Reorganization. J Neurosci 25:699–705

Noreña AJ, Eggermont JJ (2006) Enriched acoustic environment after noise trauma abolishes neural signs of tinnitus. Neuroreport 17:559–563

Noreña AJ, Farley BJ (2013) Tinnitus-related neural activity: theories of generation, propagation, and centralization. Hear Res 295:161–171

Noreña AJ, Moffat G, Blanc JL, Pezard L, Cazals Y (2010) Neural changes in the auditory cortex of awake guinea pigs after two tinnitus inducers: salicylate and acoustic trauma. Neuroscience 166:1194–1209

Ochi K, Eggermont JJ (1996) Effects of salicylate on neural activity in cat primary auditory cortex. Hear Res 95:63–76

Okamoto H, Stracke H, Stoll W, Pantev C (2010) Listening to tailor-made notched music reduces tinnitus loudness and tinnitus-related auditory cortex activity. Proc Natl Acad Sci U S A 107:1207–1210

Oostenveld R, Fries P, Maris E, Schoffelen J-M (2011) FieldTrip: Open source software for advanced analysis of MEG, EEG, and invasive electrophysiological data. Comput Intell Neurosci 2011:156869

Ortmann M, Müller N, Schlee W, Weisz N (2011) Rapid increases of gamma power in the auditory cortex following noise trauma in humans. Eur J Neurosci 33:568–575

Pantev C, Roberts LE, Elbert T, Ross B, Weinbruch C (1996) Tonotopic organization of the sources of human auditory steady-state responses. Hear Res 101: 62-74

Pape J, Paraskevopoulos E, Bruchmann M, Wollbrink A, Rudack C, Pantev C (2014) Playing and Listening to Tailor-Made Notched Music: Cortical Plasticity Induced by Unimodal and Multimodal Training in Tinnitus Patients. Neural Plast 2014:1–10

Pascual-Marqui RD, Lehmann D, Koukkou M, Kochi K, Anderer P, Saletu B, Tanaka H, Hirata K, John ER, Prichep L, Biscay-Lirio R, Kinoshita T (2011) Assessing interactions in the brain with exact low-resolution electromagnetic tomography. Philos Trans A Math Phys Eng Sci 369:3768–3784

Paul BT, Bruce IC, Bosnyak DJ, Thompson DC, Roberts LE (2014) Modulation of Electrocortical Brain Activity by Attention in Individuals with and without Tinnitus. Neural Plasticity 2014.

Peelle JE, Gross J, Davis MH (2013) Phase-locked responses to speech in human auditory cortex are enhanced during comprehension. Cereb Cortex 23:1378–1387

Petkov CI, Kang X, Alho K, Bertrand O, Yund EW, Woods DL (2004) Attentional modulation of human auditory cortex. Nat Neurosci 7:658–663

Petrides M, Alivisatos B, Frey S (2002) Differential activation of the human orbital, mid-ventrolateral, and mid-dorsolateral prefrontal cortex during the processing of visual stimuli. Proc Natl Acad Sci U S A 99:5649–5654

Phillips J, McFerran D (2010) Tinnitus retraining therapy (TRT) for tinnitus. Cochrane Libr

Pienkowski M, Eggermont J (2009) Recovery from reorganization induced in adult cat primary auditory cortex by a band-limited spectrally enhanced acoustic environment. Hear Res

Pineda JA, Moore FR, Viirre E (2008) Tinnitus treatment with customized sounds. Int Tinnitus J 14:17–25

Rae CD (2014) A guide to the metabolic pathways and function of metabolites observed in human brain 1H magnetic resonance spectra. Neurochem Res 39:1–36

Raichle ME, MacLeod AM, Snyder AZ, Powers WJ, Gusnard DA, Shulman GL (2001) A default mode of brain function. Proc Natl Acad Sci U S A 98:676–682.

Ramanathan D, Tuszynski MH, Conner JM (2009) The basal forebrain cholinergic system is required specifically for behaviorally mediated cortical map plasticity. J Neurosci 29:5992–6000

Rao RP, Ballard DH (1999) Predictive coding in the visual cortex: a functional interpretation of some extra-classical receptive-field effects. Nat Neurosci 2:79–87.

Rauschecker JP, Leaver AM, Muhlau M (2010) Tuning out the noise: Limbic-auditory interactions in tinnitus. Neuron 66:819–826.

Ray S, Maunsell JHR (2011) Different origins of gamma rhythm and high-gamma activity in macaque visual cortex. PLoS Biol 9:e1000610

Ray S, Niebur E, Hsiao SS, Sinai A, Crone NE (2008) High-frequency gamma activity (80-150Hz) is increased in human cortex during selective attention. Clin Neurophysiol 119:116–133

Reyes SA, Salvi RJ, Burkard RF, Coad M Lou, Wack DS, Galantowicz PJ, Lockwood AH (2002) Brain imaging of the effects of lidocaine on tinnitus. Hear Res 171:43–50

Risey J, Guth P, Amedee R (1995) Furosemide Distinguishes Central and Peripheral Tinnitus. Int Tinnitus J 1:99–103

Roberts L, Moffat G, Bosnyak D (2006) Residual inhibition functions in relation to tinnitus spectra and auditory threshold shift. Acta Otolaryngol 556:27–33

Roberts LE, Bosnyak DJ, Bruce IC, Gander PE, Paul BT (2015) Evidence for differential modulation of primary and nonprimary auditory cortex by forward masking in tinnitus. Hear Res 327:9–27

Roberts LE, Husain FT, Eggermont JJ (2013) Role of attention in the generation and modulation of tinnitus. Neurosci Biobehav Rev 37:1754–1773

Roberts LE, Moffat G, Baumann M, Ward LM, Bosnyak DJ (2008) Residual inhibition functions overlap tinnitus spectra and the region of auditory threshold shift. J Assoc Res Otolaryngol 9:417–435

Robertson D, Bester C, Vogler D, Mulders WHAM (2013) Spontaneous hyperactivity in the auditory midbrain: relationship to afferent input. Hear Res 295:124–129

Ruttiger L, Ciuffani J, Zenner H-P, Knipper M (2003) A behavioral paradigm to judge acute sodium salicylate-induced sound experience in rats : a new approach for an animal model on tinnitus. Hear Res 180:39–50.

Sadaghiani S, Hesselmann G, Kleinschmidt A (2009) Distributed and antagonistic contributions of ongoing activity fluctuations to auditory stimulus detection. J Neurosci 29:13410–13417

Sarter M, Givens B, Bruno JP (2001) The cognitive neuroscience of sustained attention: where top-down meets bottom-up. Brain Res Rev 35:146–160

Sarter M, Hasselmo ME, Bruno JP, Givens B (2005) Unraveling the attentional functions of cortical cholinergic inputs: interactions between signal-driven and cognitive modulation of signal detection. Brain Res Brain Res Rev 48:98–111

Sarter M, Parikh V (2005) Choline transporters, cholinergic transmission and cognition. Nat Rev Neurosci 6:48–56

Schaette R, Kempter R (2006) Development of tinnitus-related neuronal hyperactivity through homeostatic plasticity after hearing loss: a computational model. Eur J Neurosci 23:3124–3138

Schaette R, McAlpine D (2011) Tinnitus with a normal audiogram: physiological evidence for hidden hearing loss and computational model. J Neurosci 31:13452–13457

Schecklmann M, Landgrebe M, Poeppl TB, Kreuzer P, Männer P, Marienhagen J, Wack DS, Kleinjung T, Hajak G, Langguth B (2013a) Neural correlates of tinnitus duration and distress: a positron emission tomography study. Hum Brain Mapp 34:233–240

Schecklmann M, Lehner A, Poeppl TB, Kreuzer PM (2013b) Auditory cortex is implicated in tinnitus distress : a voxel-based morphometry study. :1061–1070.

Schlee W, Mueller N, Hartmann T, Keil J, Lorenz I, Weisz N (2009) Mapping cortical hubs in tinnitus. BMC Biol 7:80

Schlee W, Weisz N, Bertrand O, Hartmann T, Elbert T (2008) Using auditory steady state responses to outline the functional connectivity in the tinnitus brain. PLoS One 3:e3720

Schmidt SA, Akrofi K, Carpenter-Thompson JR, Husain FT (2013) Default mode, dorsal attention and auditory resting state networks exhibit differential functional connectivity in tinnitus and hearing loss. PLoS One 8:e76488

Schneider P, Andermann M, Wengenroth M, Goebel R, Flor H, Rupp A, Diesch E (2009) Reduced volume of Heschl's gyrus in tinnitus. Neuroimage 45:927–939

Schönwiesner M, Novitski N, Pakarinen S, Carlson S, Tervaniemi M, Näätänen R (2007) Heschl's gyrus, posterior superior temporal gyrus, and mid-ventrolateral prefrontal cortex have different roles in the detection of acoustic changes. J Neurophysiol 97:2075–2082

Scott B, Lindberg P (2000) Psychological profile and somatic complaints between help-seeking and non-help-seeking tinnitus subjects. Psychosomatics 41:347–352

Searchfield GD, Kobayashi K, Sanders M (2012) An adaptation level theory of tinnitus audibility. Front Syst Neurosci 6:46

Sedley W, Gander PE, Kumar S, Oya H, Kovach CK, Nourski KV, Kawasaki H, Howard MA, Griffiths TD (2015) Intracranial Mapping of a Cortical Tinnitus System using Residual Inhibition. Curr Biol:1–7

Sedley W, Teki S, Kumar S, Barnes GR, Bamiou D-E, Griffiths TD (2012a) Single-subject oscillatory γ responses in tinnitus. Brain 135:3089–3100

Sedley W, Teki S, Kumar S, Overath T, Barnes G, Griffiths T (2012b) Gamma band pitch responses in human auditory cortex measured with magnetoencephalography. Neuroimage 59:1904–1911

Seki S, Eggermont JJ (2002) Changes in cat primary auditory cortex after minor-to-moderate pure-tone induced hearing loss. Hear Res 173:172–186

Seki S, Eggermont JJ (2003) Changes in spontaneous firing rate and neural synchrony in cat primary auditory cortex after localized tone-induced hearing loss. Hear Res 180:28–38

Sereda M, Adjamian P, Edmondson-Jones M, Palmer AR, Hall DA (2013) Auditory evoked magnetic fields in individuals with tinnitus. Hear Res 302:50–59

Shargorodsky J, Curhan GC, Farwell WR (2010) Prevalence and characteristics of tinnitus among US adults. Am J Med 123:711–718

Shore SE (2005) Multisensory integration in the dorsal cochlear nucleus: unit responses to acoustic and trigeminal ganglion stimulation. Eur J Neurosci 21:3334–3348

Shore SE, Koehler S, Oldakowski M, Hughes LF, Syed S (2009) Dorsal cochlear nucleus responses to somatosensory stimulation are enhanced after noise-induced hearing loss. Eur J Neurosci 27:155–168.

Shulman A, Strashun AM, Seibyl JP, Daftary A, Goldstein B (2000) Benzodiazepine receptor deficiency and tinnitus. Int Tinnitus J 6:98–111

Singer W, Gray CM (1995) Visual feature integration and the temporal correlation hypothesis. Annu Rev Neurosci 18:555–586.

Smits M, Kovacs S, de Ridder D, Peeters RR, van Hecke P, Sunaert S (2007) Lateralization of functional magnetic resonance imaging (fMRI) activation in the auditory pathway of patients with lateralized tinnitus. Neuroradiology 49:669–679

Song JJ, Vanneste S, De Ridder D (2015) Dysfunctional noise cancelling of the rostral anterior cingulate cortex in tinnitus patients. PLoS One 10:e0123538

Spaak E, Bonnefond M, Maier A, Leopold DA, Jensen O (2012) Layer-specific entrainment of γ-band neural activity by the α rhythm in monkey visual cortex. Curr Biol 22:2313–2318

Stefanics G, Hangya B, Hernádi I, Winkler I, Lakatos P, Ulbert I (2010) Phase entrainment of human delta oscillations can mediate the effects of expectation on reaction speed. J Neurosci 30:13578–13585

Stein A, Engell A, Junghoefer M, Wunderlich R, Lau P, Wollbrink a, Rudack C, Pantev C (2015a) Inhibition-induced plasticity in tinnitus patients after repetitive exposure to tailor-made notched music. Clin Neurophysiol 126:1007–1015

Stein A, Engell A, Lau P, Wunderlich R, Junghoefer M, Wollbrink A, Bruchmann M, Rudack C, Pantev C (2015b) Enhancing inhibition-induced plasticity in tinnitus - spectral energy contrasts in tailor-made notched music matter. PLoS One 10:e0126494

Stein A, Engell A, Okamoto H, Wollbrink A, Lau P, Wunderlich R, Rudack C, Pantev C (2013) Modulatory Effects of Spectral Energy Contrasts on Lateral Inhibition in the Human Auditory Cortex: An MEG Study. PLoS One 8:e80899

Steriade M, McCormick D a, Sejnowski TJ (1993) Thalamocortical oscillations in the sleeping and aroused brain. Science 262:679–685

Stolzberg D, Chen G-D, Allman BL, Salvi RJ (2011) Salicylate-induced peripheral auditory changes and tonotopic reorganization of auditory cortex. Neuroscience 180:157–164

Stolzberg D, Salvi RJ, Allman BL (2012) Salicylate toxicity model of tinnitus. Front Syst Neurosci 6:28

Stolzberg D, Hayes SH, Kashanian N, Radziwon K, Salvi RJ, Allman BL (2013) A novel behavioral assay for the assessment of acute tinnitus in rats optimized for simultaneous recording of oscillatory neural activity. J Neurosci Methods 219:224–232

Stypulkowski PH (1990) Mechanisms of salicylate ototoxicity. Hear Res 46:113–146.

Sun W, Deng A, Jayaram A, Gibson B (2012) Noise exposure enhances auditory cortex responses related to hyperacusis behavior. Brain Res 1485:108–116

Sun W, Lu J, Stolzberg D, Gray L, Deng A., Lobarinas E, Salvi RJ (2009) Salicylate increases the gain of the central auditory system. Neuroscience 159:325–334

Tadin D, Lappin JS, Gilroy LA, Blake R (2003) Perceptual consequences of centre – surround antagonism in visual motion processing. Nature 424:312–315.

Tallon-baudry C, Bertrand O (1999) Oscillatory gamma activity in humans and its role in object representation. 3:151–162.

Tallon-Baudry C, Bertrand O, Hénaff M-A, Isnard J, Fischer C (2005) Attention modulates gamma-band oscillations differently in the human lateral occipital cortex and fusiform gyrus. Cereb Cortex 15:654–662

Tass PA, Adamchic I, Freund H-J, von Stackelberg T, Hauptmann C (2012) Counteracting tinnitus by acoustic coordinated reset neuromodulation. Restor Neurol Neurosci 30:137–159

Tiesinga PH, Fellous J-M, Salinas E, José J V, Sejnowski TJ (2004) Inhibitory synchrony as a mechanism for attentional gain modulation. J Physiol Paris 98:296–314

Tkác I, Starcuk Z, Choi IY, Gruetter R (1999) In vivo 1H NMR spectroscopy of rat brain at 1 ms echo time. Magn Reson Med 41:649–656

Tucker DA, Phillips SL, Ruth RA, Clayton WA, Royster E, Todd AD (2005) The effect of silence on tinnitus perception. Otolaryngol Head Neck Surg 132:20–24

Turken AU, Dronkers NF (2011) The neural architecture of the language comprehension network: converging evidence from lesion and connectivity analyses. Front Syst Neurosci 5:1

Turner JG, Brozoski TJ, Bauer CA, Parrish JL, Myers K, Hughes LF, Caspary DM (2006) Gap detection deficits in rats with tinnitus: a potential novel screening tool. Behav Neurosci 120:188–195

Van der Loo E, Gais S, Congedo M, Vanneste S, Plazier M, Menovsky T, Van de Heyning P, De Ridder D (2009) Tinnitus intensity dependent gamma oscillations of the contralateral auditory cortex. PLoS One 4:e7396

Van Kerkoerle T, Self MW, Dagnino B, Gariel-Mathis M-A., Poort J, van der Togt C, Roelfsema PR (2014) Alpha and gamma oscillations characterize feedback and feedforward processing in monkey visual cortex. Proc Natl Acad Sci 111

Van Veen BD, van Drongelen W, Yuchtman M, Suzuki A (1997) Localization of brain electrical activity via linearly constrained minimum variance spatial filtering. IEEE Trans Biomed Eng 44:867–880

Vanneste S, Heyning P Van De, Ridder D De (2011a) Contralateral parahippocampal gamma-band activity determines noise-like tinnitus laterality: a region of interest analysis. Neuroscience 199:481–490

Vanneste S, Plazier M, der Loo E Van, de Heyning P Van, Congedo M, De Ridder D (2010a) The neural correlates of tinnitus-related distress. Neuroimage 52:470–480

Vanneste S, Plazier M, van der Loo E, Van de Heyning P, De Ridder D (2010b) The differences in brain activity between narrow band noise and pure tone tinnitus. PLoS One 5:e13618

Vanneste S, Plazier M, van der Loo E, Van de Heyning P, De Ridder D (2011b) The difference between uni- and bilateral auditory phantom percept. Clin Neurophysiol 122:578–587

Vanneste S, Song J-J, De Ridder D (2013a) Tinnitus and musical hallucinosis: the same but more. Neuroimage 82:373–383

Vanneste S, van de Heyning P, De Ridder D (2011c) The neural network of phantom sound changes over time: a comparison between recent-onset and chronic tinnitus patients. Eur J Neurosci 34:718–731

Vanneste S, Van De Heyning P, De Ridder D (2015) Tinnitus: A Large VBM-EEG Correlational Study Langguth B, ed. PLoS One 10:e0115122

Vanneste S, van Dongen M, De Vree B, Hiseni S, van der Velden E, Strydis C, Joos K, Norena A, Serdijn W, De Ridder D (2013b) Does enriched acoustic environment in humans abolish chronic tinnitus clinically and electrophysiologically? A double blind placebo controlled study. Hear Res 296:141–148

Voisin J, Bidet-Caulet A, Bertrand O, Fonlupt P (2006) Listening in silence activates auditory areas: a functional magnetic resonance imaging study. J Neurosci 26:273–278

Wang H, Brozoski TJ, Turner JG, Ling L, Parrish JL, Hughes LF, Caspary DM (2009) Plasticity at glycinergic synapses in dorsal cochlear nucleus of rats with behavioral evidence of tinnitus. Neuroscience 164:747–759

Wang X-C, Du X-X, Tian Q, Wang J-Z (2008) Correlation between choline signal intensity and acetylcholine level in different brain regions of rat. Neurochem Res 33:814–819

Wei L, Ding D, Sun W, Xu-Friedman MA, Salvi R (2010) Effects of sodium salicylate on spontaneous and evoked spike rate in the dorsal cochlear nucleus. Hear Res 267:54–60

Weisz N, Hartmann T, Dohrmann K, Schlee W, Norena A (2006) High-frequency tinnitus without hearing loss does not mean absence of deafferentation. Hear Res 222:108–114

Weisz N, Hartmann T, Muller N, Lorenz I, Obleser J (2011) Alpha rhythms in audition: cognitive and clinical perspectives. Front Psychol 2:73

Weisz N, Moratti S, Meinzer M, Dohrmann K, Elbert T (2005a) Tinnitus perception and distress is related to abnormal spontaneous brain activity as measured by magnetoencephalography. PLoS Med 2:e153

Weisz N, Müller S, Schlee W, Dohrmann K, Hartmann T, Elbert T (2007) The neural code of auditory phantom perception. J Neurosci 27:1479–1484

Weisz N, Wienbruch C, Dohrmann K, Elbert T (2005b) Neuromagnetic indicators of auditory cortical reorganization of tinnitus. Brain 128:2722–2731

Wepsic JG (1966) Multimodal sensory activation of cells in the magnocellular medial geniculate nucleus. Exp Neurol 15:299–318

Whittington M, Traub R, Jefferys J (1995) Synchronized oscillations in interneuron networks driven by metabotropic glutamate receptor activation. Nature 373:612–615

Wienbruch C, Paul I, Weisz N, Elbert T, Roberts LE (2006) Frequency organization of the 40-Hz auditory steady-state response in normal hearing and in tinnitus. Neuroimage 33:180–194

Wineland AM, Burton H, Piccirillo J (2012) Functional connectivity networks in nonbothersome tinnitus. Otolaryngol Head Neck Surg 147:900–906.

Womelsdorf T, Fries P, Mitra PP, Desimone R (2006) Gamma-band synchronization in visual cortex predicts speed of change detection. Nature 439:733–736

Wyart V, Tallon-Baudry C (2008) Neural dissociation between visual awareness and spatial attention. J Neurosci 28:2667–2679

Yang G, Lobarinas E, Zhang L, Turner J, Stolzberg D, Salvi R, Sun W (2007) Salicylate induced tinnitus: behavioral measures and neural activity in auditory cortex of awake rats. Hear Res 226:244–253

Yang S, Weiner BD, Zhang LS, Cho S-J, Bao S (2011) Homeostatic plasticity drives tinnitus perception in an animal model. Proc Natl Acad Sci U S A 108:14974–14979.

Zeng F-G (2013) An active loudness model suggesting tinnitus as increased central noise and hyperacusis as increased nonlinear gain. Hear Res 295:172–179

Zhang JS, Kaltenbach JA, Godfrey DA, Wang J (2006) Origin of hyperactivity in the hamster dorsal cochlear nucleus following intense sound exposure. J Neurosci Res 84:819–831

Zhang X, Yang P, Cao Y, Qin L, Sato Y (2011) Salicylate induced neural changes in the primary auditory cortex of awake cats. Neuroscience 172:232–245

Zhou J, Shore S (2004) Projections from the trigeminal nuclear complex to the cochlear nuclei: a retrograde and anterograde tracing study in the guinea pig. J Neurosci Res 78:901–907

Zöger S, Svedlund J, Holgers K-M (2006) Relationship between tinnitus severity and psychiatric disorders. Psychosomatics 47:282–288